CRM-GEOTHERMAL DELIVERABLE D2.1

REPORT IDENTIFYING PRE-EXISTING SOURCES OF DATA AT THE SELECTED SITES

Summary:
We provide a background to several sites being investigated within this project, and identify possibly useful sources of information that could be interrogated or modelled later in the project in order to provide further understanding of the sites. We specifically do not provide a critical analysis or interpretation of the data, just identify the types of it and where it can be found.

Authors:
Chris Rochelle, British Geological Survey, UK, Geochemist
Michael Bau, Constructor University Bremen, Germany, Biogeochemist
Alper Baba, Izmir Institute of Technology, Türkiye, Geologist/Hydrogeologist
Simona Regenspurg, Helmholtz Centre Potsdam, GFZ, Germany, Geochemist
Andri Stefánsson, Haskoli Islands, Iceland, Geologist
Tolga Ayzit, Izmir Institute of Technology, Türkiye, Geologist, PhD student
Hazel Farndale, Geothermal Engineering Ltd, UK, Business Development Manager
Amy Peach-Gibson, Geothermal Engineering Ltd, UK, Geothermal Geoscientist
Richard Shaw, British Geological Survey, UK, Geologist
Alistair Salisbury, Cornish Lithium Plc, UK, Geologist
Serhat Tonkul, Izmir Institute of Technology, Türkiye, Geochemist, PhD student
Chris Yeomans, Cornish Lithium Plc, UK, Geologist, Research Manager

Funded by
the European Union

Title:	Report identifying pre-existing sources of data at the selected sites
Lead beneficiary:	UKRI-BGS
Other beneficiaries:	CL, GEL, GFZ, IZTECH, JUB, PWG, UoI, UoN
Due date:	31 December 2022
Nature:	Public
Diffusion:	e.g. all Partners, WP-partners
Status:	Final
DOI:	10.5281/zenodo.7495744
License information:	CC-BY-4.0
Recommended Citation:	Rochelle, C., Bau, M., Baba, A., Regenspurg, S., Stefánsson, A., Ayzit, T., Farndale, H., Peach-Gibson, A., Shaw, R., Salisbury, A., Tonkul, S. and Yeomans, C. The Horizon Europe CRM-geothermal project: Deliverable 2.1 - Report identifying pre-existing sources of data at the selected sites, Zenodo, 138pp, DOI: 10.5281/zenodo.7495744
ORCID:	Simona Regenspurg – ORCID: 0000-0002-4327-1439 Michael Bau – ORCID: 0000-0002-7746-3762 Alper Baba – ORCID: 0000-0001-5307-3156 Serhat Tonkul – ORCID: 0000-0002-8572-1565 Tolga Ayzit – ORCID: 0000-0001-5710-0713 Andri Stefansson – ORCID: 0000-0002-0439-193X Hazel Farndale – ORCID: 0000-0001-8977-1415 Richard Shaw – ORCID: 0000-0002-7691-4568
Document code:	CRM-GEOTHERMAL_D.2.1

Revision history	Author	Delivery date	Summary of changes and comments
Version 01	CR	20.12.2022	Deliverable contributions from all partners assembled and checked.

Approval status			
	Name	Function	Date
Deliverable responsible	Chris Rochelle	Geochemist	20/12/2022
WP leader	Chris Rochelle	Geochemist	20/12/2022
Project Coordinator	Katrin Kieling	Project manager	21/12/2022

Funded by the European Union and UKRI through Innovate UK. Views and opinions expressed are however those of the author(s) only and do not necessarily reflect those of the European Union or HADEA. Neither the European Union nor the granting authority can be held responsible for them.

TABLE OF CONTENTS

FIGURES

TABLES

1 EXECUTIVE SUMMARY

This report is a published product of the 'CRM-geothermal' project - an EU-funded, Horizon Europe project which aims to develop a novel and potentially disruptive technology solution that can help satisfy the European needs for critical raw materials (CRM) combined with energy production.

This report identifies sources of pre-existing data that underpin datasets and models for the sites being investigated in the 'CRM-geothermal' project. These sites are:

- High enthalpy volcanic geothermal areas - Reykjanes, Iceland; Tuzla, Turkey
- Low salinity water in fractured crystalline rock – Cornwall, UK
- Saline water in sedimentary basins – northern Germany
- Alkaline geothermal area – Olkaria, Kenya
- Metamorphosed flysch – Seferihisar, Turkey

Information on each of these is reported in a separate chapter. This report provides a brief introduction to the study areas and identifies the broad types of data and datasets already generated. It does not discriminate between open-file and restricted information, just identifying what exists. There has been no attempt to interpret those data in the report – this will be part of other Work Packages within the project.

2 INTRODUCTION TO THE STUDY AREAS

Geothermal fluids often carry high amounts of elements that the EU considers as critical raw materials (CRM), and preliminary calculations show that even a single borehole has the potential to produce single-digit percentages of the EU needs. Combined extraction of heat and minerals maximises returns on investment, minimises environmental impact, requires no additional land use, leaves no mining legacies, has near-zero carbon footprint, and enables domestic supplies of CRM. The 'CRM-geothermal' project aims to open up a potentially huge untapped resource and deploy solutions to help Europe fulfil the strategic objectives of the EU Green Deal and the Agenda for Sustainable Development.

2.1 OUTLINE OF WORK

To assess overall supply potential, the 'CRM-geothermal' project will enlarge an existing geothermal fluid atlas by collecting new data and sampling boreholes for their CRM content in Europe and East Africa. It is important however, to also utilise existing information as a foundation for updated datasets and new models, which for some sites could be extensive. Hence, we bring together sources of information, in order that more detailed investigations in the project can more efficiently access the data they need.

This report identifies sources of pre-existing data that underpin datasets and models for the sites being investigated in the 'CRM-geothermal' project. These sites are:

- High enthalpy volcanic geothermal areas - Reykjanes, Iceland; Tuzla, Turkey
- Low salinity water in fractured crystalline rock – Cornwall, UK
- Saline water in sedimentary basins – Groß Schönebeck, northern Germany
- Alkaline geothermal area – Olkaria, Kenya
- Metamorphosed flysch – Seferihisar, Turkey

Information on each of these study sites is reported in a separate chapter, authored by different partners within the project. We aim to provide a brief introduction to each of the study areas and identify the broad types of data and datasets already in existence. We purposefully do not discriminate between open-file and restricted information, just identifying what exists. Access to some of the information and datasets should therefore be via the experts who author each chapter. There has been no attempt to provide a detailed interpretation of those data presented in the report – this will be part of other Work Packages within the overall project.

2.2 LOCATION OF THE STUDY SITES

The following 5 chapters present summaries of available geological, geochemical and other data related to geothermal areas in several countries in Europe and Africa, with special focus on England, Germany, Iceland, Kenya and Turkey (2 sites), see Figures 2.1 and 2.2. Although there is some variation in detail and extent, it is hoped that the chapters provide a useful resource to enable quick identification and checking of data holdings – many of which are openly available. However, much of the data on crustal fluids reflect conditions at <1000 m deep, often less than this, and are only abundant for the near surface.

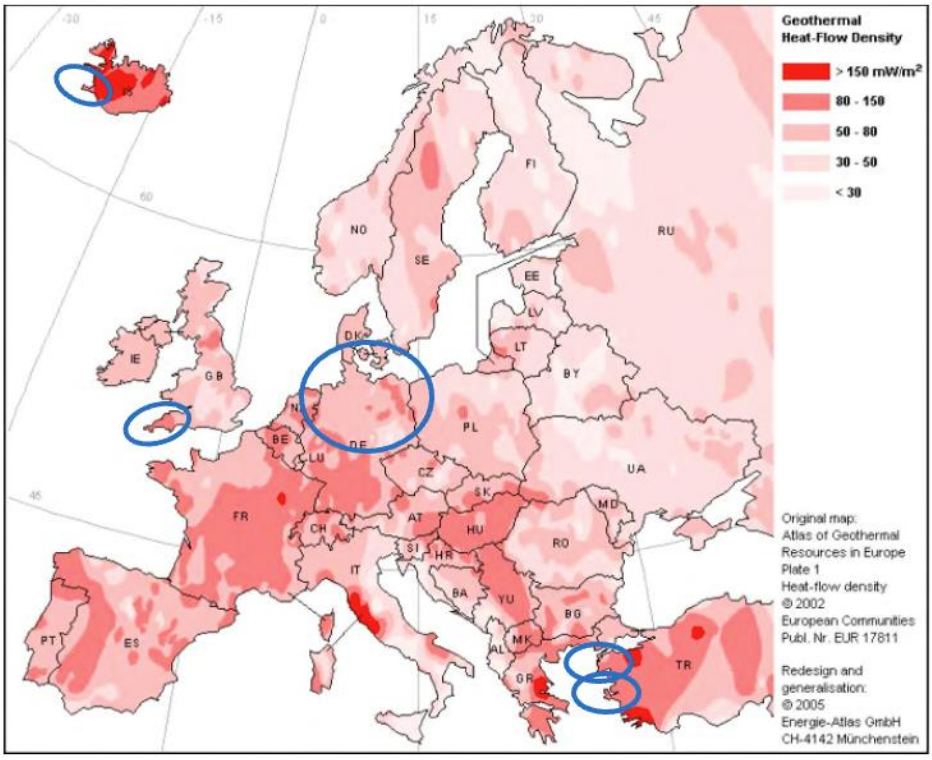

Figure 2.1. The five European study site areas on a generalised heat flow density map, based on the Atlas of Geothermal Resources in Europe (after Hurter and Haenel, 2002)

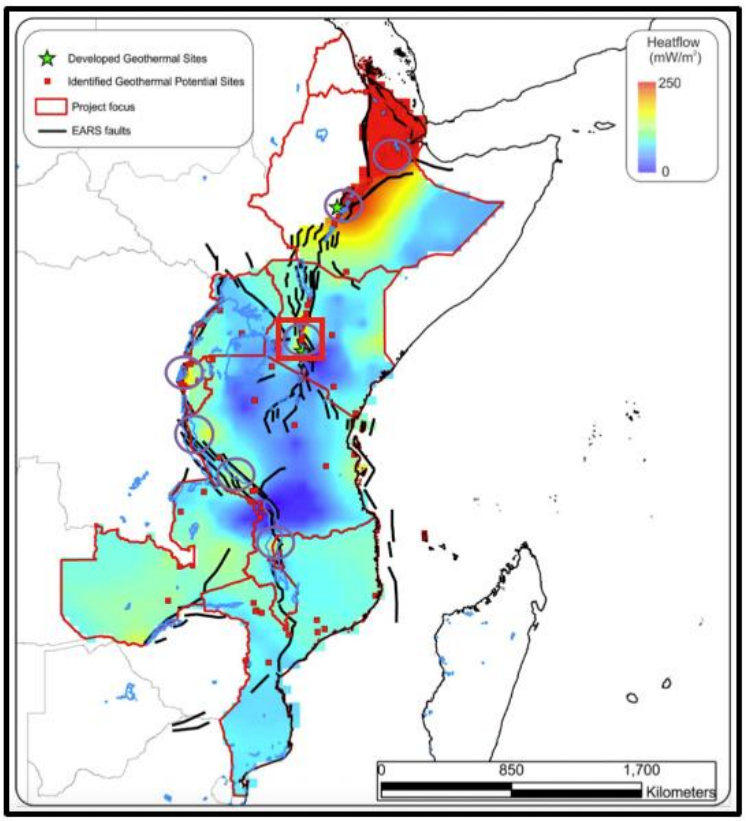

Figure 2.2. The Olkaria, Kenya, study site area (red box) in relation to east African major crustal lineaments and modelled heat flow (after Jones, 2020)

Fluid chemical data below 1000 m are scarce and limited to areas targeted for deep drilling – such as geothermal sites and hydrocarbon exploration. In general, hydraulic conductivity and the magnitude of fluid flow are low at depth, and fracture permeability is a key factor in fluid movement. The composition and salinity of brines and waters at depth varies considerably between countries reported here. Usually concentrations of total dissolved solids (TDS) increase with depth, with the highest values found below 1000 m. Having said that, the deep waters of south-west England do not follow this trend and, though they are enriched in elements such as lithium, are of relatively low salinity.

The first two sites are high enthalpy volcanic geothermal areas, and they are described in Section 3. The first of these sites is the **Reykjanes geothermal system**, Iceland. This site is a basalt-hosted, seawater-dominated active geothermal system located on the southwestern tip of the Reykjanes Peninsula, and is an on-land extension of the Mid-Atlantic Ridge. The geothermal field hosts a 100MW geothermal power plant that was commissioned in 2006. 39 boreholes have been drilled into the geothermal system reaching depths of 1036-4500 m including the second Iceland Deep Drilling Project borehole, IDDP-2. The average reservoir temperature is around 300 °C, though the IDDP-2 borehole reached temperatures of approximately 450 °C. The hydrothermal fluids are enriched in chloride and carry notable concentrations of metals such as Cu, Zn, Pb, and also some Ag and Au. The concentrations of Cu, Zn, and Pb are similar to those in 'black smoker' discharges.

The second high enthalpy geothermal site, the **Tuzla geothermal field**, is described in the second part of Section 3, and is one of the most important geothermal fields in Turkey in terms of temperature. Many studies have been carried out to investigate the geology of the region and to determine the characteristics of the geothermal system. The geothermal field is quite complex, being a hybrid formed by an overlying magmatic-controlled geothermal reservoir in volcanic rocks, and a deeper reservoir consisting of a fault-controlled system in metamorphic basement rocks. Geothermal boreholes have been drilled by both the government and private companies, reaching bottom-hole temperatures of up to 175 °C, with produced waters up to 165 °C at the wellhead.

Until recently, deep geothermal energy research in the UK was limited to the Hot Dry Rock programme of the 1980s, where 3 boreholes in Cornwall were used on a test system at 2-2.5 km. In recent years however, increased interest in renewable energy has led to significant industry investment in **south-west England**, which is the focus of Section 4. Deep geothermal boreholes have been drilled (to about 5 km) into two radiogenic granites:

- The Carnmenellis Granite at United Downs (aimed at power production ± a smaller amount of heat).
- The Saint Austell Granite at the Eden Project (aimed at heat extraction [and potentially a smaller amount of power in the future]).

Both reached bottom-hole temperatures of over 180 °C. Shallower drilling (to 1.8 km) is also ongoing to investigate the potential for dissolved lithium resources, ± low enthalpy water. Lithium concentrations of up to approximately 260 mg/L have been found in the relatively dilute, Mg-poor waters.

The fourth area described in Section 5 is at **Groß Schönebeck, northern Germany**, and is part of the North German Basin. This is a rift basin forming part of a larger structure stretching in two directions; in a north-south direction from the Southern Baltic Sea and North Sea across northern Germany to the German Mittelgebirge (low mountain range), and in an east-west direction from Poland to the Netherlands. Various of the formations within the basin are exploited for geothermal purposes: Rotliegend sandstones and underlying Permocarboniferous Volcanic rocks, Bunter sandstone, Muschelkalk (limestone), Upper Keuper (various sandstones), and Jurassic Hettang sandstone. Extraction of raw materials from geothermal fluids is already considered and tested for brines from the Upper Rhine Valley (a continental sedimentary basin in a rift valley), where methods of lithium extraction are also being investigated at several geothermal sites (e.g. Insheim, Bruchsal).

The most southerly of the sites is **Olkaria, Kenya**, and this is the focus of Section 6. This site is part of the East African Rift System (EARS) was initiated around 45 Ma ago, and there is a close association between doming, rifting and alkaline magmatism. The volcanic activity and hence the geothermal potential are the highest in the northeastern part of the EARS (Djibouti, Ethiopia, Kenya, Tanzania), with estimated geothermal resources >20 GW. However, at present it is only utilized in Kenya (c. 700 MW_e) and Ethiopia (c. 10 MW_e). In Kenya, the focus has been in the central Kenya rift, and in particular at **Olkaria.** Drilling started in 1956, and currently there are over two hundred deep wells down to 3 km, producing water to about 240 °C. In some areas, temperatures at >2 km are >400 °C. Many of the hot springs have alkaline pH, up to c. 10 and are typically Na-HCO_3 or Na-Cl type waters with high fluoride content. Little emphasis has been placed upon the potential enrichment of critical metals in the geothermal waters in the EARS, including those of the rare earth elements (REE), and hence this is an area in need of more detailed investigation.

The final site is described in Section 7, which is at **Seferihisar**, Turkey. This geothermal field lies south of the one at Tuzla. It is a high enthalpy area again, but with the geothermal reservoir located within the Bornova Flysch Zone, which consists of deformed Maastrichtian–Paleocene greywacke and shale with Mesozoic limestone and ophiolite blocks. Geothermal activities in the Seferihisar area have been known since before Roman times, and the numerous 35-70 °C springs in the region have been used traditionally for bathing and washing purposes. Over 40 boreholes have explored the geothermal field, with most present-day produced waters in the vicinity of the Tuzla Fault Zone varying between 90-150 °C. However, in deep (to 2.1 km) boreholes intended for power production, bottom-hole temperatures of over 205 °C have been recorded. The meteoric-derived waters are Na/K-Cl dominated, and are relatively saline.

2.3 REFERENCES

HURTER S. and HAENEL, R., 2002. Atlas of Geothermal Resources in Europe. Directorate-General for Research and Innovation, European Commission. GGA, Hannover, Germany. 92p., 89 plates. pp.47-49. ISBN92-828-0999-4.

JONES, D. J. R. 2020. A summary of the East Africa Rift Temperature and Heat flow Model (EARTH). British Geological Survey Open Report, OR/20/006. 24pp.

SCHWARZ, G., RIPA, M., THUNHOLM, B., SHAW, R.A., BATEMAN, K., DEADY, E., LUSTY, P., RAMALHO, E.C., MATOS, J.X., CARVALHO, J.G., PERȘA, D., MARINCEA, S., BALTREȘ, A., COSTEA, C., DUMITRAȘ, D., PREDA, G., BISEVAC, V. and FERNANDEZ, I. 2016. CHPM2030 Deliverable D1.2 - Report on data availability. CHPM2030 project, University of Miskolc, Hungary, 241pp.

3 HIGH-ENTHALPY VOLCANIC GEOTHERMAL AREAS

Authors:
For Section 3.1: Andri Stefánsson
Haskoli Islands, Iceland
For Section 3.2: Alper Baba, Serhat Tonkul
Izmir Institute of Technology, Turkey

In this section we consider two high-enthalpy sites:

- Reykjanes in Iceland
- Tuzla in Turkey

These sites are important as they involve the highest temperatures involved in this study, and fluid chemistry and rates of fluid-rock reactions will be at the more extreme end of the range covered during the CRM-geothermal project.

3.1 REYKJANES, ICELAND

The Reykjanes geothermal system is a basalt-hosted, seawater-dominated active geothermal system located on the southwestern tip of the Reykjanes Peninsula, SW Iceland. Its presence results from a crustal thermal anomaly associated with the on-land extension of the Mid-Atlantic Ridge. The Reykjanes geothermal field is one of the smallest high-temperature fields in Iceland, with surface manifestations and altered ground covering an area of ~1 km^2. The average reservoir temperature is ~300°C with a natural heat flow of ~130 MWth (Friðriksson et al., 2006). The geothermal field has been explored for decades and currently hosts a 100 MW geothermal power plant that was commissioned in 2006. Since 1956, 39 boreholes have been drilled into the geothermal system reaching depths of 1036 m to 4500 m including the second Iceland Deep Drilling Project borehole, IDDP-2. The discharge fluid rate is 520 kg/s.

3.1.1 Geological and geothermal background

The Reykjanes Peninsula consists of young, highly permeable basaltic formations, and is tectonically active and transected by an intense NE–SW trending fault zone, the continuation of the median fault zone of the Mid-Atlantic Ridge (Björnsson et al., 1970). The Reykjanes volcanic and geothermal system is the westernmost system in Iceland's western neovolcanic zone (Figure 3.1). This volcanic system is characterized by oblique extensional tectonics and episodic fissure eruption volcanism (Thordarson and Larsen, 2007). The Reykjanes Peninsula lacks central volcanoes with shallow secondary magma chambers; rather heat is provided to the geothermal system through dikes intruded at depth (Gudmundsson, 1995). The most recent volcanic eruptions at Reykjanes occurred in 2021 and 2022, and were fed directly from the mantle (Halldórsson et al., 2022).

The Reykjanes Peninsula lies less than 40 m above sea level, and the rocks within the system are highly faulted and porous. Rainwater can enter the system easily, as a result of the high permeability, and outside of the Reykjanes geothermal area a thin lens of fresh water (< 30 m thick) overlies the seawater that comprises most of the groundwater (Sigurdsson, 1986). Continuous tectonic and magmatic activity facilitates the circulation of groundwater and seawater through the basaltic crust (Fridriksson et al., 2006). The Reykjanes thermal area sits at the center of swarms of active faults that facilitate hydrologic convection, where seawater intrusions occur below about 1500 m depth (Kadko et al., 2007). The high heat of the thermal area causes the groundwater to flow nearly to the surface, and this results in pressures that are below those of adjacent groundwaters of similar elevations outside the geothermal system (Tómasson and Kristmannsdóttir, 1972).

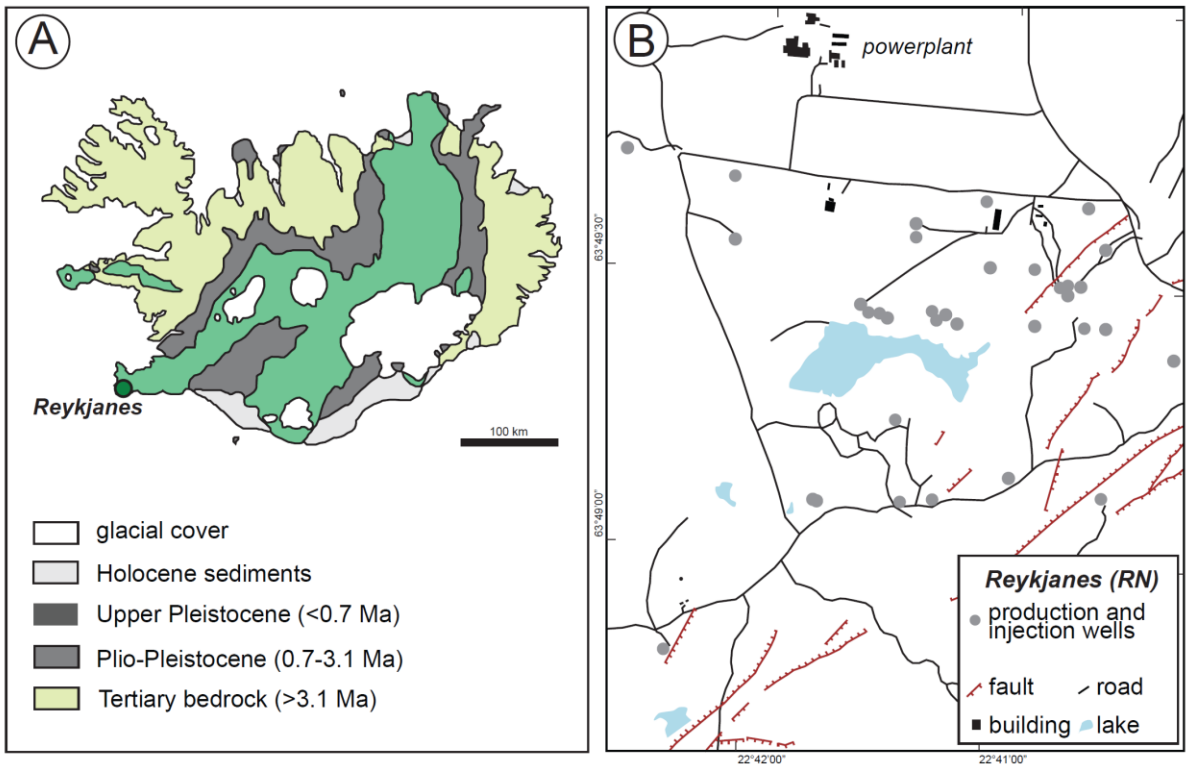

Figure 3.1. Geology of Iceland, and the location of the Reykjanes geothermal field, showing boreholes and powerplant.

The Reykjanes geothermal system is centered in a prominent rift-zone graben, however, many of the associated faults are covered by Holocene lavas and not exposed at the surface (Figure 3.2). This is especially true on the western side of the peninsula where young (< 2 ka) lava flows dominate (Friðleifsson et al., 2014). The orientation of feed zones and the temperature distribution has led to the development of a model that has upflow at Reykjanes controlled by the intersection of a NE–SW trending zone of normal faults and fissures, with a short N–S fracture and NW–SE transform fault (Sigurðsson, 2010).

The upper ~1 km of the Reykjanes system is dominated by hyaloclastite tuff, breccias, pillow basalts, and tuffaceous and marine sediments. The deeper parts of the system are composed primarily of basaltic lavas and diabase dikes (Marks et al., 2010). Altered tuffaceous and sedimentary successions at depths of 400 to 800 m act as a cap-rock to the hydrothermal system (Friðleifsson et al., 2014). A low resistivity anomaly at ~10 km below the surface of the Reykjanes geothermal system has been interpreted as a dense, partially molten, sheeted-dike complex or a large cooling gabbroic intrusion, and likely serves as the heat engine that drives the shallower hydrothermal system (Friðleifsson et al., 2014).

Upflowing hydrothermal fluids in the Reykjanes geothermal system first boil at a depth of ~1300 m and follow the boiling point with depth curve until they reach the base of the cap rock at roughly 700 m (Franzson et al., 2002; Friðleifsson et al., 2014). Deeper in the reservoir, conditions follow an adiabatic gradient through a freely convecting zone down to a minimum depth of ~2.5 km for most parts of the field (Franzson et al., 2002). With further increase in depth, temperature rises due to conductive heat transfer indicating low permeability in these regions (e.g., Friðriksson et al., 2015). Measured reservoir temperatures at Reykjanes are commonly in the range of 280 °C to 300 °C, however, temperatures as high as ~350 °C have been measured (Friðriksson et al., 2015).

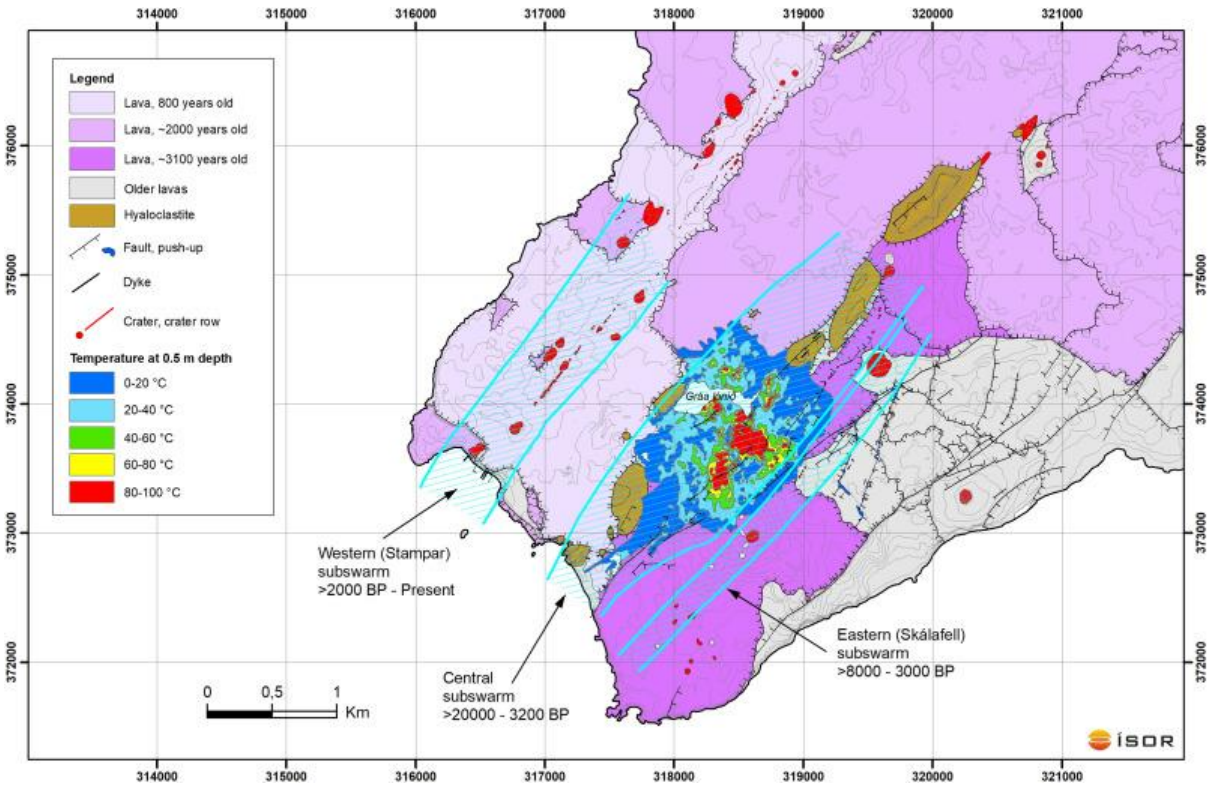

Figure 3.2. Location of the Reykjanes geothermal field in relation to its middle fissure zone. The geothermal field is observed at surface through soil temperatures whereas the reservoir temperature is ~300°C in feed zones, mainly at depth of 1700-2200 m (from Sæmundsson et al., 2020).

3.1.2 Fluids and dissolved resources

The hydrothermal fluids at Reykjanes are characterized by elevated chloride concentrations and mildly acid pH values (Arnórsson, 1978) and considered to be predominantly of seawater origin with addition of minor meteoric water (Pope et al., 2009). The range of salinity (~0.1 and 3.5 wt.% NaCl) and the light δ^2H signature of presently circulating fluids (Pope et al., 2009) suggest that glacially-derived freshwater dominated the system at some time during the Pleistocene (Franzson et al., 2002). The pH of the hydrothermal fluids is about 5.5, lower than is typically the case in other hydrothermal fluids of meteoric water origin in Iceland (Stefánsson and Arnórsson, 2002; Kaasalainen et al., 2015).

The major element chemistry of the hydrothermal fluids represents an equilibrium composition at the relevant reservoir temperatures. For example, the dissolved concentrations of silica, sodium, potassium, calcium, sulphate, and carbonate are controlled by the solubilities of quartz, albite, K-feldspar, anhydrite, and calcite. Fluoride activity is thought to be controlled by an ionic exchange reaction where it substitutes for hydroxyl groups in phyllosilicates. The ratios of individual cations and hydrogen ion are governed by ionic exchange equilibria with hydrothermal minerals, probably smectite and chlorite (Arnórsson, 1978).

The hydrothermal fluids at depth have a relatively high concentration of many metals and metaloids. Concentrations include 154–2431 µM Fe (9–140 ppm), 207–261 µM Cu (14–17 ppm), 79–393 µM Zn (5–27 ppm), 0.6–1.4 µM Pb (120–290 ppb), 6–31 nM Au (1–6 ppb), and 250–960 nM Ag (28–107 ppb) and ~900 µM Li (6.3 ppm), orders of magnitude greater than seawater concentrations. Fluids discharged at surface from the same wells have often orders of magnitude lower metal concentrations due to precipitation caused by depressurisation boiling. The concentrations of Cu, Zn, and Pb in the high-temperature reservoir liquids at Reykjanes are similar to those in the highest-temperature black smoker discharges (Figure 3.3) (Hardardóttir et al., 2009).

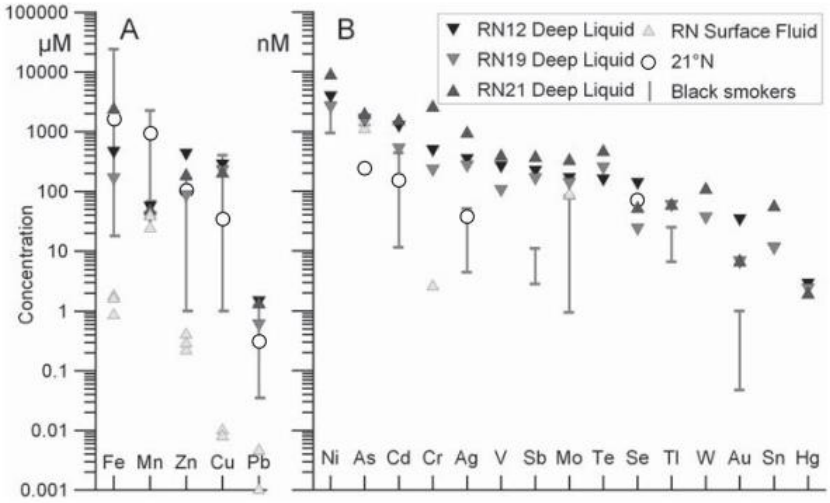

Figure 3.3. Trace element concentrations in reservoir hydrothermal fluids at Reykjanes, and one sample collected from surface (from Hardardóttir et al., 2009).

The second Iceland Deep Drilling borehole, IDDP-2, was drilled at Reykjanes in 2016–2017 by deepening an earlier borehole, RN-15. The total depth reached was 4659 m (Fridleifsson et al., 2020). Today, this is the deepest high-temperature geothermal borehole in the world. At ~4500 m depth, the metabasalt and metagabbro show hydrothermal alteration at ~700-900 °C. Paragenetically later alteration assemblages record continuing alteration down to 600 °C in the latest-stage, crosscutting veins (Zierenberg et al., 2021). Hydrothermal fluids were not directly recovered from depth, but based on fluid inclusion analysis, two separate phases exist: an H_2O-rich vapor and an Fe-K–rich brine containing 2000 µg/g Cu, 3.5 µg/g Ag, 1.4 µg/g U, and 0.14 µg/g Au. Occasionally, the fluid inclusions coexist with rhyolite melt inclusions. These findings indicate that the borehole intersected high-energy vapor, which is valuable for energy production, and discovered a potentially ore-forming brine (Bali et al., 2020).

3.1.3 Alteration mineralogy and trace element concentration

The alteration mineralogy in the subsurface of the Reykjanes geothermal system is primarily based on analysis of drill cuttings of rocks, both crystalline basalt and hyaloclastite fragments. Host rocks of the Reykjanes geothermal system are extensively altered by the circulating hydrothermal fluids. A prograde geothermal alteration assemblage is developed with depth consisting of mixed layered clays and chlorite in the top 700 m followed by an alteration zone composed of mainly chlorite, quartz, epidote and anhydrite (Franzson et al., 2002). At depths >1200 m, actinolite appears within the alteration mineral assemblage (Figures 3.4 and 3.5).

The alteration shows distinct characteristics. Hyaloclastite fragments are typically highly altered, whereas basalts from the same depth interval are commonly minimally altered. Additionally, alteration assemblages differ in the two rock types, with hyaloclastite hosting secondary epidote, prehnite, chlorite, titanite, garnet, plagioclase, clinopyroxene, and quartz. Basalt alteration includes albitization, uralitization, and at advanced stages of alteration, replacement of secondary albite by potassium feldspar. Titanite typically occurs as fine-grained disseminated crystals forming discontinuous rims around minerals that have been replaced by chlorite. Vein minerals include calcite, quartz, prehnite, epidote, hydrothermal clinopyroxene, and, rarely, anorthite that appears to be of hydrothermal origin. Although crosscutting relationships can be difficult to distinguish from cuttings alone, a number of veins that intersect both crystalline basalt and hyaloclastite have different assemblages than the groundmass they cut (e.g. epidote-hydrothermal clinopyroxene cutting relatively fresh basalt) (Marks et al., 2010).

The interaction of the host rocks with the hydrothermal fluids results in substantial trace element mass changes with elements including Ba, Zn, Cu, Ni, Sr, Rb, As and Cd being enriched in the altered rocks. Barium is for example contained in K-feldspars, whereas Fe, Mn and Sr are enriched in carbonates and elements like Au, Cu, Ni, Pb and Zn in sulfide minerals (Figures 3.6 and 3.7) (Libbey and Williams-Jones, 2016a; 2016b). Based on these findings it has been concluded that the Reykjanes geothermal system is an active equivalent to an epithermal ore-deposit.

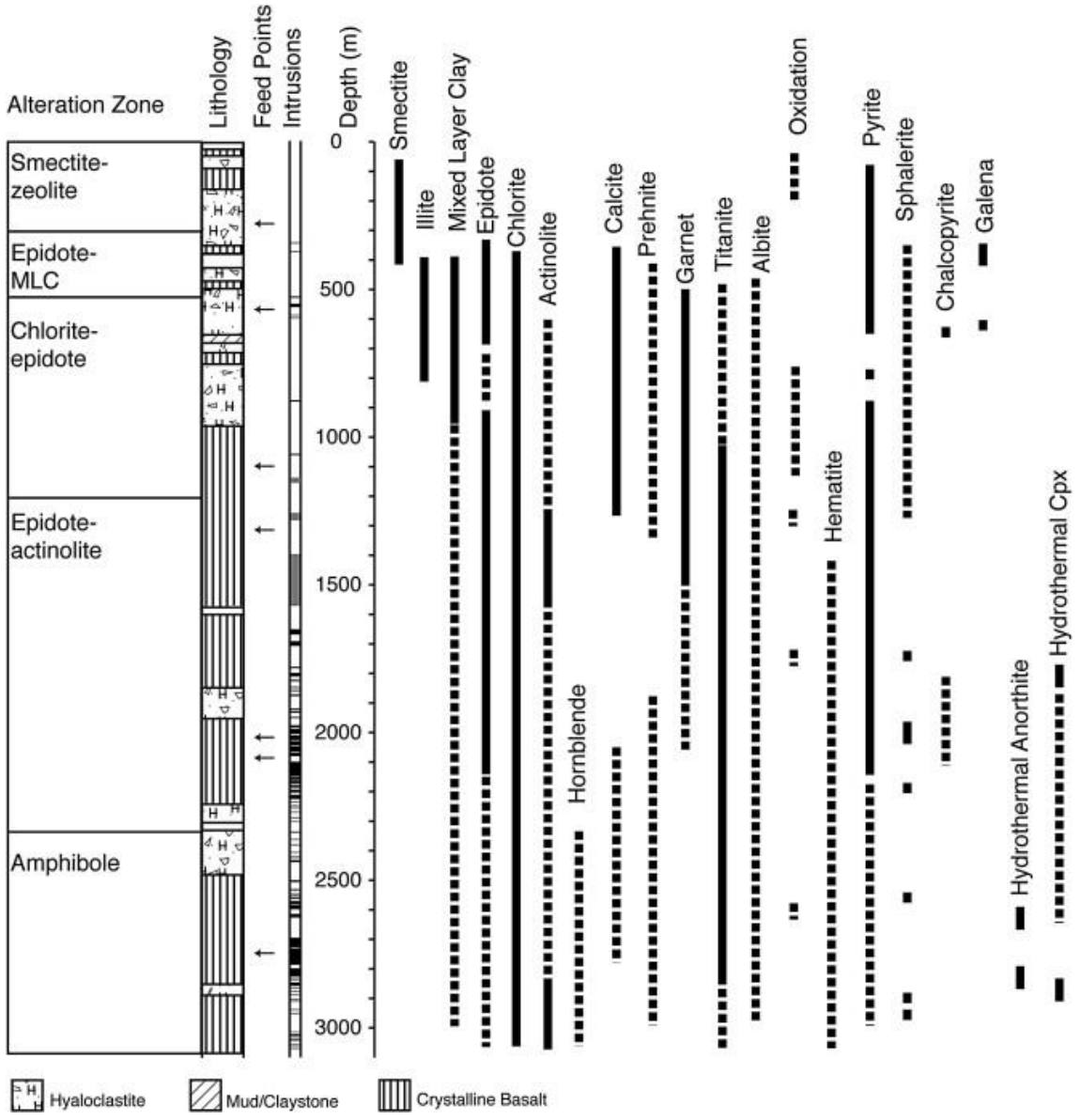

Figure 3.4. Lithostratigraphy, alteration zones, and distribution of secondary minerals (below the smectite zone) with depth in RN-17. Feed points are inferred from loss of circulation and temperature logs, all are considered to be minor (Marks et al., 2010).

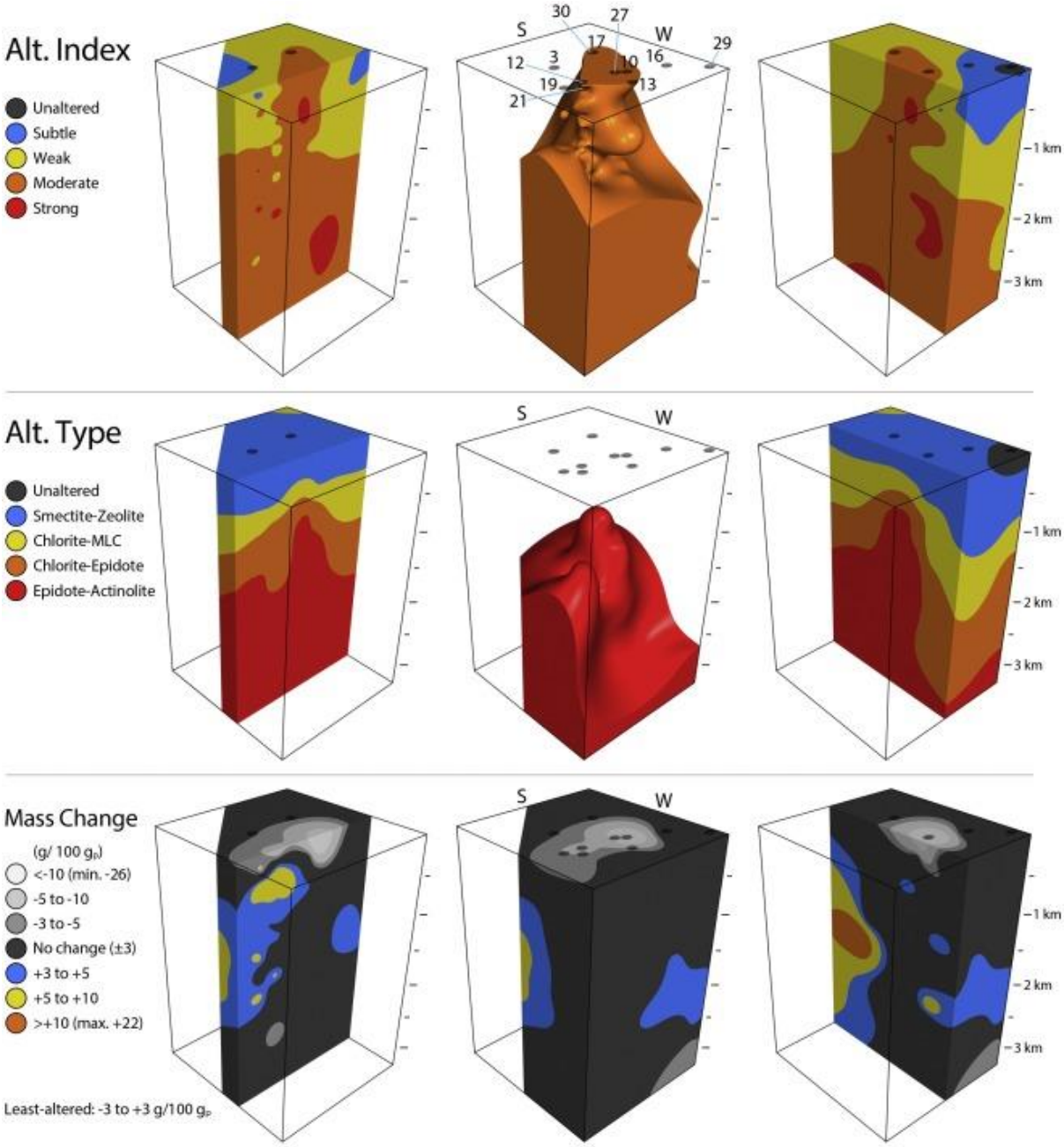

Figure 3.5. Alteration index and type, and calculated elemental mass changes for the Reykjanes geothermal system (Libbey and Williams-Jones, 2016a).

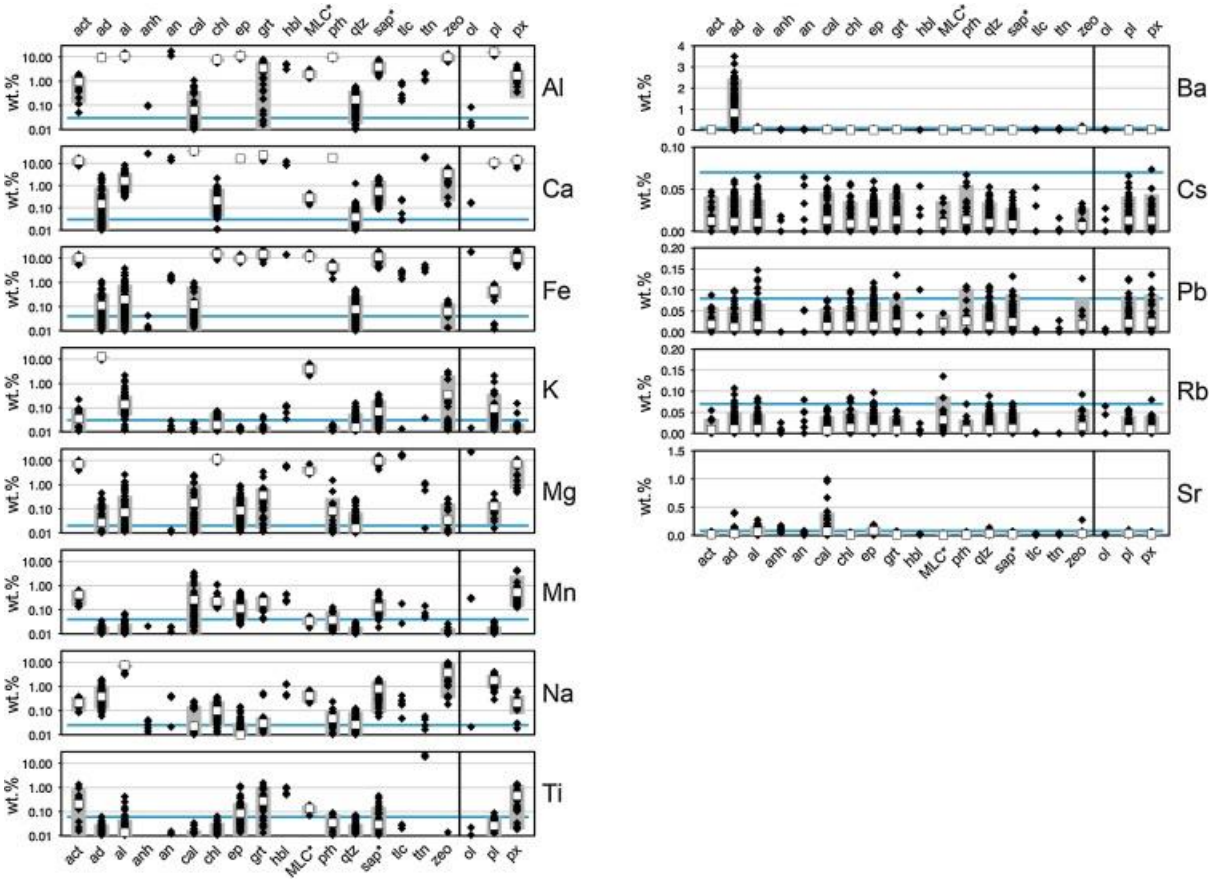

Figure 3.6. Major and trace element concentration in altered rocks in Reykjanes (Libbey and Williams-Jones, 2016b).

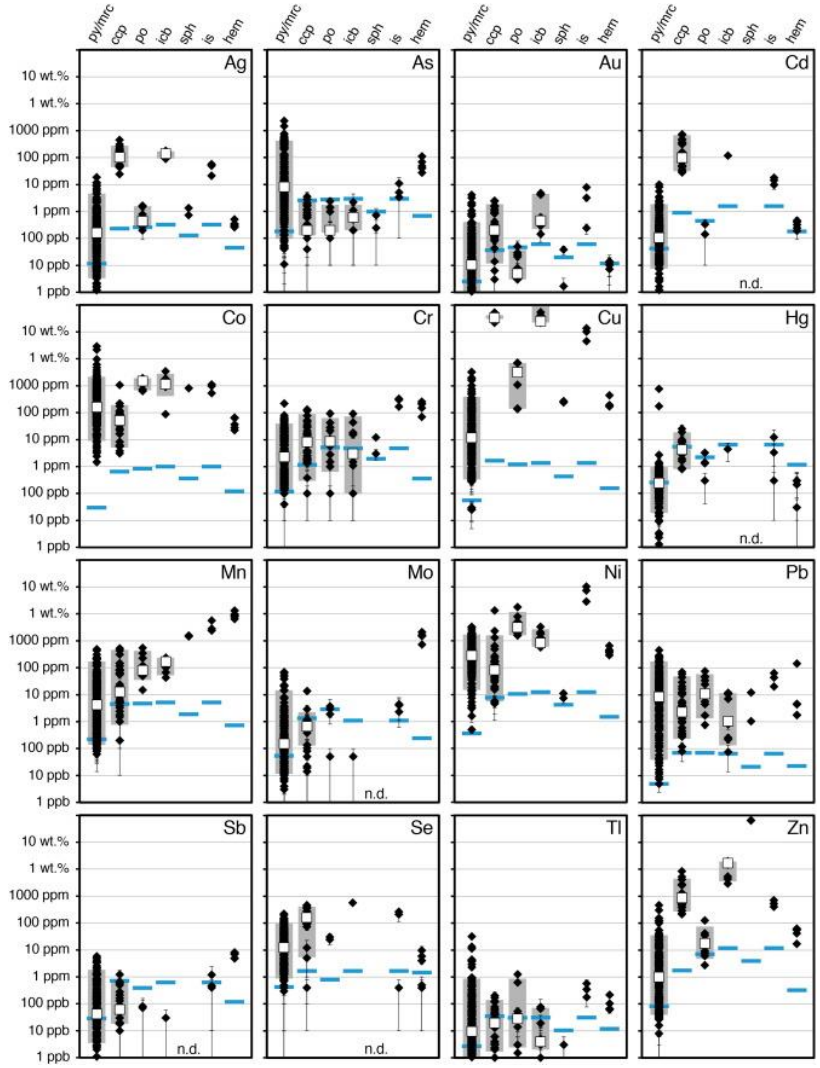

Figure 3.7. Trace element concentrations in sulfide minerals and hematite in the Reykjanes geothermal system (after Libbey et al., 2016b)

3.1.4 Scales

Geothermal mineral deposits (scales) are common in pipelines at Reykjanes. In particular, sulfide and silica scales are common. These mineral scales have formed under a range of conditions from high pressures and temperatures at depth (>2 km) to being associated with boiling, and pressure decreases in surface pipelines. Many of these scales are enriched in trace elements, including; Cu, Zn, Cd, Co, Te, V, Ni, Mo, W, Sn, Fe and S in higher pressure and temperature scales, and Zn, Cu, Bi, Pb, Ag, As, Sb, Ga, Hg, Tl, U and Th in lower temperature and pressure scales at the surface. A number of elements (e.g. Co, Se, Cd, Zn, Cu, and Au) are deposited at both high- and low-pressure scales. Boiling and destabilization of metal-bearing aqueous complexes are the dominant control on the deposition of most metals (particularly Au). Other metals (e.g. Cu and Se) may also have been transported in the vapor phase. Very large enrichments of Au, Ag and Pb in the scales (e.g. 948 ppm Au, 23,200 ppm Ag, and 18.8 wt.% Pb) have been noted in some cases (e.g. Grant et al., 2020; Hardardóttir et al., 2010).

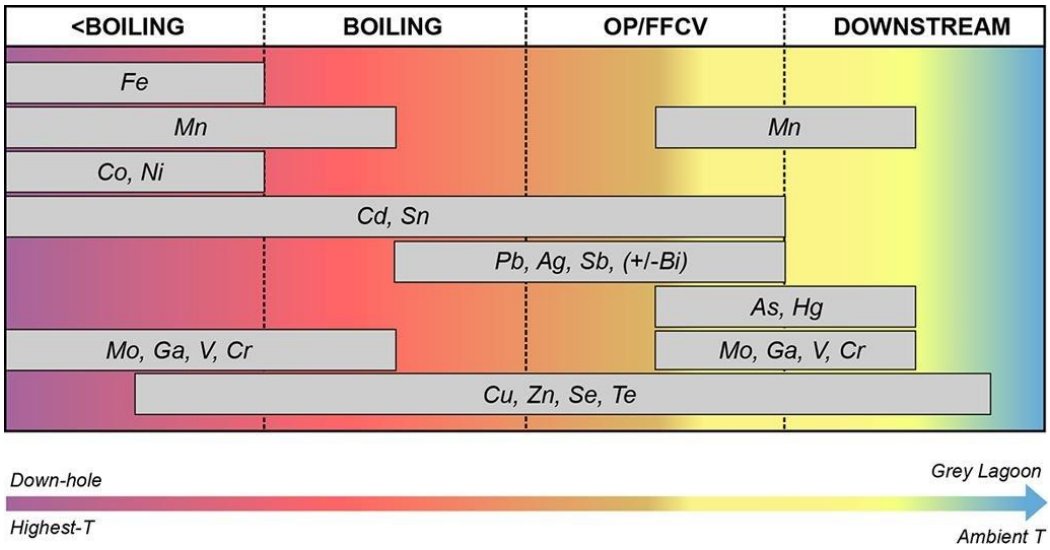

Figure 3.8. Conditions of various mineral scale formations at Reykjanes (after Grant et al., 2020)

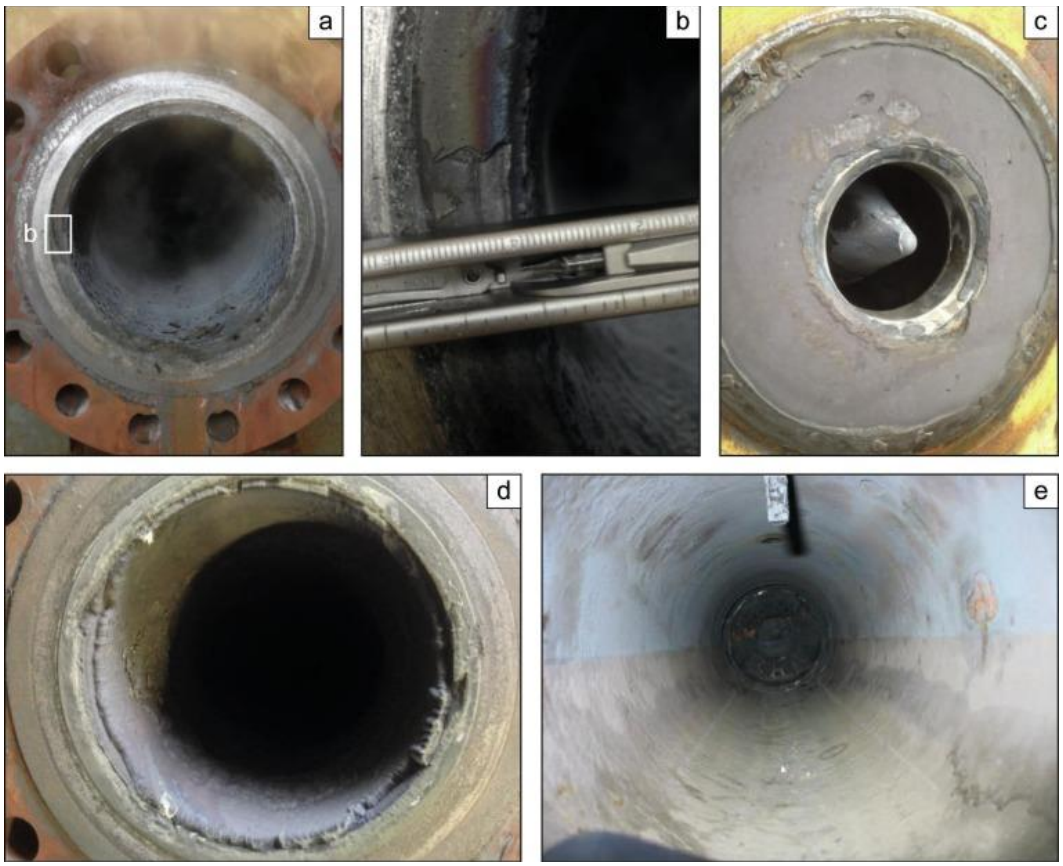

Figure 3.9. Photographs of scales in surface geothermal well pipes. A) Looking upstream in high-pressure well RN-11. Blue Cu-(Fe)-sulfide scales < 0.5 cm in thickness are predominant in the base of the pipe. B) Close-up image of scale on the upstream side of the OP in high-pressure well RN-11. The scale thickness is ~0.5 cm. C) Scales on the downstream side of the OP and FFCV in low-pressure well RN-13B. Grey scales on the OP are dominantly sphalerite scales, and scales on the FFCV have a slight blue tint indicating more Cu-(Fe)-sulfides than on the OP. The scale thickness is < 0.5 cm. D) Looking downstream in high-pressure well RN-14. Blue Cu-(Fe)-sulfides are dominant. The scale thickness at the base of the pipe is approximately 2 cm. E) Looking upstream from the orifice plate towards the wellhead in high-pressure well RN-22. There is a thin coat of blue (Cu-Fe-sulfide) lining the pipe where steam would have been dominant, and gray where liquid was dominant (from Hardardóttir, 2010).

3.1.5 Geothermal exploration and exploitation

Exploration of the Reykjanes geothermal filed started in 1956 when the first well was drilled. The field was investigated extensively in the years 1968-1970 when additional 7 exploration wells were drilled. Drilling for power production commenced in 1998. Currently, 34 wells have been drilled, and 18 of them are contributing to steam provision with an average temperature of 290 °C down the wells. The single-flash condensing-type geothermal power plant was commissioned in 2006 with a total capacity of 100 MW and with approximately 96 MW net electrical output to the grid (Figure 3.10). Design of the power plant has two major unique features; one is having one of the highest turbine inlet steam pressure in the world (18 bar) in order to impede silica scaling in exposed components. Another specific feature of the plant is the use seawater for cooling, excluding cooling towers. The Reykjanes power plant is run by HS Orka, hf. This is a privately-owned company who has developed geothermal and other renewable energy applications since 1975.

Figure 3.10. Reykjanes geothermal powerplant (source: https://icelandmag.is/article/radioactive-waste-discovered-a-reykjanes-peninsula-geothermal-power-plant).

3.1.6 Summary and conclusions

The Reykjanes geothermal system is a basalt-hosted, seawater-dominated active geothermal system located on the southwestern tip of the Reykjanes Peninsula, SW Iceland. The average reservoir temperature is approximately 300 °C and hosts a 100 MW geothermal power plant.

The geothermal alteration shows depth zone distribution; a prograde geothermal alteration assemblage with mixed layered clays and chlorite at the top, followed by zones mainly of chlorite, quartz, epidote and anhydrite and appearance of amphiboles at greater depths.

The hydrothermal fluids represent modified seawater with addition of meteoric water. The major element composition is controlled by mineral-fluid equilibria. The reservoir hydrothermal fluids are enriched in many trace metals and metaloids that are often deposited in boreholes and pipelines upon

depressurisation and boiling to form metal-enriched scales containing high concentrations of for example Pb, Zn, Cu, Ag and Au.

3.1.7 References

ARNÓRSSON, S. 1978. Major element chemistry of the geothermal sea-water at Reykjanes and Svartsengi, Iceland. Mineral. Mag., 42, 209-220.

BALI, E., et a. (2020) Geothermal energy and ore-forming potential of 600°C mid-ocean-ridge hydrothermal fluids. geology, 48, 1221–1225.

BJÖRNSSON, S., ARNÓRSSON, S., TÓMASSON, J. 1970. Exploration of the Reykjanes thermal brine area. Geothermics, 56, 2380-2391.

FRANZSON, H., THORDARSON, S., BJÖRNSSON, G., GUDLAUGSSON, S., RICHTER, B., FRIDLEIFSSON, G., THORHALLSSON, S. 2002. Reykjanes high-temperature field SW-Iceland. Geology and hydrothermal alteration of well rn-10. 27th Stanford Workshop on Geothermal Reservoir Engineering, pp. 233-240.

FRIÐDRIKOSSON, TH., KRISTJÁNSSON, B.R., ÁRMANNSSON, H., MARGRÉTARDÓTTIR, E., ÓLAFSDÓTTIR, S., CHIODINI, G. 2006. CO2 emissions and heat flow through soil, fumaroles, and steam heated mud pools at the Reykjanes geothermal area, SW Iceland Appl. Geochem., 21, 1551-1569.

FRIDLEIFSSON, G.O., et al. (2020) The Iceland Deep Drilling Project at Reykjanes: Drilling into the root zone of a black smoker analog. J. Volcanol. Geotherm. Res. 391, 106435.

FRIDLEIFSSON, G.Ó., SIGURDSSON, Ó., THORBJÖRNSSON, D., KARLSDÓTTIR, R., GÍSLASON, TH., ALBERTSSON, A., ELDERS, W.A. 2014. Preparation for drilling well iddp-2 at Reykjanes. Geothermics, 49, 119-126.

FRIDRIKSSON, TH., STEFÁNSSON, A., ÓSKARSSON, F., EYJÓLFSDÓTTIR, E., SIGURDSSON, Ó. 2015. fluid chemistry scenarios anticipated for iddp-2 to be drilled in Reykjanes, Iceland.Proc. World Geothermal Congress, Melbourne, Australia, 19–25 April 2015, p. 8.

GRANT, H.L.J., HANNINGTON, M.D., HARDARDÓTTIR, V., FUCHSA, S.H., SCHUMANN, D. 2020. Trace metal distributions in sulfide scales of the seawater-dominated Reykjanes geothermal system: Constraints on sub-seafloor hydrothermal mineralizing processes and metal fluxes. Ore Geology Reviews 116, 103145.

GUDMUNDSSON, A. 1995. Dynamics of volcanic systems in Iceland: example of tectonism and volcanism at juxtaposed hot spot and mid-ocean ridge systems. Annu. Rev. Earth Planet. Sci., 28, 1-22.

HALLDÓRSSON, S.A. et al. 2022. Rapid shifting of a deep magmatic source at Fagradalsfjall volcano, Iceland. nature 609, 529-534.

HARDARDÓTTIR, V., BROWN, K.L., FRIDRIKSSON, TH., HEDENQUIST, J.W., HANNINGTON, M.D., THORHALLSSON, S. 2009. Metals in deep liquid of the Reykjanes geothermal system, southwest Iceland: implications for the composition of seafloor black smoker fluids. Geology, 37, 1103-1106

HARDARDÓTTIR, V., HANNINGTON, M., HEDENQUIST, J., KJARSGARRD, I., HOAL, K. 2010. Cu-rich scales in the Reykjanes geothermal system, Iceland. Econ. Geol., 105, 1143-1155.

KAASALAINEN, H., STEFÁNSSON, A., GIROUD, N., ARNÓRSSON, S. 2015. The geochemistry of trace elements in geothermal fluids, Iceland. Appl. Geochem., 62, 207-223.

KADKO, D., GRONVOLD, K., BUTTERFIELD, D. 2007. Application of radium isotopes to determine crustal residence times of hydrothermal fluids from two sites on the Reykjanes Peninsula, Iceland. Geochim. Cosmochim. Acta, 71, 6019-6029.

LIBBEY, R.B., WILLIAMS-JONES, A.E. (2016A) Lithogeochemical approaches in geothermal system characterization: An application to the Reykjanes geothermal field, Iceland. Geothermics, 64, 61-80.

LIBBEY, R.B., WILLIAMS-JONES, A.E. (2016B) Compositions of hydrothermal silicates and carbonates as indicators of physicochemical conditions in the Reykjanes geothermal system, Iceland. Geothermics 64, 15-27.

MARKS, N., SCHIFFMAN, P., ZIERENBERG, R.A., FRANZSON, H., FRIDLEIFSSON, G.Ó. 2010. Hydrothermal alteration in the Reykjanes geothermal system: Insights from Iceland deep drilling program well RN-17. J. Volcanol. Geoth. Res., 189, 172-190.

POPE, E.C., BIRD, D.K., ARNÓRSSON, S., FRIDRIKSSON, T., ELDERS, W.A., FRIDLEIFSSON, G.Ó. 2009. Isotopic constraints on ice age fluids in active geothermal systems: Reykjanes, Iceland. Geochim. Cosmochim. Acta, 73, 4468-4488.

SÆMUNDSSON K., SIGURGEIRSSON, M.Á., FIRDLEIFSSON, G.Ó. 2020. Geology and structure of the Reykjanes volcanic system, Iceland. j. volcanol. geotherm. res. 391, 106501.

SIGURDSSON, F. 1985. Jarðvatn og vatnajarðfræði á utanverðum Reykjanesskaga. Orkustofnun. (Nationa Energy Authority) Report os-85075/vod-06.

SIGURDSSON, O. 2010. The Reykjanes seawater geothermal system—Its exploitation under regulatory constraints. Proceedings of the World Geothermal Congress, Bali, Indonesia, p. 7.

STEFÁNSSON, A., ARNÓRSSON, S. 2002. Gas pressures and redox reactions in geothermal systems in Iceland. Chemical Geology 190, 251-271.

THORDARSON, T, LARSEN, G. 2007. Volcanism in Iceland in historical time: volcano types, eruption styles and eruptive history. J. Geodyn., 43, 118-152.

TÓMASSON, J., KRISTMANNSDÓTTIR, H. 1971. High temperature alteration minerals and thermal brines, reykjanes, iceland. contr. mineral. petrol., 36, 123-137.

ZIERENBERG, R.A., FIRDLEIFSSON, G.O., ELDERS, W.A., SCHIFFMAN, P., FOWLER, A.P.G. (2021) Active Basalt Alteration at Supercritical Conditions in a Seawater-Recharged Hydrothermal System: IDDP-2 Drill Hole, Reykjanes, Iceland. Geochemistry, Geophysics, Geosystems, 22, e2021GC009747.

3.2 TUZLA GEOTHERMAL FIELD

Tuzla geothermal field (TGF) is one of the most important geothermal fields in Türkiye in terms of temperature. Numerous studies have been carried out to determine the geology of the region and to determine the characteristics of the geothermal system. Geothermal wells have been drilled in this power plant by private companies and the government. In the geothermal wells, temperatures are approximately 174 °C at the well-bottom and 166 °C at the wellhead. There are two reservoirs in the TGF. The first of these reservoirs is hosted by volcanic rocks, and the second by metamorphic rocks, which are basement rocks. There are also radionuclide-rich granite rocks that cut the basement rocks. The TGF is currently recharged from the first reservoir. Many Magneto Telluric (MT) studies were carried out by private companies in the TGF in 2006, and the tectonic features of the field were examined in detail. The Tuzla geothermal field represents an active geothermal regime. The shallow geothermal system associated with hydrothermal activity following Miocene magmatism/volcanism was formed by the overlapping of a deeply recharged geothermal system that emerged with the development of the Tuzla fault. Therefore, the geothermal system resulted in the development of reservoirs at two different depths and characteristics. Accordingly, the Tuzla Geothermal Field is a hybrid geothermal field formed by overlying a magmatic-controlled geothermal system with a normal fault-controlled active geothermal system.

Tuzla is the most complex geothermal field in northwestern Türkiye, some 80 km south of the city of Çanakkale and 5 km from the Aegean Coast (Figure 3.11). In the TGF there are currently 4 geothermal wells (3 production wells, 1 reinjection well) with depths varying between 539 and 871 m.

Figure 3.11: Power plant at the Tuzla geothermal field.

3.2.1 Geological background of Tuzla Geothermal field

The geothermal field is observed at surface through elevated soil temperatures, whereas the reservoir temperature is approximately 300°C in feed zones, mainly at depth of 1700-2200 m (Sæmundsson et al., 2020).

Tuzla geothermal field and its surroundings, located in the north of Türkiye, have been the subject of various geological research before, due to both being in an active fault zone and being one of the most important geothermal fields in Türkiye (Ercan and Türkecan, 1985; Karamanderesi, 1986; Mützenberg, 1990; Şamilgil, 1983; Şener and Gevrek, 2000). Paleozoic-aged metamorphic rocks form the basement of the Tuzla field, and mainly consist of quartzite, calcschist, chlorite, biotite, muscovite schist, and marbles. Metamorphic rocks consist of different types of rocks according to the chemistry, type, environment, and facies of the primary rock and the degree of metamorphism they have undergone. Marbles, which are

accepted as the most important lithological unit forming the second reservoir in the TGF, are exposed over a very wide area. A simplified geological map of the study area is given in Figure 3.12.

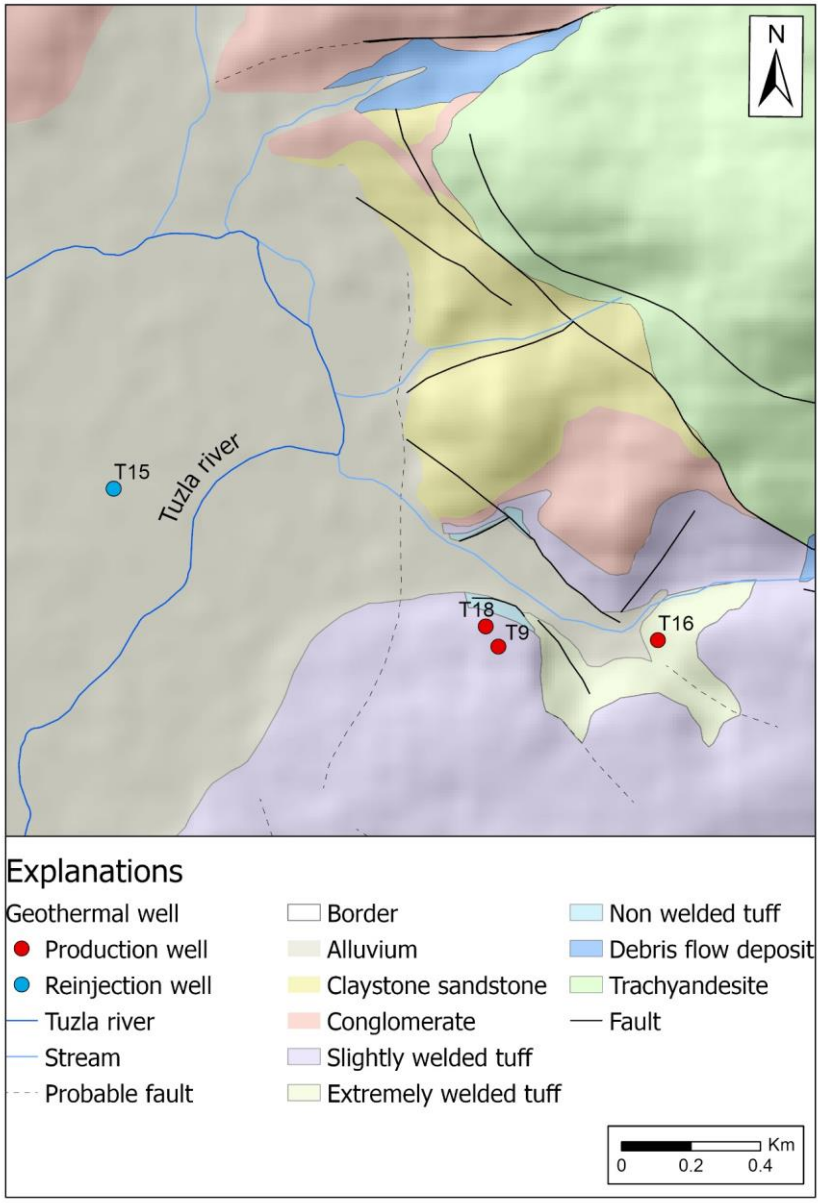

Figure 3.12: Geological map of the Tuzla geothermal field.

The thickness of the marble in the field is about 200 m (Şimşek et al., 2005). The marbles in the schists are seen as a single thick level. Thick marble levels are generally white and coarsely crystalline. Volcanic rocks are generally composed of latite type lava, rhyolitic tuff and agglomerates, and ignimbrites, together with effective volcanism. Various types of lava (andesite, dacite, etc.) were also observed in the geothermal field. Volcanism was active throughout the entire Miocene time. The ignimbrites formed in the last stage of the volcanism in the region are covered by sediments of Upper Miocene-Pliocene age, consisting of conglomerate, sandstone, limestone, and clayey limestone alternations. The Quaternary-aged alluvium, located at the top of the stratigraphic section, formed the Tuzla plain. Tuzla Plain consists of alluvial permeable units consisting of gravel, sand, and clay with a thickness of up to 100 m from the edge of the Tuzla Stream valley to the middle and contains groundwater. Tuzla geothermal water represents the active thermal regime and is a region associated with hydrothermal activity following Miocene volcanism (Şener and Gevrek, 2000). Volcanic rocks form the reservoir of the geothermal fluid. Miocene-aged volcanic rocks in the study area were affected by faults in the NW-SE direction. Around these faults, which

provide the formation of hot water springs, silicic and argillic alteration are clearly observed. Currently, the active thermal regime in TGF is associated with volcanism. Major geological structures in the study area are controlled by N-S and NW-SE trending faults. N-S directional fault systems are located at the boundary of Neogene sediments and Quaternary alluvium. Neogene sandstone and claystone are cap rocks of the system. There are many springs along N-S directional fault systems. The 3D conceptual model of the TGF is given in Figure 3.13. While creating the conceptual model, borehole logs of all 4 wells in the field were used to obtain a more accurate model. The model was obtained using licensed Leapfrog Geothermal software.

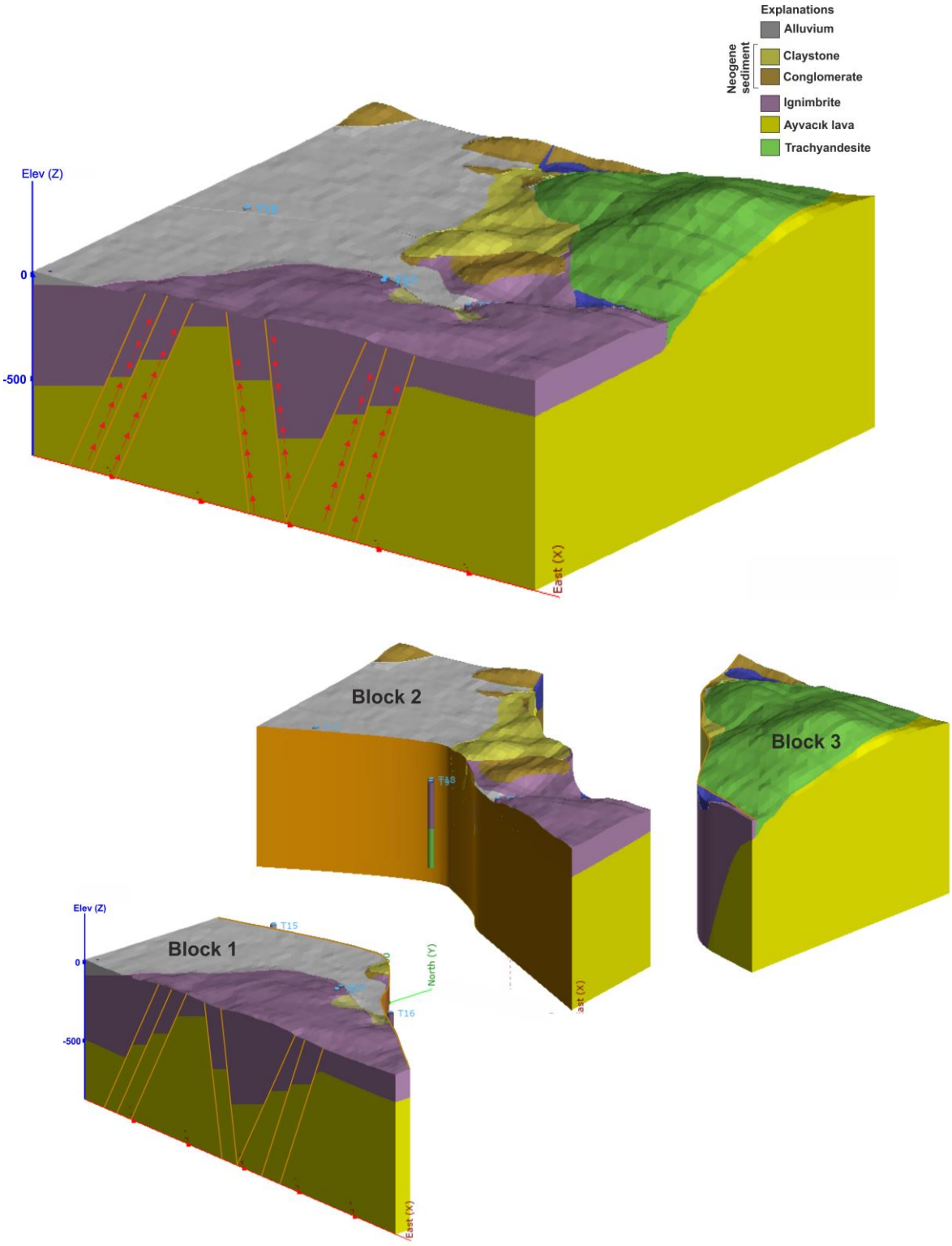

Figure 3.13: 3D conceptual model of the Tuzla geothermal field.

3.2.2 Geothermal exploration and exploitation

Geothermal study of the Tuzla field began some 20 years ago by a geological and volcanological survey (Alpan 1975; Şamilgil 1966; Erdoğan 1966; Ürgun 1971; Öngür 1973). These were followed by a geophysical survey (Demirörer 1971; Ekingen 1972). Based on this survey about 10 thermal gradient wells were drilled to 50 - 100 m depth in 1974. High temperatures (145 °C) were met at about 50 m depth in some of these wells, and due to vigorous boiling within the wells two of them were lost in blowouts (Karamanderesi and Öngür 1974). The result of these studies gave reason for the drilling of deep exploration wells. Two deep wells were drilled in the field in 1982 and 1983, T-1 to 814 m depth and T-2 to 1020 m depth. Circulation losses were experienced in both wells, and the highest temperature measured was 173 °C. Since then, a detailed study of the surface alteration has been published (Gevrek and Şener 1985) showing three surface alteration zones to be present, silica zone, a montmorillonite zone, and illite zone. A detailed investigation of the hydrothermal alteration of well T-2 is presented in section 3.3.1.

Tuzla geothermal system is divided into two; deep and shallow reservoirs. The shallow reservoir can rise to the surface with the help of faults, especially within the thick volcanic cover in the region. This system can be easily seen in the geothermal field and hot water outlets in the Tuzla region (Figure 3.14). The hot water springs exit at more than 50 points and show a temperature change between 30-102 °C (Erişen et al., 1996). In shallow drillings, temperatures were recorded up to 174 °C, and an artesian flow of 30-90 l/s was found. In addition, it is known that recrystallized limestone was encountered under the volcanic cover in deep geothermal wells. Conceptually, the hot fluid of the Tuzla fault system is thought to have dispersed convectively into permeable carbonate levels at depth. Therefore, the deep geothermal reservoir in the region is probably recharged from the Tuzla fault system and spreads convectively within the carbonate system, and gains the feature of a deep geothermal reservoir. Temperatures were recorded in this reservoir as 130-135 °C, and an artesian flow of 40 l/s was found.

Reservoir 1 (Shallow reservoir):

Hosted by fractured structures developed in latitic andesite, trachyte, and trachyandesites within Miocene volcanic (Şamilgil, 1983; Şimşek, 2008, 2009).

Reservoir 2 (Deep reservoir):

Hosted by metamorphic units consisting of marble, calcschist, and quartzite. Terrestrial-lacustrine sedimentary rocks and Pliocene-PlioQuaternary units outcropping in the Tuzla geothermal field form the cover rock.

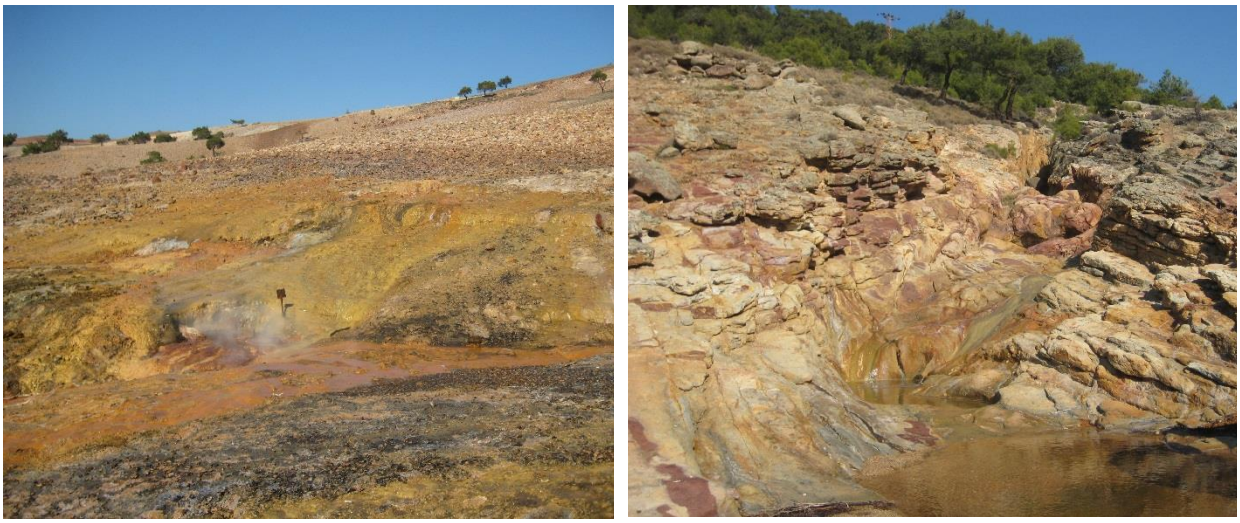

Figure 3.14: Geothermal outflows in the Tuzla geothermal field.

3.2.3 Mineralization and alteration

A comprehensive study of cross-cutting vein relationships and mineralogical evolution suggests at least two hydrothermal events in the TGF. The first hydrothermal event, involved high temperature conditions, resulting in contact metamorphic calc-silicate mineralization, including garnet, epidote, chlorite, sphene, magnetite, actinolite, diopsite and prehnite. The second hydrothermal event, which relates to the present-day hydrothermal system is evidenced by smectite, mixed layer clay, kaolinite, mica, pyrite, haematite, quartz, calcite, barite and gypsum.

In the lower part of the well, calcite-quartz veins are found in the granodiorite and monzonite intrusions, while clear cross-cutting evidence was not found between these and the high- temperature calc-silicate minerals. The high temperature calc-silicate mineralization, however, is lacking in well T-1, as are intrusive rocks, which is then taken to imply that the calc-silicate mineralization in T-2 is related to an episode of contact metamorphism (Figure 3.15). Therefore, two hydrothermal mineralizing periods are realized from the lower part of well T-2; that of early contact metamorphism (garnet, magnetite and diopside) and associated high-temperature hydrothermal system (chlorite, epidote, sphene, actinolite), followed by the superimposition of the present-day calcite-quartz-clay mineralization. Evidence of a high-temperature hydrothermal system established by the granodiorite and monzonite intrusive activity is therefore not found in the overlying subaerial volcanics. This implies that the high-temperature hydrothermal activity of late Tertiary age pre-dates the volcanic extrusive rocks, which confirms the chronological order of volcanic rocks gathered from outside the Tuzla field. Evidently, this rules out the other possibility of a contemporaneous origin of the intrusive and extrusive rocks in the Tuzla field (after Karamanderesi, 1986).

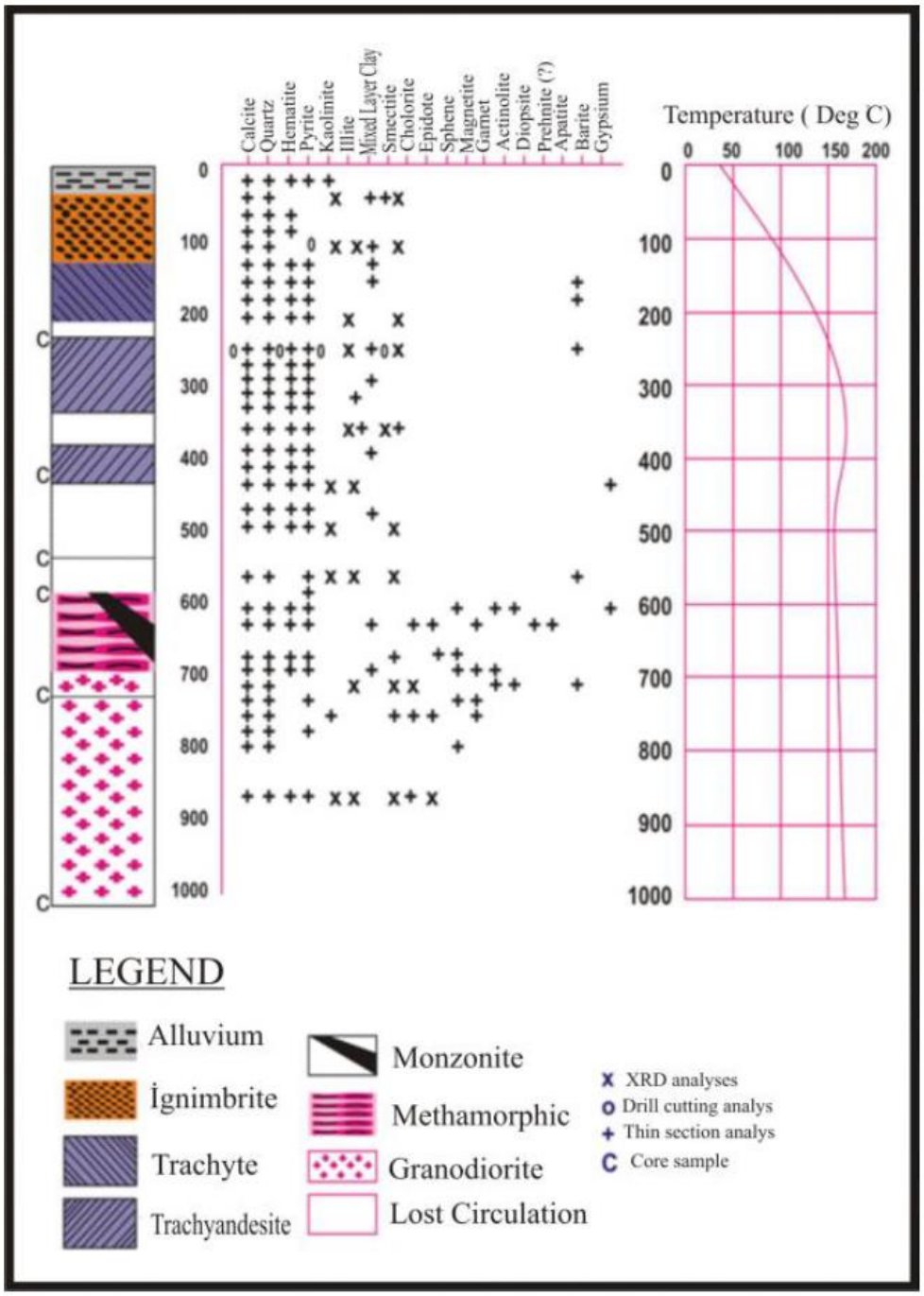

Figure 3.15: T-2 (not active) well; distribution of minerals, temperature and mineralization zones (after Karamanderesi, 1986).

3.2.4 Fluids and dissolved resources

3.2.4.1 Water Chemistry of the Tuzla Geothermal Fluids

TGF is an interesting area in Türkiye from the point of its temperature and dissolved ions in the water. At the surface, the waters reach temperatures of 32-86 °C. The chloride concentration of Tuzla geothermal brine reaches 38 g/L, which is nearly twice the concentration of seawater, and is termed “brine” water. On the other hand, the sodium concentrations reach up to 19 g/L The total outflow of water from approximately 100 springs in the TGF field is estimated to be close to 50 L/s. In geothermal waters from the TGF, the average pH and EC values range from 5.6 to 7.65 and from 83.2 to 86.2 mS/cm, respectively

(Figures 3.16 and 3.17). The pH in the system is changing continuously. The water from the wells is acidic due to an excess of free CO_2 (free mineral acidity) which is the result of the high partial pressure of this gas in the well. The temperature of geothermal fluid in well T9, T16 and T18 in Tuzla geothermal site is 164 °C, 166 °C and 169 °C respectively. In the TGF, Na^+ and Cl^- are the dominant ions in the geothermal brine. NaCl water composition indicates a marine origin and also water-rock interactions. That said, continuous water rock interactions are the primary reason for the high salt content in the geothermal waters. The fact that the geothermal waters in the TGF are NaCl type is an indicator of hydrothermal activity. Active seismicity and hydrothermal activity in the region facilitate the upflow of geothermal fluid from depth. The rising geothermal water cools to some extent and is diluted by mixing with groundwater. The emergence of geothermal brine can be as a result of extensional tectonic regime where lithosphere is thinner and uplift occurs due to isostasy (Keisuke, 1978). Active seismicity in the region makes it easier for bine to ascend from depth. The ascending brine is to some extent cooled and diluted by mixing with groundwater. The outflowing of NaCl-rich thermal brine indicates the presence of hydrothermal activity (Mützenberg, 1997; Baba et al., 2009).

The range of concentrations of minor components the geothermal waters are: B = 24.4 to 26.3 ppm; Al = 4.61 to 4.78 ppm; Li = 20.8 to 22.6; Fe = 5.49 to 6.48; Mn = 3.84 to 4.73; and Ba = 6.21 to 6.82 ppm (Fig. 3.18). The concentrations of other elements are notably lower: Co = 31-59 ppb; Ni = 12-28; Pb = 10-100; and Cu = 20-29 ppb. The highest Pb values are in well T15 and T18 (Fig. 3.19). Sr concentrations in geothermal fluids range from 132 to 143 ppm. High Sr concentrations in the geothermal waters are associated with volcanic rocks (Fig. 3.20).

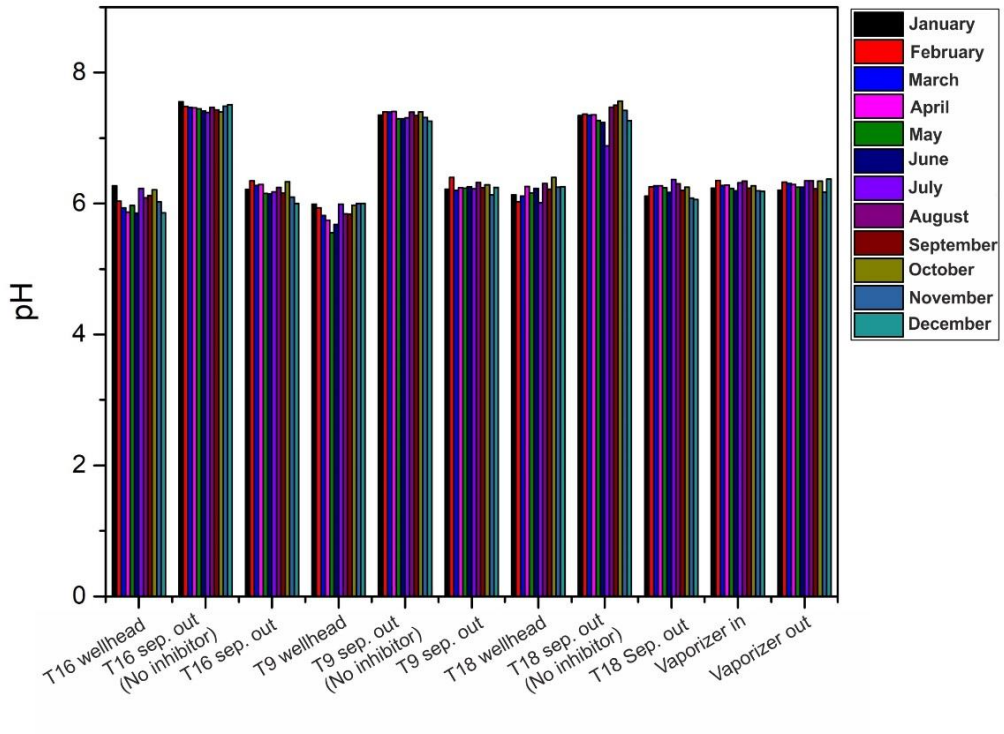

Figure 3.16: pH change in the TGF over a one-year period.

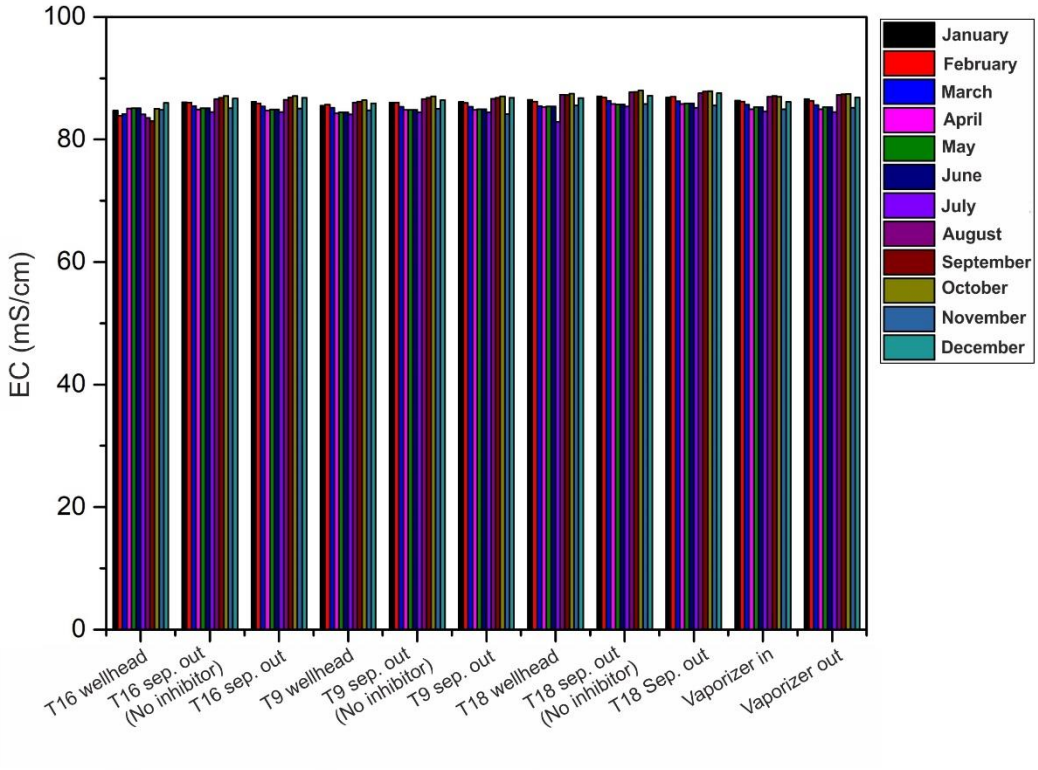

Figure 3.17: Electric conductivity (EC) change in the TGF over a one-year period.

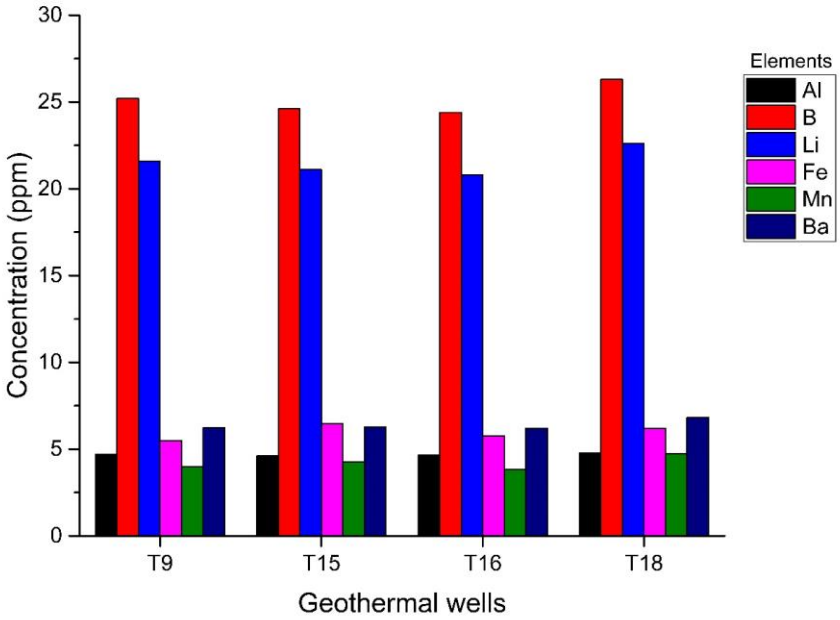

Figure 3.18: Metal concentrations in the geothermal wells (in ppm).

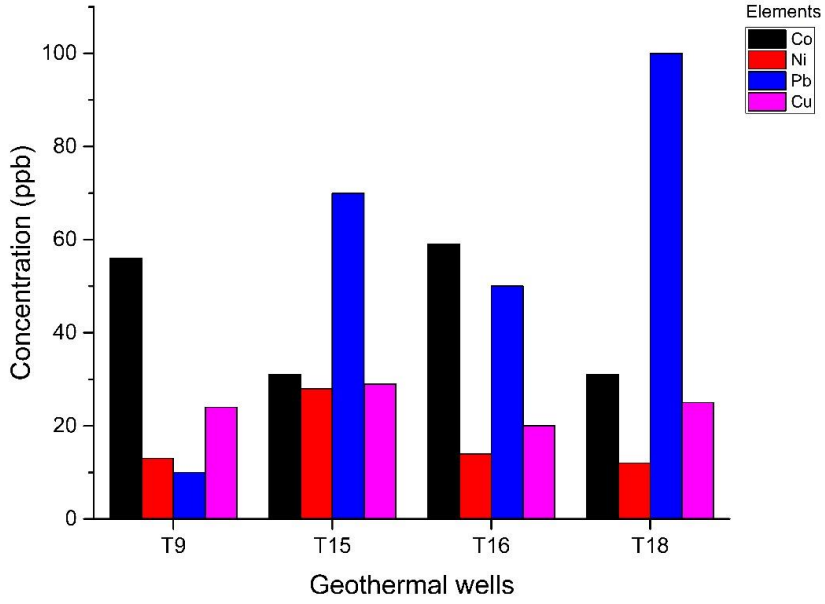

Figure 3.19: Trace metal concentrations in the geothermal wells (in ppb).

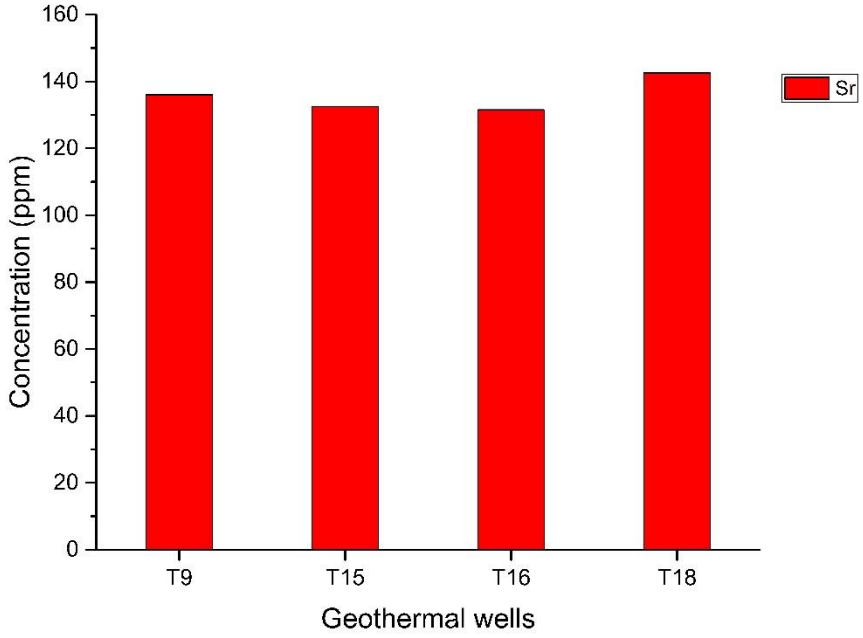

Figure 3.20: Sr concentrations in the geothermal wells (in ppm)

3.2.4.2 Scale Properties of the TGF

The TGF is hosted by rhyolite lavas and pyro-clastic deposits. Base zone consists of calcschist, quartzite and marble, which are metamorphic rocks that include quartz, orthoclase, albite and mica minerals. The metamorphic rocks are covered by andesitic volcanic rocks; trachyandesite, trachyte and rhyodacitic ignimbrite. These rocks, especially trachyandesite, include quartz, calcite minerals that are highly altered

and covered by sediments and alluvium (Demir et al., 2014; Baba et al., 2008, 2009). The currently active thermal regime in Tuzla is associated with volcanism.

The geothermal fluid undergoes physical and chemical changes during operation, causing scale problems that reduce powerplant efficiency. Depending on the temperature and pressure changes in the reservoir, the geothermal fluid whose physical and chemical properties change causes scaling problems in wells, pipelines, and surface equipment. Deposition of silicate scaling is the main handicap in Tuzla geothermal systems (Figure 3.21). This problem reduces the efficiency of the geothermal power plant and causes economic losses. Scaling caused by the geothermal fluid was discovered immediately after the start of operation. The type scaling is special and has not been encountered at other geothermal systems in Türkiye.

Although silicate-based scaling is main problem, PbS (Galena) and $CaCO_3$ (Calcite) were detected in the downhole and the surface pipelines (Figure 3.21).

Figure 3.21: Scale formation in the borehole system of the TGF.

3.2.4.3 Sources of dissolved elements

The TGF is called hyper-saline geothermal system due to high ion concentration, which occurs by the interaction between water and volcanic rocks in TGF. The electrical conductivity (EC) value of Tuzla fluid reaches 97.2 mS/cm. Also, the chloride concentration reaches 38,000 ppm in the fluid, and the sodium concentrations of the geothermal fluid can reach up to 19,000 ppm. The temperatures of the geothermal fluids range from 32-86 °C at the surface, while the reservoir temperatures range from 145-200 °C. Therefore, the TGF is significantly remarkable due to its temperature and dissolved ion concentrations in the aqueous solution.

Geothermal studies on the TGF have been ongoing since 1966. The general geological and volcanological characteristics have been studied by Samilgil (1966), Erdogan (unpublished data, 1966 *MTA Report* [Geothermal energy possibility of survey and tectonic mapping of Tuzla hot springs and surrounding]), Ürgun (1971), Öngür (unpublished data, 1973 *MTA Report* [Volcanology and geological report of Canakkale Tuzla geothermal area, Ankara]), and Alpan (1975). Geophysical surveys were carried out by Demirörer (unpublished data, 1971 *MTA Report* [Resistivity survey of Tuzla-Kestanbol hot springs and surrounding]) and Ekingen (1972). Hydrogeological characteristics of the geothermal waters in the TGF were studied by some researchers (Baba et al., 2005; 2008; 2009).

As mentioned in previous section, the TGF is located near recent volcanic activity areas. The slightly acidic NaCl Tuzla brine flows out of places where the permeability is high (i.e. fault and fracture zones). Eventually, the geothermal brine diffuses into shallower aquifers, which change its fluid chemistry. The high concentrations of Mg and Fe are attributed to the dissolution of ferromagnesium minerals within

Miocene volcanic rocks which consist of trachyte, andesite, and trachyte andesite in the TGF (Demir et al., 2014). Highly altered, these rocks include quartz, K-feldspar, biotite, amphibole, sanidine, chalcopyrite, pyrite and hematite (Karamanderesi and Öngür, 1974). The high trace metal content in the hot-saline waters of the TGF results from rapid evolution of anoxic conditions in brines (Drever, 1997) and reduction of the sulphite (SO_3) formed by reactions with trace elements. B and Sr concentrations in geothermal fluids are extremely high in the TGF. This is related to volcanic rocks, but may also be controlled by the degassing of magma bodies. Of these trace metals, Zn and Pb are known to build stable chloride complexes at high temperatures (White, 1968). Also, Tuzla brine includes silica (SiO_2) (189–225 ppm). Quartz is soluble in the brine in the reservoir under high pressure and high temperature (Newton and Manning, 2000). The lithium concentrations of the geothermal waters in the TGF can reach up to 22 ppm, and are attributed to manganese oxide and aluminum hydroxide in the volcanic reservoir system (Demir et al., 2014).

3.2.5 Conclusions

Geothermal fluids often contain high concentrations of dissolved metals and a mixture of gasses, some of which are of commercial interest. Some elements, such as Li, are already known to occur in economically-relevant concentration in geothermal fluids and extraction efforts are underway. Although other elements also occur in relevant concentrations in geothermal fluids (brine and gas phase) or in precipitates (solid phase forming in geothermal settings = scaling/scales), large-scale commercial extraction has not been undertaken so far. It was recently found that salty metal-rich brines (containing e.g. Cu, Li, Zn, Au, Ag) exist in active and dormant volcanoes across the world, and a commercial use was considered.

The geothermal fluids from the Tuzla geothermal reservoir are enriched in Li and Sr with values up to 23 ppm and 142 ppm respectively, and the Tuzla geothermal field may be a future target resource for Li recovery in Türkiye. The geothermal waters also contain notable concentrations of other metals, such as Pb and Co, which can lead to various types of scaling problems (calcite, silica, lead).

Based on existing information about the TGF, in WP2 of the CRM-geothermal project we aim to:

- Determine the source and mobility of critical elements in the brine, in order to predict the sustainability of extraction. Also to provide guidance for future exploration for new CRM-rich geothermal systems.
- Characterize the process of CRM enrichment and mobilization in high-enthalpy geothermal system (e.g. the Tuzla Geothermal Field).
- Calculate how long the extraction of CRM is economically viable before the brine becomes depleted.

3.2.6 References

Alpan, S. (1975). Geothermal energy exploration in Türkiye. In: 2nd United Nation Symposium on the Development and Use of Geothermal Resources, San Francisco, CA, USA, p. 25.

Baba, A., & Deniz, O. (2005). Determine of potential, application and environmental properties of geothermal resources in Biga Peninsulla. TUBITAK Project, C AYDAG-104Y082.

Baba, A., Deniz, O., Ozcan, H., Erees, S.F., Cetiner, S.Z. (2008). Geochemical and radionuclide profile of Tuzla geothermal field, Türkiye. Environ. Monit. Assess. 145 (1–3),361–374.

Baba, A., Yuce, G., Deniz, O., & Ugurluoglu, D. Y. (2009). Hydrochemical and isotopic composition of Tuzla geothermal field (Canakkale-Türkiye) and its environmental impacts. Environmental Forensics, 10(2), 144-161.

Demir, M. M., Baba, A., Atilla, V., & Inanlı, M. (2014). Types of the scaling in hyper saline geothermal system in northwest Türkiye. Geothermics, 50, 1-9.

Demirörer, M. (1971). Resistivity Survey of Tuzla-Kestanbol Hot Springs and Sur- rounding, MTA report, Ankara (unpublished).

Drever, I. (1997). The Geochemistry of Natural Waters, Surface and Groundwater Environments, third ed. Prentice Hall, Upper Saddle River, NJ, pp. 164–178.

Ekingen, A. (1972). Gravimetric Survey of Ezine – Ayvacik – Bayramic Surrounding, MTA report, no.: 4859, Ankara.

Ercan, T., & Türkecan, A. (1985). Bati Anadolu-Ege adalari-Yunanistan ve Bulgaristan'daki plütonlarin gözden geçirilisi. Paper presented at the Ketin simpozyumu.

Erdoğan, E. (1966). Geothermal Energy Possibility of Survey and Tectonic Mapping of Tuzla Hot Springs and Surrounding, MTA report, Ankara (unpublished).

Erişen, B., Akkuş, L, Uygur, N. & Koçak, A. (1996). Türkiye Jeotermal Envanteri, MTA Genel Müdürlüğü, 480s., Ankara. Euro-Med Seismological Centre (EMSC) http://www.emsccsem.org/#2

Gevrek, A.İ. & Şener, M. (1985). Çanakkale-Tuzla jeotermal sahasının hidrotermal alterasyon etüdü: MTA Rap. (baskıda), Ankara

Karamanderesi, I. H., & Öngur, T. (1974). The report of gradient wells finished of Tuzla (Canakkale) geothermal field. MTA report, (5524).

Karamanderesi, I. H. (1986). Hydrothermal alternation in well Tuzla T-2, Canakkale, Türkiye: United Nations University.

Keisuke, I. (1978). Ascending flow between the descending lithosphere and the over- lying asthenosphere. J. Geophys. Res. 83, 262–268.

Mützenberg, S. R. (1990). Westliche Biga-Halbinsel (Canakkale, Türkei): Beziehung zwischen geologie, tektonik und entwicklung der thermalquellen. ETH Zurich.

Mützenberg, S. (1997). Nature and origin of the thermal springs in the Tuzla area, Western Anatolia, Türkiye, Active Tectonic of Northwestern Anatolia – The Marmara Poly-Project. In: Schindler, C., Pfister, M. (Eds.), vdf hochschulverlag AG an der. ETH, Zurich, pp. 301–317.

Newton, R. C., & Manning, C. E. (2000). Quartz solubility in concentrated aqueous NaCl solutions at deep crust-upper mantle metamorphic conditions: 2–15 kbar and 500–900 C. Geochim. Cosmochim. Acta, 64, 2993-3005.

Öngür, T. (1973). Volcanology and Geological Report of Canakkale Tuzla Geothermal Area, MTA Report, Ankara (unpublished).

Şâmilgil, E., (1983). Çanakkale jeotermal alanları ve Tuzla sondajları: Türkiye Jeoloji Kongresi Bült., 4, 147-158. Zanettin, B., 1984, Proposed new chemical dassification of volcanic rocks: Episodes, 7/4, 19-20.

Şamilgil, E. (1966). Hydrogeological Report of Geothermal Energy Possibility Survey of Hot Springs of Kestanbol and Tuzla village of Canakkale. MTA report, no.: 4274, Ankara.

Şener, M., & Gevrek, A. I. (2000). Distribution and significance of hydrothermal alteration minerals in the Tuzla hydrothermal system, Canakkale, Türkiye. Journal of Volcanology and Geothermal Research, 96(3-4), 215-228.

Şimşek, Ş., Yıldırım, N., & Gülgör, A. (2005). Developmental and environmental effects of the Kızıldere geothermal power project, Türkiye. Geothermics, 34(2), 234-251.

Şimşek, Ş. (2008). Çanakkale-Tuzla Jeotermal Alanı T-7E Ve T-8E Arama/Üretim Kuyularının Jeoloji-Hidrojeoloji Değerlendirme Raporu. TUZLA JEOTERMAL ENERJİ A.Ş, 62 s.

Şimşek, Ş. (2009). Çanakkale-Tuzla Jeotermal Alanı T-9E Ve T-15E Arama/Üretim Kuyularının Jeoloji-Hidrojeoloji Değerlendirme Raporu. TUZLA JEOTERMAL ENERJİ A.Ş, 82 s.

Ürgun, S. (1971). The geology of Tuzla – Kestanbol (Canakkale) Surrounding and Geothermal Energy Possibility, MTA report, no.: 4664, Ankara.

White, D.E. (1968). Environments and generations of some base metal ore deposits. Econ. Geol. 63 (4), 301–335.

4 LOW SALINITY WATER IN FRACTURED CRYSTALLINE ROCK (CORNWALL, UK)

Authors:
Chris Rochelle, Richard Shaw (British Geological Survey, UK)
Hazel Farndale, Amy Peach-Gibson (Geothermal Engineering Ltd, UK)
Alistair Salisbury, Chris Yeomans (Cornish Lithium Plc, UK)

4.1 INTRODUCTION

Until recently, geothermal energy research in the UK has been limited, partly due to a lack of high-enthalpy resources, but also because of the availability of cheap fossil fuels during the 1980s and 1990s. Previous research focussed on three main aspects: (1) a nationwide appraisal of heat flow; (2) energy generation from hot brines in deep, hyper-saline aquifers (HSA); and (3) energy generation from enhanced geothermal systems (EGS) in hot dry rocks (Busby, 2010).

Heat flow measurements (Lee *et* al., 1987; Downing and Gray, 1986; Rollin, 1995; Rollin *et al.*, 1995; Barker *et al.*, 2000) place UK background heat flow at about 52 mW m^2, with elevated values associated with buried granites in north-eastern England and radiogenic granites in south-west England. The average UK geothermal gradient is approximately 26 °C km^{-1}, although locally it can exceed 35 °C km^{-1}.

The radiogenic granites of south-west England were assessed for their Hot Dry Rock (HDR) geothermal energy potential as part of the HDR project during the 1970s and 1980s. This programme of work was largely undertaken by the Camborne School of Mines to assess the performance of an EGS in the Carnmenellis granite, in south-west England. The test site operated a set of deep (between 2–2.5 km) boreholes to assess the feasibility of developing a full-scale commercial HDR system at about 5–6 km depth.

In recent years, increased interest in renewable energy technologies has led to significant industry investment in south-west England. Geothermal Engineering Limited (GEL) and Eden Geothermal Limited (EGL) have conducted deep (to 5 km) drilling to investigate the geothermal potential of the Carnmenellis and St Austell granites, and Cornish Lithium Plc (CL) have conducted shallower drilling (to 1.8 km) to investigate the potential of shallower resources for lithium in geothermal fluids at several targets along the Porthtowan Fault Zone.

South-west England, and in particular the region on the northern side of the Carnmenellis Granite, was chosen as a potential pilot study site for the CRM-geothermal project because of the relatively large amount of data available for that region – resulting from both its status as a historically important orefield and because of the history of geothermal research in the area.

The sections below are largely based on Shaw et al. (2016) and Schwarz et al (2016), updated to include information from several recent studies in Cornwall. Their aim is to describe some of the complexities of the geology of the region and the several stages of fluid movement associated with the granite bodies.

4.2 GEOLOGICAL BACKGROUND

4.2.1 The geology of south-west England

The geology and metallogenesis of south-west England is complex and has been the subject of extensive scientific research for more than two centuries. It was during the eighteenth century (c. 1778) that William Pryce first attempted to synthesise the geology, mining practices and metallurgy of the region. A number of important papers followed in the early to mid-nineteenth century (Phillips, 1814; De La Beche, 1839; Henwood, 1843) that sought to explain the role of granite and circulating fluids in the formation of south-west England's mineral deposits. This extensive metallogenic province, covering the county of Cornwall and part of the county of Devon from Land's End to Dartmoor, is termed the 'Cornubian Orefield'. Significant advances were made during the twentieth century in understanding the formation of the Cornubian Orefield, with the publication of numerous papers by Dines (1934 and 1956) and Hosking

(1950, 1951, 1952, 1964, and 1969). Geoscience research during the past forty years has sought to refine many of the earlier theories and concepts by the application of geochronology (Chesley *et al.*, 1993; Chen *et al.*, 1993; Clark *et al.*, 1993; Clark *et al.*, 1994; and Darbyshire, 1995), isotope studies (Rouse and Colman, 1976; Darbyshire and Shepherd, 1994; and Shail *et al.*, 2003) and fluid inclusion research (Williamson *et al.*, 1997; Gleeson *et al.*, 2000; 2001; Williamson *et al.*, 2000; and Müller and Halls, 2005).

Regional geological mapping by the British Geological Survey at 1:50 000 scale, and airborne geophysical (i.e. magnetic and radiometric) and remote sensing (i.e. LiDAR) surveys, flown as part of the TELLUS South West project, have further contributed to the geological knowledge base. Comprehensive reviews of the geology of south-west England can be found in Selwood *et al.* (1998), LeBoutillier (2002) and Shail and Leveridge (2009), and references therein.

A brief chronology of major geological events in south-west England, from oldest to youngest, includes:

(1) The development of a series of middle Palaeozoic (410–345 Ma), east-west trending volcano-sedimentary basins (from east–west these are the: North Devon Basin; Culm Basin; Tavy Basin; South Devon Basin; Looe Basin and; Gramscatho Basin) (Figure 4.1) that have been inverted, deformed and subjected to low-grade metamorphism (Parker, 1989; Shail, 2014);
(2) Variscan continental collision, during the mid-Carboniferous (331–329 Ma), resulted in significant crustal shortening and the development of NNW-trending thrust sheets (Parker, 1989; Shail, 2014);
(3) Crustal extension and orogenic collapse during the late Carboniferous and lower Permian resulting in extensive granitic magmatism (295–270 Ma) and associated hypothermal (300–600 °C) Sn-W greisens, and mesothermal (200–300 °C) Sn-Cu mineralisation hosted by E-W-trending mineral lodes. Following granite emplacement widespread Pb-Zn mineralisation developed in N-S-trending crosscourses, many of which are re-activated NNW-trending thrust sheets (Parker, 1989; LeBoutillier, 2002; Shail *et al.*, 2014);
(4) Cyclic periods of uplift, erosion and sedimentation throughout the Jurassic and Cretaceous (Parker, 1989; Shail *et al.*, 2014) resulting in the current landscape (e.g. exposure of granite roof zones at the existing land surface).

Emplacement of the Cornubian batholith into largely Devonian sedimentary rocks caused large-scale heating and thermal alteration. These metamorphic rocks in south-west England are locally known as 'killas'. Although these rocks are not economically important in themselves, fractures within them host a significant proportion of the region's mineral deposits (e.g. polymetallic mineral veins, or 'lodes'). The 'killas' comprises a series of Devonian (410–355 Ma) marine-deposited sandstones, siltstones, mudstones and rare carbonates that were regionally metamorphosed to sub-green schist facies during the Variscan Orogeny. As a result of granite emplacement, the low-grade regional metamorphism has been locally overprinted by higher-grade contact metamorphism, to produce a series of aluminosilicate and/or cordierite-bearing slates (Selwood, *et al.*, 1998).

The current surface expression of the Cornubian Batholith comprises six large granite plutons. From west to east these are: the offshore Isles of Scilly (120 km^2), Land's End (190 km^2), Carnmenellis (135 km^2), St Austell (85 km^2), Bodmin (220 km^2), and Dartmoor (650 km^2) (Figure 4.1). The subsurface extent of the Cornubian Batholith is estimated to be about 250 km in length and has an approximate width of between 40 and 60 km (Willis-Richards and Jackson, 1989; Scrivener, 2006). However, there is uncertainty about the true size of the Cornubian Batholith because current models are based on a small amount of data (e.g. gravity measurements and a very limited number of deep drill holes). Similarly, there is some uncertainty about the true thickness and shape of the granite plutons. 2D-gravity modelling of the Carnmenellis, St Austell and Bodmin granites indicates they are tabular bodies with an estimated thickness of between three and four kilometres, whilst the larger Dartmoor pluton is estimated to be about nine kilometres thick (Taylor, 2007). However, seismic refraction data suggest that the depth of the base of the batholith (i.e. its lower contact with the killas) is variable, ranging from about seven and eight kilometres beneath the Bodmin and Carnmenellis granites, respectively, to about ten kilometres beneath the Dartmoor granite (Brooks, 1984; Shail *et al.*, 2014).

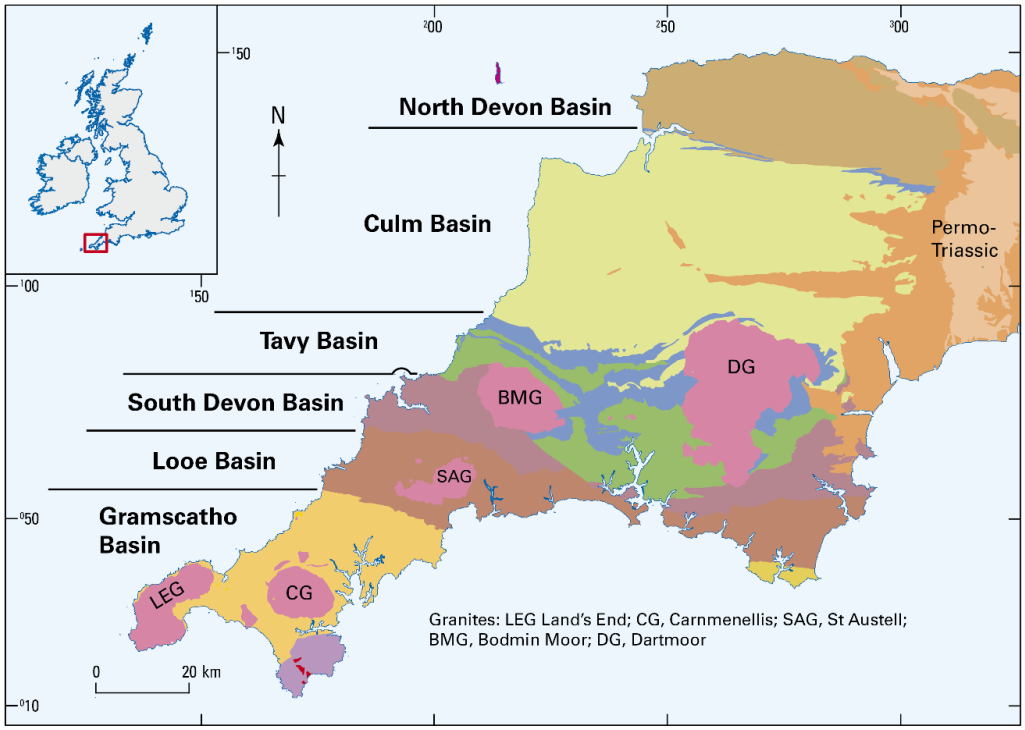

Figure 4.1: Simplified geological map of south-west England showing the distribution of sedimentary basins and the location of the granites (re-drawn from BGS mapping data and Shail and Leveridge, 2009).

Radiometric dating (U-Pb in monazite and zircon) suggests that the extensive granitic magmatism observed in south-west England occurred over an about 20 million year period, between about 293 Ma and 274 Ma, although separate intrusive episodes can be identified in some of the individual plutons (Chen *et al.*, 1993; Chesley *et al.*, 1993; Clark *et al.*, 1994). In terms of age, the plutons can be broadly divided into two groups: (1) the older (>290 Ma) Bodmin Moor, Isles of Scilly and Carnmenellis granites, and; (2) the younger (<286 Ma) Land's End, St Austell and Dartmoor granites (Figure 4.2).

Compositionally the granites are all peraluminous granites that are enriched in elements such as K, B, F, Li, U, Th, Sn, Rb and Pb. A notable feature of Cornubian granites is their high uranium content (with an average of about 12 ppm for all plutons), which is largely controlled by the distribution of accessory minerals such as uraninite and monazite (Chappell and Hine, 2006; Scrivener, 2006). Importantly it is the radioactive decay of uranium, thorium and potassium in the Cornubian granites that is responsible for their high heat production through radioactive decay (Chappell and Hine, 2006).

The granites of south-west England can be categorised mineralogically into three broad groups: (1) biotite granite; (2) topaz granite; and (3) tourmaline granite. However, minor variants also exist, including Li-mica granite and fluorite granite (Exley *et al.*, 1983; Floyd *et al.*, 1993; Manning *et al.*, 1996; Simons *et al.*, 2016). Textural variations are also used to distinguish sub-classes of the granites e.g. fine-grained tourmaline granite (Manning *et al.*, 1996) (Figure 4.2). The older granites (Bodmin Moor, Isles of Scilly, and Carnmenellis) can be distinguished from the younger granites (Land's End, St Austell and Dartmoor) by their texture, composition (peraluminosity), isotopic signature (εNd) and rare earth element (REE) patterns. These differences may reflect increased mantle-melting and possibly increased amounts of crustal melting during formation of the younger granites, probably in response to higher temperatures in the lower crust. However, it remains unclear why temperatures increased, and if this change was transitional, or an abrupt change in response to a discrete tectonic event (Stone, 1995; 1997; 2000a; 2000b; Shail *et al.*, 2014).

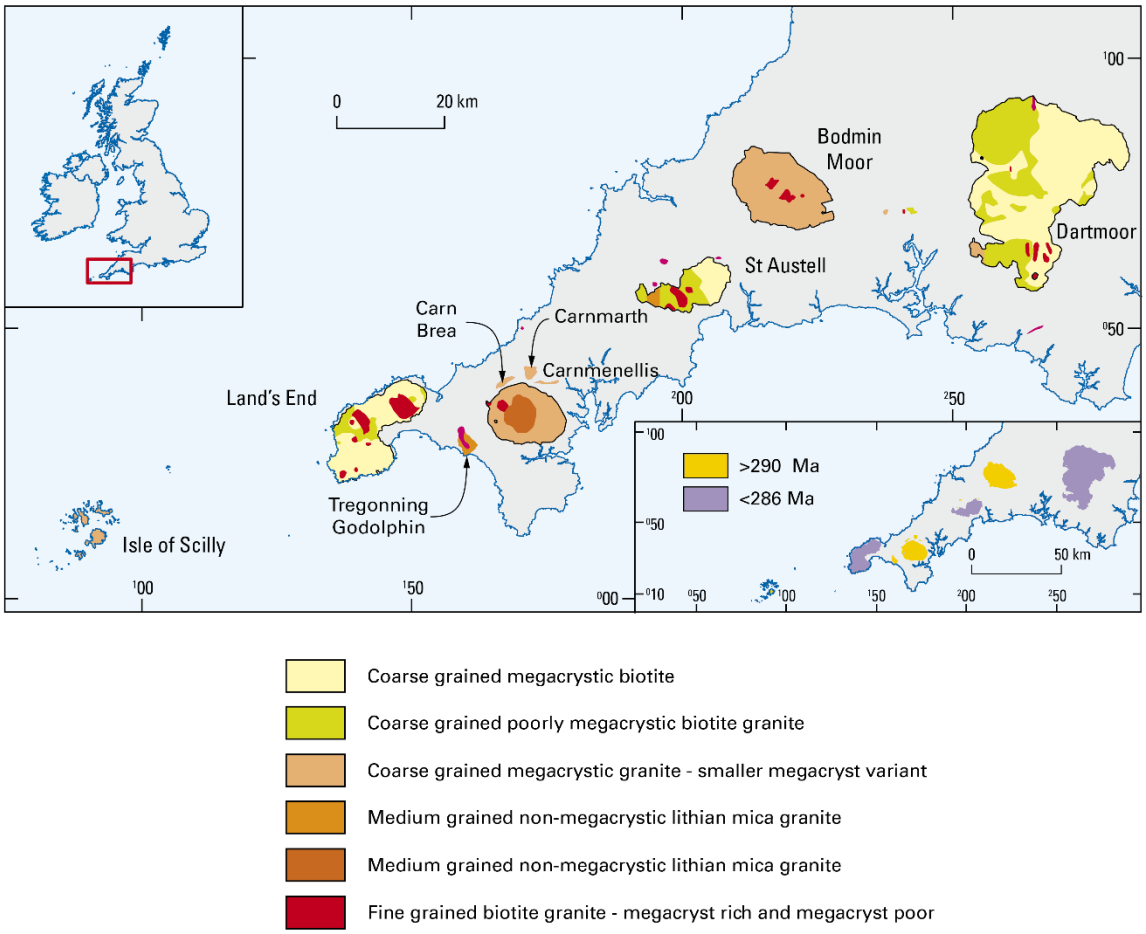

Figure 4.2: Map showing the principal mineralogical and textural variations in the Cornubian Batholith. It combines subdivision into biotite and lithian-mica granites with a textural scheme based primarily on mean matrix grainsize and the size and abundance of alkali feldspar megacrysts - compiled from Exley and Stone (1964, 1982) Stone and Exley (1985), Hawkes and Dangerfield (1978), Dangerfield and Hawkes (1981), Exley et al. (1983), Floyd et al. (1993), Manning et al. (1996), Manning (1998) and Shail et al. (2014). In-set map shows the distribution of granite ages: Dartmoor, St Austell and Land's End (in purple) are <286 Ma, whereas Bodmin, Carnmenellis and Isle of Scilly (in yellow) are older (>290 Ma).

In summary, the region has been studied for more than 200 years and a large amount of academic and industry data exist that describes the relationship between magmatism and mineralisation. The abundance of magmatism and mineralisation across south-west England warrants its status as a globally significant metallogenic province. Complimentary geological mapping and airborne geophysical surveys have further refined the interpretation of the geological evolution of the region. There is continuous digital geological mapping at 1:50,000 scale, complimentary regional datasets (e.g. LiDAR, airborne geophysics, etc.), and a 3D model of the geology at 1:625,000 scale. Though much data exist, there are still some limitations which present uncertainty in terms of extrapolating information and data at surface to any significant depth. For example, the majority of the primary data is related to the shallow sub-surface (<1 km, and often <200 m), and there has also been no regional deep geophysical investigation.

4.2.2 Mineralisation

The Cornubian Orefield has a complex, protracted (c. 100 Ma), multi-stage history of polymetallic mineralisation. Mineralisation comprises a variety of styles, ranging from Devono-Carboniferous syngenetic mineralisation, to recent placer and kaolin deposits. There is a long history of mineralisation-related research in south-west England, with a particular focus on granite-related hydrothermal tin and tungsten-bearing deposits.

Although historically the south-west region was major metal producer, the Drakelands Sn-W deposit (operated by Tungsten West Limited) is the only active metal mine in south-west England. It is hosted

within and around a dyke-like body of porphyritic granite, known as the Hemerdon Granite that forms a cupola to the south-west of the main body of the Dartmoor Granite. The deposit is one of the world's largest tungsten deposits containing 35.7 million tonnes at a grade of 0.18% WO_3 and 0.03% Sn (Wolf Minerals, 2015). The previous owners of the mine (Wolf Mineral Limited) estimated that the Drakelands operation has a production capacity of more than 3,000 tonnes of tungsten concentrate per annum (Wolf Minerals, 2015).

4.2.2.1 Historical production

Historically, the south-west region was a major metal producer. Mineral deposits in the region were predominantly exploited for tin, tungsten, arsenic, zinc, lead and copper (Dines, 1956; Shail *et al.*, 2014; Burt *et al.*, 2015). Approximate quantities of metal production in south-west England are shown in Table 4.1.

Table 4.1: Estimated total mineral and metal production from south-west England. After Dines (1956), Alderton (1993) and South Crofty PLC (1988-1998). Adapted from LeBoutillier (2002).

Mineral or metal (Tonnes)	
Sn metal	2,770,000
Cu metal	2,000,000
Fe ore	2,000,000
Pb metal	250,000
As (as As_2O_3)	250,000
Pyrite	150,000
Mn ores	100,000
Zn metal	70,000
W (as WO_3)	5,600
U ore	2,000
Ag ore	2,000
Ag metal (from sulphide ore)	250
Co-Ni-Bi ores	500
Sb ores	300
Mo metal	Minor
Au metal	Minor
Barite	500,000
Fluorite	10,000
Ochre/umber	20,000
Kaolinite (china clay)	150,000,000

4.2.2.2 Mineralisation styles in south-west England

Several main stages of mineralisation have been identified, forming over about a 100 Ma period between the early Permian and the late Triassic. The mineralisation can be broadly divided on the basis of its timing relative to granite emplacement as:

1) *Pre-granite* orebodies of the sedimentary-exhalative type and shear-zone hosted Au-Sb mineralisation
2) *Granite-related* mineralisation, comprising: a) greisens and sheeted vein complexes, and b) polymetallic sulfide lodes
3) *Post-granite* mineralised Pb-Zn-Ag crosscourses (highlighted in Table 4.2).

Figure 4.3 provides an overview of the fluid chemistry of these mineralisation styles.

Pre-granite mineralisation

This comprises:

1) Stratiform mineralisation that contains sub-economic enrichments in base metals (Scrivener *et al.,* 1989; Scrivener, 2006). The main commodities associated with the early stratiform mineralisation are iron and base metals.
2) Metamorphogenic quartz-carbonate veins that typically contain Sb-As-(Au) (Clayton *et al.*, 1990). Orogenic shear-hosted Au-Sb-Ag mineralisation is limited to basinal argillaceous lithologies with significant volumes of basic volcanic rocks. It is also spatially associated with NNW-trending shear zones (Stanley *et al.*, 1990). Fluid chemistry and structural data indicate that the quartz-Au-Sb veins were precipitated early from CO_2-rich metamorphic fluids with fluid inclusion homogenisation temperatures (Th) in the range 315–280 °C (Clayton *et al.*, 1990).

Granite-related mineralisation

This formed largely during the early to mid-Permian. These mineral deposits were historically of the greatest economic importance and were exploited for tin, tungsten, arsenic and base metals. *Granite-related* mineralisation includes skarns and pegmatites, greisens and sheeted vein deposits, and the main-stage polymetallic deposits. Localised skarn deposits have resulted from the thermal alteration of calc-silicate minerals that have been altered by boron-rich fluids (Scrivener 2006). Volumetrically these skarns are insignificant, thus reflecting the lack of carbonate-rich rocks in the region.

Greisen occurrences are restricted in extent, but common immediately adjacent to all plutons, including the Isles of Scilly Granite (Grant and Smith, 2012; Sullivan *et al.*, 2013; Shail *et al.*, 2014). Greisen wall rock alteration is characterised by the development of secondary mica around sheeted veins and in stockworks. It occurs in the granite (endogranite) and the surrounding host rocks (exogranite). Endogranitic greisens occur at St. Michaels Mount (Floyd *et al.*, 1993), Cligga Head (Hall 1971; Jackson and Moore 1977), and Hemerdon (Beer and Scrivener, 1982), while exogranitic greisens occur in the Tregonning and St Austell granites (Dominy *et al.*, 1995). The greisens comprise closely spaced quartz-tourmaline veins up to 0.1 m wide that host wolframite, cassiterite, stannite, arsenopyrite and other sulfides. Fluid inclusions indicate that the greisen-bordered veins were precipitated over a wide range of temperatures (Figure 4.3). Greisens represent the earliest occurrence of significant fracture controlled magmatic-hydrothermal mineralisation in south-west England (Shail *et al.*, 2014). Greisen bordered, sheeted veins and quartz-(feldspar)-wolframite lodes formed within 2–3 Ma of granite emplacement, and overlap with muscovite cooling ages for the host/adjacent pluton (Chen *et al.*, 1993; Chesley *et al.*, 1993).

Polymetallic lodes containing cassiterite and chalcopyrite, and subordinate arsenopyrite, sphalerite, galena and localised wolframite post-date the greisen bordered, sheeted veins. These lodes were historically the main source of tin and copper in the region. The complex structure and mineralogy of these deposits, and their strong spatial association with granite bodies, reflect the protracted magmatic-hydrothermal activity associated with their formation (Scrivener 2006). These polymetallic lodes are generally orientated E-W and developed between 269–259 Ma, although there is a suggestion that this reflects the dating of more than one paragenetic episode (Chen *et al.*, 1993; Clark *et al.*, 1993). These lodes mark the final contribution of magmatic-hydrothermal fluids to mineralisation in south-west England (Shail *et al.,* 2014).

Post-granite mineralisation

This formed by east-west extension during regional extension-driven subsidence in the Permian and resulted in the formation of north-south-trending fracture systems. Subsequent fracture-controlled ingress of metal-complexing basinal fluids from Permo-Triassic sedimentary successions into the Variscan basement resulted in the stripping of metals from metalliferous source rocks, and the formation of what

is known as 'crosscourse' mineralisation (Scrivener *et al.*, 1994). This comprises north-south-trending polymetallic veins dominated by lead, zinc and copper, which locally host antimony-bearing minerals. The crosscourse mineralisation postdates the granite related Sn-W-Cu mineralisation by 30–40 Ma (Scrivener *et al.*, 1994). The crosscourse veins were primarily exploited for lead, zinc, silver, fluorite and baryte, typically within Devonian and Carboniferous successions. The name 'crosscourse' is a local miners' term for these structures that cut across, and often displace, the mineral veins that they were exploiting.

Other mineralisation

In addition to the styles of mineralisation described above, there are a number of less significant types of mineralisation (not described in detail here). These include: syn-granite tourmaline-tin veins (Scrivener 1982; Bromley 1989); tourmaline breccias (London *et al.*, 1995; Müller and Halls 2005); post-granite, low temperature manganese and iron replacement deposits; and gold-carbonate veins (Jackson *et al.*, 1989). Following granite emplacement, descending meteoric water resulted in alteration of feldspar, leading to high levels of kaolinisation in the St Austell and Dartmoor granites (good overview of this late-stage alteration can be found in: Sheppard, 1977; Bray and Spooner, 1983; and Bristow and Exley, 1994).

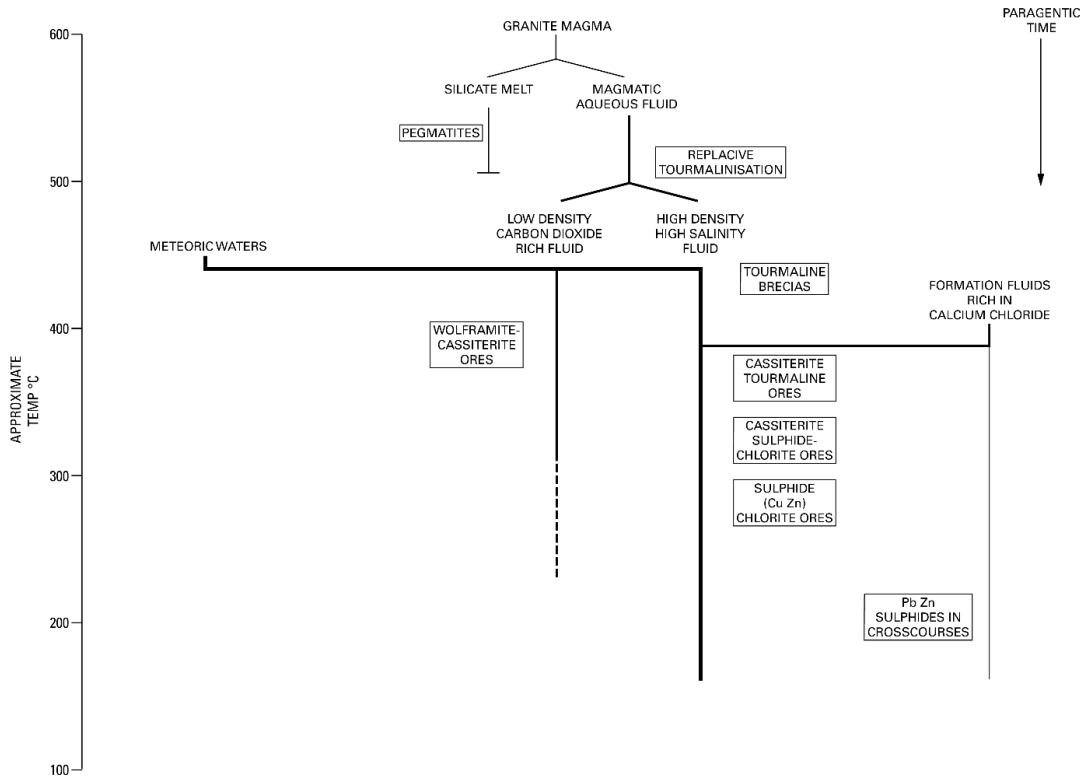

Figure 4.3: Overview of the evolution of mineralising fluids in south-west England (after Leveridge *et al.*, 1990).

Pre-granite mineralisation	**Main ore minerals**				
1) Rifting and passive margin development (early Devonian- Carboniferous) sedimentary-exhalative (SedEx) mineralisation	Haematite	Siderite	Galena	Sphalerite	
2) Variscan convergence and continental collision (late Devonian-Carboniferous) shear zone hosted Au-Sb + base metal mineralisation	Gold	Bournonite	Sphalerite	Chalcopyrite	Tetrahedrite
Granite-related mineralisation					
3) Early post-Variscan extension and magmatism (early Permian)					
a) Magnetite-silicate skarns developed in metabasaltic hosts	Magnetite	Cassiterite			
b) Sulfide-silicate skarns developed in calc-silicate granite hosts	Cassiterite	Arsenopyrite	Pyrite	Chalcopyrite	Pyrrhotite
c) Greisen-bordered sheeted vein complexes	Wolframite	Cassiterite	Chalcopyrite	Sphalerite	Bismuthinite
d) Quartz-tourmaline veins and breccias	Cassiterite	Haematite			
e) Polymetallic sulfide lodes	Cassiterite	Chalcopyrite	Wolframite	Arsenopyrite	Sphalerite
Post-granite mineralisation					
4) Episodic intraplate rifting and inversion (late Permian – Cenozoic)					
a) Crosscourse Pb-Zn ± F, Ba mineralisation	Galena	Sphalerite	Arsenopyrite	Chalcopyrite	

Table 4.2: Summary of mineralisation styles in the south-west England (Cornubian) orefield (adapted from Andersen, et al. 2016).

In summary, the south-west of England is a historically important mining region and has produced a significant range and volume of metals - though the region is best known for its tin and copper production. Mineralisation in south-west England can be categorised into broad styles that have been related to the timing of granite emplacement (i.e. pre-granite, granite-related, and post-granite). The most significant mineralisation in south-west England from an economic perspective is related to magmatic-hydrothermal activity associated with granite emplacement. Importantly a significant, and growing, body of research and data exist on this mineralisation (e.g. geochronology, fluid composition, mineralogy, geochemistry) and there is a good understanding of how magmatism, fluids and large-scale structures have interacted to produce economic mineralisation. That said, there are still some limitations. For example, there is significant uncertainty about the form and scale of mineralisation below 1 km, and the distribution of data coverage is generally skewed towards areas where economic mineralisation has been exploited or commercial mineral exploration has occurred.

4.3 GEOTHERMAL EXPLORATION AND EXPLOITATION

4.3.1 The Hot Dry Rock (HDR) research programme

In 1984, a programme of work, funded by the UK Department of Energy (DEn) and the Commission of the European Communities (CEC), was undertaken by the British Geological Survey (BGS) to assess the UK for its geothermal potential. Over the same time period (1977–1984) the Camborne School of Mines (CSM) was assessing the feasibility of creating HDR geothermal systems at a test site at the Rosemanowes quarry, on the Carnmenellis granite, in Cornwall (Figure 4.4). The assumption was made that the behaviour and characteristics of a HDR system (Figure 4.5) could be modelled using geochemistry, geophysics, and physical properties. Between 1985–1989 the Department of Energy and the Commission of the European Communities funded a detailed geochemical investigation of the HDR site at Rosemanowes. These investigations were undertaken by the BGS, the then NERC Isotope Geology Centre (NIGC), the University of Bath (UoB) and CSM. In 1987 an informal working group (the UK Hot Dry Rock Geochemistry Group) was established to align the geochemical programme more closely with the physical properties and geophysical work being undertaken by CSM at the Rosemanowes test site.

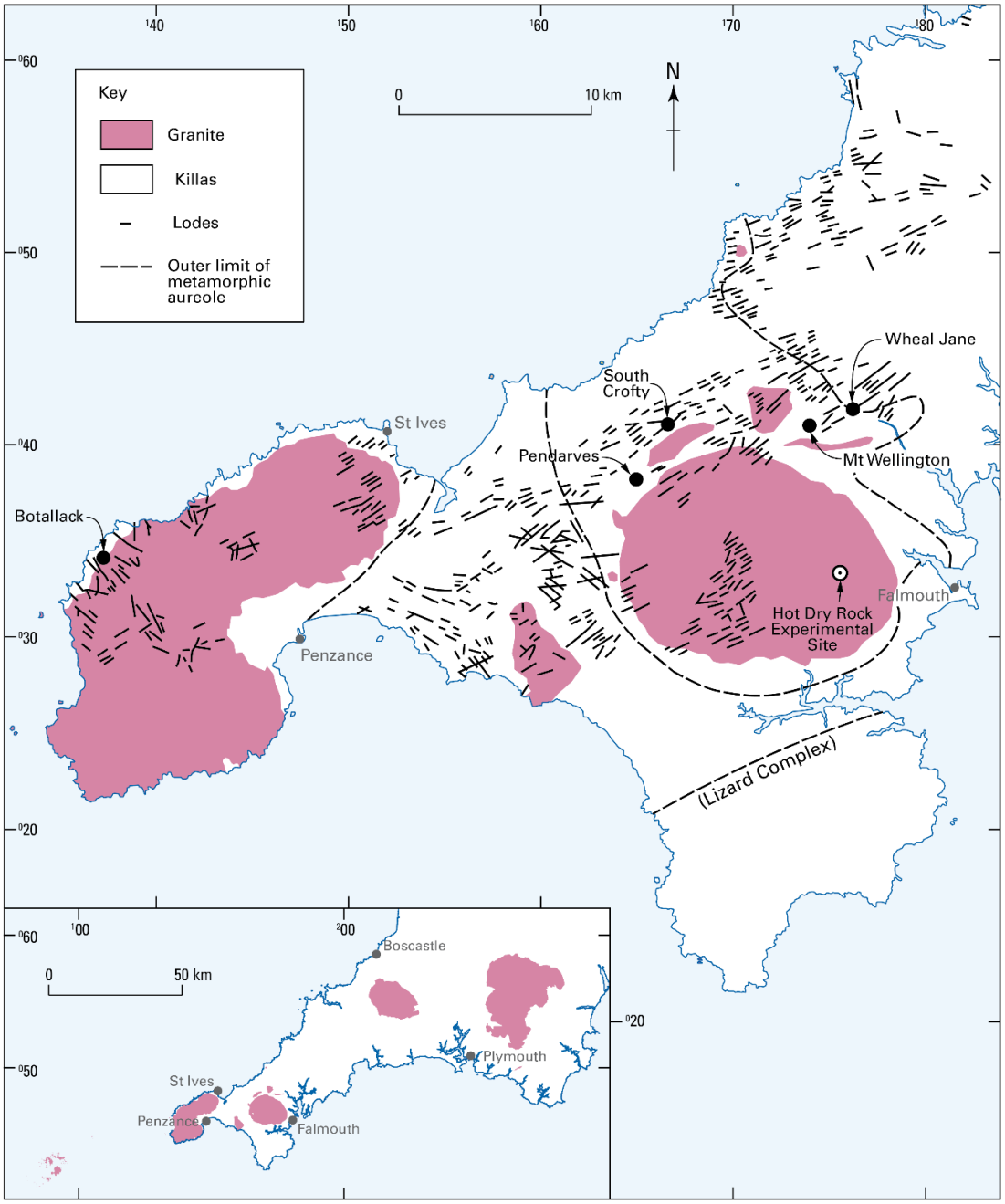

Figure 4.4: Location of the Rosemanowes HDR test site in relation to the Carnmenellis granite outcrop (re-drawn from Edmunds *et al.*, 1989).

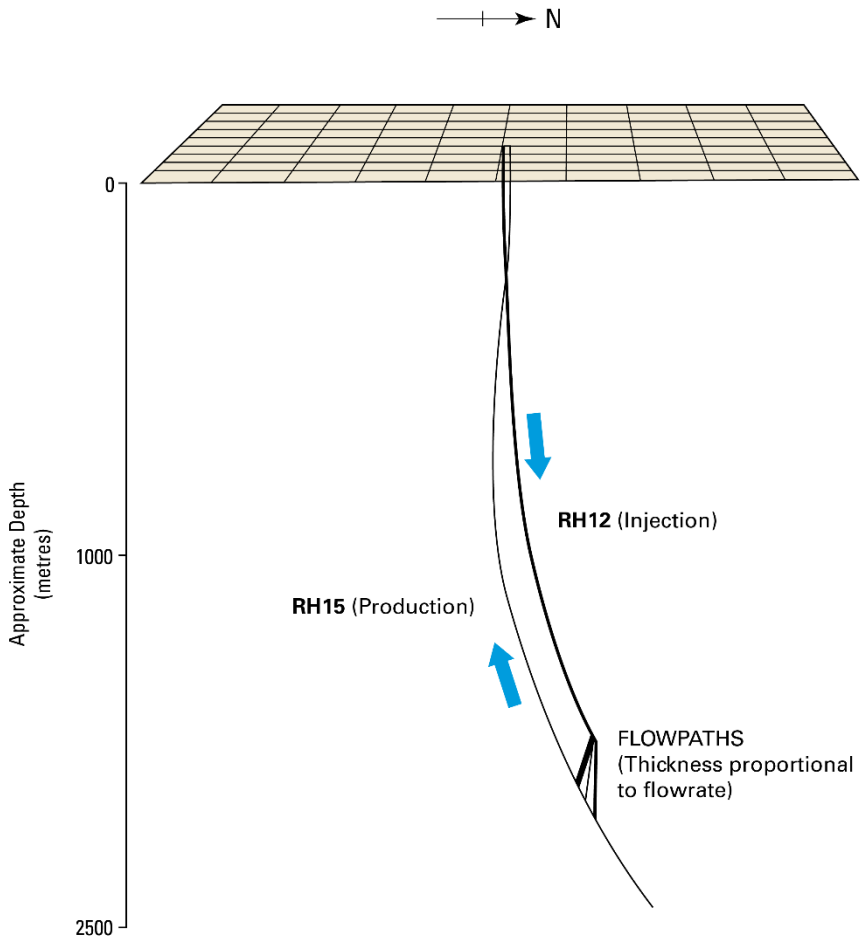

Figure 4.5: A schematic diagram showing the configuration of the 2 and 2.5 km test wells at the Rosemanowes HDR test site (re-drawn from Edmunds *et al.*, 1989).

A key output from this work was a BGS-led 7-volume report (Edmunds *et al.* 1989; Richards *et al.* 1989; Andrews *et al.* 1989; Smedley *et al.* 1989; Bromley *et al.* 1989; Savage *et al.* 1989 and; Richards *et al.* 1989) that outlines the methods and results of geochemical HDR research at the Rosemanowes test site (Edmunds, *et al.*, 1989). The first 2 volumes were summaries, with the following 5 reports containing much technical detail and data (see summary information below). Similar outputs authored by CSM describe the physical properties of the HDR system.

In summary, the main HDR report volumes comprise:

Volume 1 (Edmunds et al. 1989). This provides an overview and synopsis of the other 6 volumes.

Volume 2 (Richards et al. 1989). This provides an overview of geochemical results collected as part of the HDR programme.

Volume 3 (Andrews et al. 1989). The movement of natural radioelements (e.g. ^{226}Ra) and radiogenic noble gases (e.g. ^{222}Rn) in the HDR system were investigated to:

1) Characterise changes in reservoir surface area.
2) Develop a routine monitoring method for determining ^{222}Rn in the HDR return fluids.

3) Determine the effect of surface mineralisation and physical conditions on ^{222}Rn flux, and hence upon derived reservoir parameters.
4) Estimate the effect of fracture width variation on the radon model.
5) Assess geochemical changes in radioelement chemistry induced by HDR circulation.

The conclusions were that:

- Reservoir surface area showed a general increase as flow tests progressed.
- Tracer transit times of up to 400 hours were observed within fractures.
- Mineralised surfaces, particularly those hosting uranium-rich minerals, dramatically increase the ^{222}Rn flux of the system.
- Uranium mobilisation occurs in the system in response to fluid circulation.

Volume 4 (Smedley et al. 1989). The investigation of the hydrogeology and hydrogeochemistry of the Carnmenellis granite. Understanding natural fluid flow can be useful to HDR development as it provides an analogue to artificial short-term circulation in the HDR reservoir, and helped explain important processes, such as:

1) Granite-water interaction
2) Fluid-flow in granite
3) Solution-precipitation reactions.

The conclusions were that:

- Groundwater flow in both granite and killas is dominated by fracture permeability; primary permeability in both rock types is low. In particular, it is the north-south-tending crosscourse structures that are the most important water-conducting fractures.
- Shallow groundwater compositions show a strong affinity with the local geology and soils. In many cases the element concentrations are very lithology-specific, for example Cl, HCO_3, pH, Na, Ca, Mg levels are highest over the killas, whilst Al, Ba and Rb levels are higher over the granite.
- Saline thermal waters discharging in deep mines (depths down to 820 m) are effectively dilute palaeobrines (formed by long-term water-rock interaction) that have mixed with circulating local meteoric waters.

Volume 5 (Bromley et al. 1989 [note, this was not printed in large quantities as per the other reports]). In order to fully understand the geological constraints on HDR reservoir development the geology of the region is considered in detail. In particular, the following areas of enquiry are relevant:

1) The spatial variation in the petrological and geochemical characteristics of the granites.
2) The spatial variation in the nature of the fracture system, and the character of fracture mineralogy and adjacent wall-rock alteration.
3) The mechanisms and products of natural fluid-rock interaction under conditions similar to those pertaining in an artificial reservoir, and which might provide useful analogues for reservoir behaviour.
4) The prediction of geological conditions at depths of 5–7 km in regions where commercial reservoirs may be developed.

The conclusions were that:

- Rock at depth is likely to be an inhomogeneous mixture of vuggy, pegmatitic granite and magmatic residues (i.e. restite). Thus water-rock interaction would be significantly different from that predicted by experiments on samples of 'average' Cornubian granite.
- The ability to drill an inhomogeneous mixture of granite and restite is likely to be very different from that of standard granite alone.

- Localised zones of argillic alteration, associated with crosscourse structures at depth, may hamper drilling operations.
- North-south-trending crosscourse structures are likely to extend to significant depths and as such represent important zones of increased permeability. However, they may also lead to extensive fluid loss from the HDR system.

Volume 6 (Savage et al. 1989). Investigation of chemical reactions that take place between circulating fluids and reservoir rock in a HDR system is important, primarily because:

1) It provides an indication of the evolution of the physical characteristics of a reservoir under development (e.g. temperature).
2) It provides information about the potential lifetime of a reservoir undergoing commercial operation.

Much of this volume relates to laboratory experimental studies undertaken to evaluate the magnitude and rate of water-rock reactions, including:

a) The surface-area dependant release rate of a variety of chemical component from the Carnmenellis granite under likely *in-situ* conditions at EGS depths.
b) The investigation of the chemical reaction of Carnmenellis granite with possible circulation fluids.

The conclusions were that:

- The concentration (by weight) of elements in the output fluid from laboratory experiments was as follows (from highest to lowest): SiO_2 > Ca > Na > K > Fe > Mn > Rb > Li > Cs > Sr.
- The relative molar release rates of the elements (from highest to lowest) was: SiO_2 > Na > Ca > K > Fe > Mn > Li > Rb > Sr > Cs.
- Changes in pH were only found to affect Al (increased with increasing pH), SiO_2 (increased with increasing pH) and Fe (decreased with increasing pH).
- Use of dilute surface water as an EGS 'top-up' fluid was superior to using seawater, the latter causing potential problematical precipitation of hydrated magnesium sulphate phases.
- Bulk granite dissolution rates vary significantly from 6×10^{-10} g m^{-2} s^{-1} (expressed as SiO_2 release) at 60 °C to 5×10^{-7} g m^{-2} s^{-1} (expressed as Ca release) at 100 °C.
- Individual mineral dissolution rates also vary significantly. Experiments at 80 °C generated the following estimated rates of dissolution: $2 \times 10^{-11} - 8 \times 10^{-10}$ mol m^{-2} s^{-1} (biotite); $4 \times 10^{-11} - 2 \times 10^{-10}$ mol m^{-2} s^{-1} (oligoclase); $2 \times 10^{-10} - 4 \times 10^{-10}$ mol m^{-2} s^{-1} (labradorite) and; $1 \times 10^{-15} - 2 \times 10^{-14}$ mol m^{-2} s^{-1} (tourmaline).

Volume 7 (Richards et al. 1989). The geochemical aspects of the design and operation of a commercial HDR geothermal system in granite, in south-west England are reviewed and modelled in order to predict:

1) The composition of the circulation fluid.
2) The potential for chemical problems associated with the wells and surface plant (including effluents).
3) The rates of water-rock reactions in the HDR reservoir, and how this might affect hydraulic performance.
4) The potential use of geochemistry in characterising the performance of the HDR reservoir during and after its creation.

The conclusions were that:

- The most appropriate circulation fluid is predicted to be a mildly-saline, neutral- to mildly-alkaline local surface water, with low to moderate total sulfur (20–150 ppm SO_4) and low to moderate total sulfide (5–10 ppm H_2S).

- Silica and/or carbonate-based scaling are likely the biggest issue for wells and surface plant.
- Predicted arsenic (c. 1 ppm), boron (c. 1 ppm), fluoride (c. 10–20 ppm) and silica (c. 300 ppm) concentrations in the circulation fluid mean they could not be discharged straight into the environment without prior treatment.
- Mineral dissolution is likely to result in widening of fractures (by up to 1 mm over a 25 year lifetime) and thus will have an impact on reservoir hydraulics.
- However, the precipitation of secondary minerals (e.g. zeolites, clays and calcite) as a result of granite-water reactions would also have a potentially negative impact on porosity and reservoir hydraulics.

The data and lessons learned during the HDR project were used to underpin more recent geothermal activities in Cornwall, namely the United Downs Deep Geothermal Power project (owned, developed and operated by Geothermal Engineering Limited) and the Eden Geothermal project (managed by Eden Geothermal Limited). These activities are described in the sections below.

4.3.2 The United Downs Deep Geothermal Power project

The United Downs Deep Geothermal Power project is an endeavour by Geothermal Engineering Limited (GEL) to build upon the results of the HDR research programmes, and to utilise advances in drilling techniques and power production technology to generate 1-3 MW_e at the project site on the United Downs Industrial Estate (just north of the main surface expression of the Carnmenellis Granite, and some 10 km NNW of the HDR site).

The site at United Downs was acquired in 2010 after an extensive feasibility study into suitable drill sites within the Carnmenellis granite. In 2018/19, the drilling of directional wells UD-1 (production) and UD-2 (injection) to measured depths of 5275 m and 2393 m, respectively (Figure 4.6), successfully identified temperatures of more than 180 °C, whilst subsequent flow testing indicated the presence of enhanced permeability, with sufficient flow for a binary power plant to generate electricity in the near future.

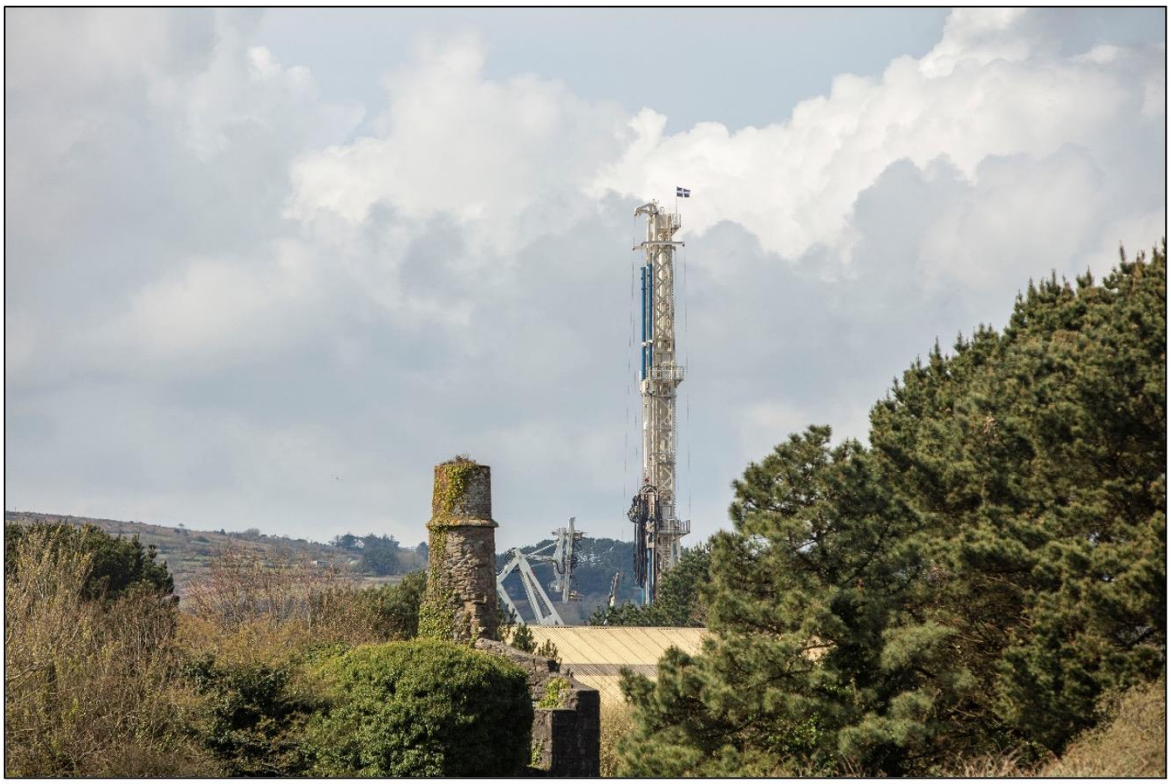

Figure 4.6: The drilling rig at the United Downs Deep Geothermal Power project near Redruth, visible behind the ruins on an engine house. (GEL photograph)

Knowledge gained during the HDR project was used to identify the geothermal target of the Porthtowan Fault Zone (PFZ), a near-vertical 200-300 m wide fracture zone known to be transmissive to water. This fault zone is found within the radiogenic Cornubian granite batholith, which underlies much of Southwest England, dramatically increasing the geothermal gradient to around 35 °C where the UK average is only 26 °C (Figure 4.7). The PFZ dips slightly to the ENE, and a production well, UD-1, was drilled to intercept the fault zone through its hanging wall at approximately 4.5 km deep (Figure 4.8).

UD-1 is the deepest and hottest geothermal borehole in the UK, and serves as a demonstration of both the technology and of the geothermal potential in SW England. Planning applications have also been submitted by GEL for further geothermal projects in Cornwall, each of which will be capable of generating around 5 MW_e.

Whilst GEL's main focus is the provision of a binary power plant at the site (requiring high fluid temperatures of >100 °C), considerations are underway regarding further uses for this geothermal resource, including the future provision of district heating (requiring temperatures of approximately 80 °C), other heat related enterprises such as a rum distillery, as well as for direct lithium extraction from the geothermal brines (requiring temperatures of approximately 40 °C).

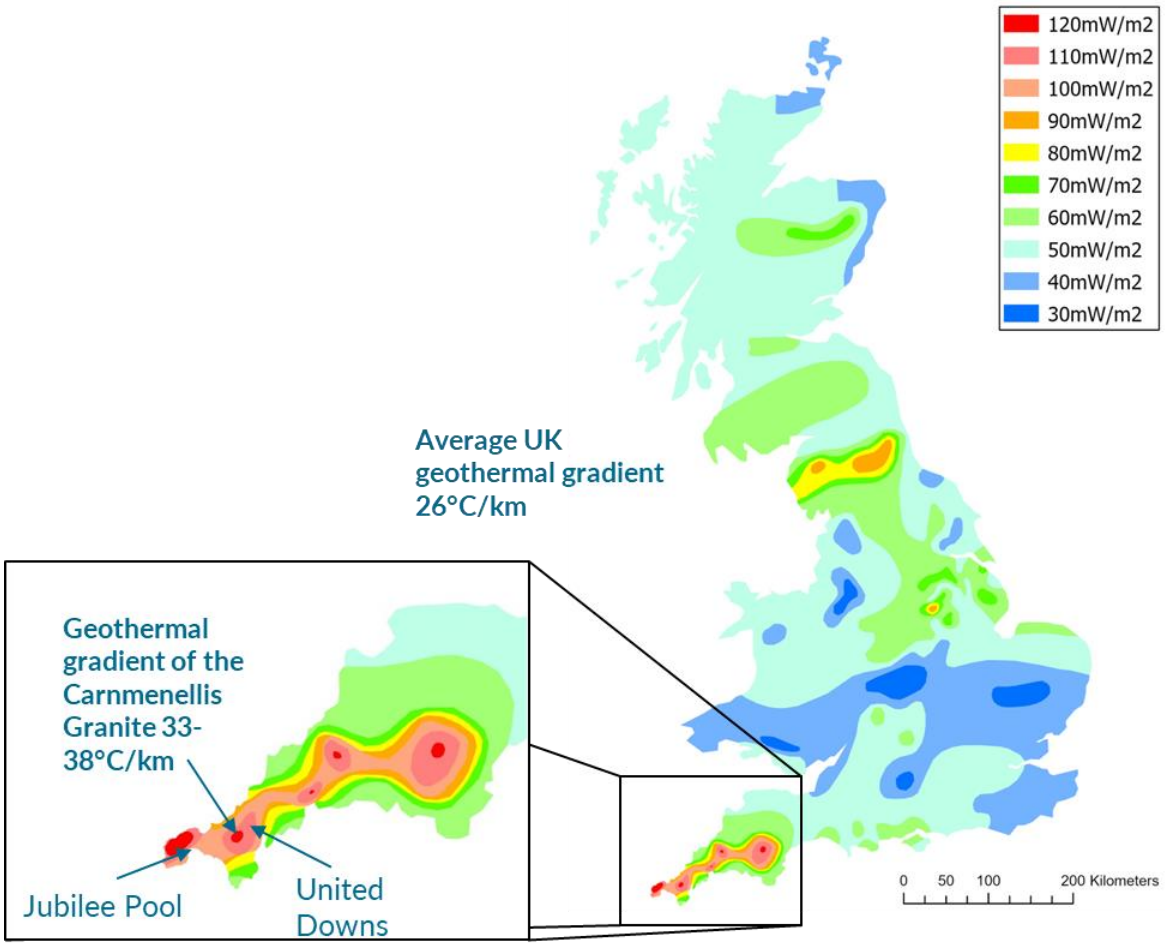

Figure 4.7: Heat map of the UK showing the high heat flow of the Cornish granite and the location of the UDDGP UK (largely based upon Busby, 2010).

GEL have already been involved in fluid testing from their deep wells at United Downs and DLE trials in conjunction with Cornish Lithium Plc (CL). These have shown globally significant concentrations of lithium at around 270 ppm in the deep geothermal brine sampled from UD-1 (from CL press release). The analysis also highlighted high Nd concentrations associated with Cornish granites and low levels of contaminants (both in terms of dissolved Mg and total dissolved solids).

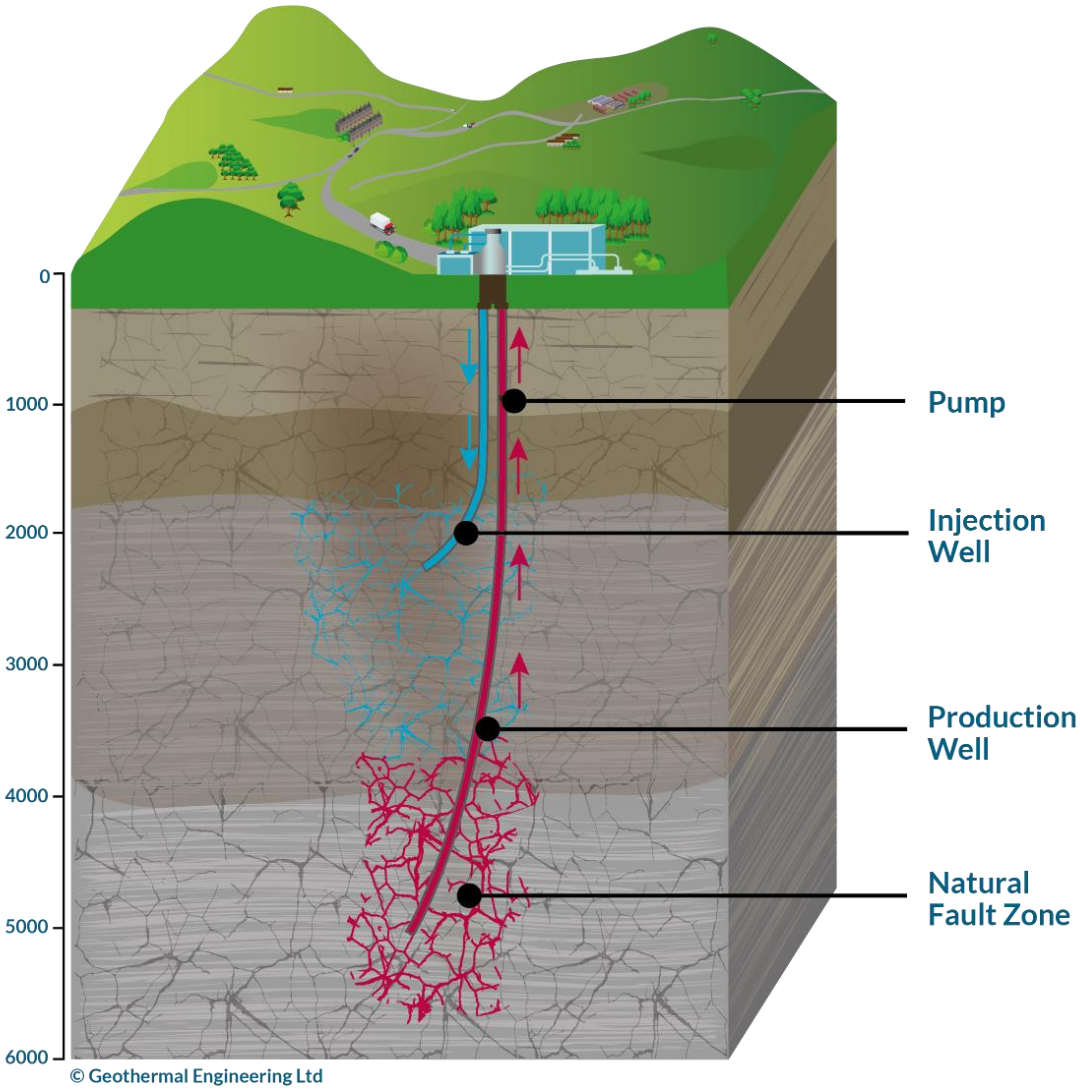

Figure 4.8: Schematic representation of the geothermal doublet at United Downs, drilled into the Porthtowan Fault Zone. (GEL image).

Considerable data have been collected through pre-drilling studies, surveying during drilling, and investigations and analyses after well completion and testing. The most significant datasets include the geochemical analysis, feasibility studies, induced seismicity mapping, local ArcGIS datasets, drilling records, hydraulic stimulation, lifetime carbon assessments and modelling. The Deep Digital Cornwall datasets covering the subsurface across Cornwall may also be available on request. Table 4.3 lists data held by the UDDGP project – much of it generated as part of GEL activities, but some of it stemming from other sources, including; the original HDR project, PhD studies, the GeoCubed project, the GWatt project, and regional datasets collected by the BGS. Only some of the data are currently publicly available, though some of the data have resulted in recent open publications (Table 4.4).

Table 4.3: List of data held by the UDDGP project.

	DATA
SEISMICITY	Earthquakes in Cornwall (1981 to 2019)
	Seismic measurements for Cornwall from BGS
	Seismic data from Rosemanowes HDR
	Naturally occurring seismicity in Cornwall
	Recorded induced seismicity during UD testing for August 2020 to July 2021
LITHOLOGY	Depth to Granite coordinates
	Cornwall Gravity data
	BGS borehole logs
	Geological cross sections of United Downs
	Bedrock and structural geology of Cornwall
	UD-1 Mineralogy from QEMSCAN
	Qtz% with depth QEMSCAN
	UD-1 Lithology, mineralogy, gamma correlation
	UD-1 XRD
	UD-1 XRF
	UD-1 Well site lithology classifications
	UD-1 Mineralogy
	UD-1 Stratigraphy
FAULTS	Structural geology (faults and fractures) of Cornwall
	Porthtowan Fault geometry
	Porthtowan fault depths and indicators
	UD-1 Geological structure and fracture characterisation
	UD-1 UXPL Fracture atlas
MINING	List of mines between Truro and Hayle
	Desk studies of mines surrounding United Downs
	Desk study of major cross courses on the western side of united mines
DRILLING	Wireline logging data
	Temperature logs
	Gas concentrations
	Fluoresceine concentration data
	MWD logs
	Tracer analysis
	Chippings logs
	SWC logging
	Losses catalogue
	Injection test data
	GEL UD1 8.5 fractures
	UD-1 Formation evaluation log
	UD-1 Daily drilling reports
	UD-1 Mud logging reports
	UD-1 Drilling evaluation logs
	UD-1 Field calliper logs

	UD-1 WellCad images/logs
	UD-1 borehole profile
	UD-1 Temperature (calculated vs measured)
	UD-1 geology summary report
	UD-1 End of well report
	UD-2 Formation evaluation log
	UD-2 formation evaluation logs/PCG gamma ray
	UD-2 Mineralogy
	UD-2 Stratigraphy
	UD-2 End of well report
GEOCHEMISTRY	Geochemical analysis for REEs & economic materials
	Geochemical analysis from Airlift and ESP testing
	Hydrogen and oxygen isotope data
	Fluid analysis report (gamma spectrometry, gross alpha/beta, properties of single stage flash, water flash gas composition, flashed water analysis, hydrocarbon molecular weights and densities, ionic species molar mass and valence.
INJECTION TESTING	UD-1 Injection testing report (key parameters of well, injection rates and pressures, flow rates, seismicity)
	UD-2 Injection testing report (key parameters of well, injection rates and pressures, flow rates)
	ESP reservoir testing results (permeability, flow rates, seismicity)
	United Downs porosity models
	ESP power consumption and motor temperature during testing

Table 4.4: List of publications associated with the UDDGP project, including the data published.

Paper	Author/s	Data	Location
An Update on the United Downs Geothermal Power Project, Cornwall, UK (Stanford 2022)	Hazel Farndale & Ryan Law	Lithology, QEMSCAN plots, key parameters of wells, structural geology (faults/linear features), seismicity, hydraulic analysis, criterial for future sites.	https://pangea.stanford.edu/ERE/db/IGAstandard/record_detail.php?id=35392
Effective Community Engagement: The United Downs Geothermal Power Project, Cornwall, UK	Jane Charman, Ryan Law, Steve Beynon & Hazel Farndale	Time line of project, community engagement strategies and outcomes	https://europeangeothermalcongress.eu/abstracts-paper/
An Update on the United Downs Geothermal Power Project, Cornwall, UK (EGC 2022)	Hazel Farndale, Ryan Law & Steve Beynon	Lithology, QEMSCAN plots, key parameters of wells, structural geology (faults/fractures/lodes), drilling mud losses, micro-seismicity, hydraulic analysis, criterial for future sites.	https://europeangeothermalcongress.eu/abstracts-paper/
An Update on the United Downs Geothermal Power Project, Cornwall, UK (GRC 2022)	Hazel Farndale, Ryan Law & Steve Beynon	Lithology, QEMSCAN plots, key parameters of wells, structural geology (faults/fractures/lodes), drilling mud losses, micro-seismicity, hydraulic analysis, criterial for future sites.	https://europeangeothermalcongress.eu/abstracts-paper/
A single multi-scale and multi-sourced semi-automated lineament detection technique for detailed structural mapping with applications to geothermal energy exploration.	Chris Yeomans, Hester Claridge, Alexander Hudson, Robin Shail, Cees Willems, Matthew Eyre & Chris Harker	Lineament detection and structural mapping.	http://mr.crossref.org/iPage?doi=10.1144%2Fqjegh2022-051
Geological Overview of the United Downs Deep Geothermal Power Project, Cornwall, UK (WGC 2020)	Lucy Cotton, Jon Gutmanis, Robin Shail, Chris Dalby, Tony Batchelor, Andy Foxford & Gavyn Rollinson	Mapping of the Porth Towan Fault Zone, lithological data, QEMSCAN plots	https://pangea.stanford.edu/ERE/db/IGAstandard/record_detail.php?id=33107
Implementation of an Induced Seismicity Protocol for the United Downs Deep Geothermal Power Project, United Kingdom EGC2022	Andrew Jupe, Ryan Law & Hazel Farndale	Induced seismicity	https://europeangeothermalcongress.eu/abstracts-paper/

An Early Numerical Prediction of the United Downs Deep Geothermal Power Project, United Kingdom (WGC 2021)	Musa D. Aliyu & Rosalind A. Archer	Fluid flow, heat transport, geomechanical process, fault permeability, mass source and sink, heat source and there-hydro-geomechanical coupling equations. Estimations of: effect of flow rate on production temperature, effect of flow rate on injection pressure, effect of flow rate on fault zone permeability, effect of production pressure on temperature, production flow rates, effect of flow rate on thermal energy extraction and effect of flow rate on impedance.	https://pangea.stanford.edu/ERE/db/IGAstandard/record_detail.php?id=32833
Geothermal exploration and reservoir modelling of the United Downs deep geothermal project, Cornwall (UK) (Geothermics, 2021)	John Reinecker, Jon Gutmanis, Andy Foxford, Lucy Cotton, Chris Dalby & Ryan Law	Mapping of faults, mines, adits, granite, surface from granite, lodes, dykes, structural dip direction. Well schematics and trajectories Lithology, structural profile (inc. fractures) of UD-1, induced seismicity, drilling mud losses. Fracture network characteristics (inc. stereonets of faults and fractures), Stress orientation derived from borehole breakouts (BO) and drilling induced tensile fractures (DITF), temperature (& gradient), C1, C2, CO_2, gamma-ray, stress, reservoir modelling.	https://www.sciencedirect.com/science/article/pii/S0375650521001838
The importance of tectonic inheritance and reactivation in geothermal energy exploration for EGS resources in SW England. (WGC 2020+1)	Chris Yeomans, Robin Shail & Matthew Eyre	Structural geology, lineament mapping	Proceedings of the World Geothermal Congress 2020+1, Reykjavik, Iceland, April - October 2021, paper 11099, 11pp.
Geothermal Power Generated From UK Granites (GWatt). (WGC2020+1)	Chris Rochelle, Jon Busby, Andrew Kilpatrick, Robin Shail, Chris Yeomans, Matthew Eyre, Sabine den Hartog, Dan Arnold, Sebastien Geiger, Andreas Busch, Peter Ledingham, Ryan Law, Caroline Carrol and	Introduction to, and overview of, the GWatt project	Proceedings of the World Geothermal Congress 2020+1, Reykjavik, Iceland, April - October 2021, 7pp.

	members of the GWatt project team		
Seismic Monitoring at the United Downs Deep Geothermal Power Project, Cornwall, UK (WGC 2020)	Andrew Jupe & Peter Ledingham	Location of seismicity associate with UDDGP	https://pangea.stanford.edu/ERE/db/IGAstandard/record_detail.php?id=33563
Education and Community Outreach Programmes at the United Downs Deep Geothermal Power Project, Cornwall, UK (WGC 2020)	Lucy Cotton, Jane Charman, Suzie Doe & Peter Ledingham	Education and community outreach overview	https://pangea.stanford.edu/ERE/db/IGAstandard/record_detail.php?id=33106
United Kingdom Country Update (WGC 2020)	Tony Batchelor, Robin Curtis & Jonathan Busby	Overview of the progress of the UK geothermal industry in 2020.	https://pangea.stanford.edu/ERE/db/IGAstandard/record_detail.php?id=33709
The United Downs Deep Geothermal Power Project (WGC 2020)	Peter Ledingham & Lucy Cotton	Overview of the UDDGP, heat flow, geology, PTF, well configuration, drilling, noise & microseismic monitoring, community & education, preliminary results.	https://pangea.stanford.edu/ERE/db/IGAstandard/record_detail.php?id=33709
The United Downs Deep Geothermal Power Project (Stanford 2019)	Peter Ledingham & Lucy Cotton	Overview of the UDDGP, heat flow, geology, PTF, well configuration, drilling, noise & microseismic monitoring, community & education.	https://pangea.stanford.edu/ERE/db/IGAstandard/record_detail.php?id=29039
The United Downs Deep Geothermal Power Project (Stanford 2019)	Peter Ledingham, Lucy Cotton & Ryan Law	Overview of the UDDGP, heat flow, geology, PTF, well configuration, drilling, noise & microseismic monitoring, community & education.	https://pangea.stanford.edu/ERE/db/IGAstandard/record_detail.php?id=29039
Integrated object-based image analysis for semi-automated geological lineament detection in southwest England.	Chris Yeomans, Robin Shail & Matthew Eyre	Lineament detection from remote sensing data	Computers and Geosciences, 123, 137-148.
Geothermal Energy Use, Country Update for United Kingdom (EGC 2016)	Robin Curtis, Ryan Law & Charlotte Adams	Policy, geothermal utilisation, deep coaxial projects, EGS/HDR projects, GSHP activity, mine water.	https://pangea.stanford.edu/ERE/db/IGAstandard/record_detail.php?id=27358
Country Update for the United Kingdom (WGC 2015)	Tony Batchelor, Robin Curtis, Peter Ledingham & Ryan Law	Policy, geothermal utilisation, deep coaxial projects, EGS/HDR projects, GSHP activity, mine water.	https://pangea.stanford.edu/ERE/db/IGAstandard/record_detail.php?id=23189
Geothermal Energy Use, Country Update for United Kingdom (EGC 2013)	Robin Curtis, Peter Ledingham, Ryan Law & Tony Batchelor	Policy, geothermal utilisation, deep coaxial projects, EGS/HDR projects, GSHP activity, mine water.	https://pangea.stanford.edu/ERE/db/IGAstandard/record_detail.php?id=19345
Revisiting Deep Geothermal Power in the United Kingdom	Ryan Law, Tony Batchelor & Pete Ledingham	New projects, geology, stress regimes, temperatures	https://pangea.stanford.edu/ERE/db/IGAstandard/record_detail.php?id=6691

Geothermal energy in the UK: The life-cycle environmental impacts of electricity production from the United Downs Deep Geothermal Power project	Andrea Paulilloa, Lucy Cotton, Ryan Law, Alberto Strioloa & Paola Lettieri	The UDDGP concept, hot-spot and scenario analysis	https://www.sciencedirect.com/science/article/abs/pii/S0959652619342805
Raspberry Shake Instruments Provide Initial Ground Motion Assessment of the Induced Seismicity at the United Downs Deep Geothermal Power Project in Cornwall, United Kingdom	Joanna M. Holmgren & Maximilian J. Werner	Raspberry shake seismicity, ground-motion analysis, local magnitude analysis	https://pubs.geoscienceworld.org/ssa/tsr/article/1/1/27/598705/Raspberry-Shake-Instruments-Provide-Initial-Ground
Down-dip circulation at the united downs deep geothermal power project maximizes heat recovery and minimizes seismicity	Quan Gan, Zijun Feng, Lei Zhoua, Honglian Li, Jun Liu & Derek Elsworth	Well pattern, induced seismicity, fault reactivation	https://www.sciencedirect.com/science/article/pii/S0375650521001644
Seismic Monitoring of the United Downs Deep Geothermal Power Project (UDDGP) Site with Public Seismic Networks	G. Rodríguez-Pradilla & J. Verdon	Seismic monitoring	https://www.earthdoc.org/content/papers/10.3997/2214-4609.202113053
Hydrothermal Numerical Simulation of Injection Operations at United Downs, Cornwall, UK	Saeed Mahmoodpour, Mrityunjay Singh, Christian Obaje, Sri Kalyan Tangirala, John Reinecker, Kristian Bär & Ingo Sass	Structural geology, lithology, flow rates/pressures,	https://www.mdpi.com/2076-3263/12/8/296/htm

4.3.3 The Eden Geothermal Project

The Eden Geothermal project is an endeavour by Eden Geothermal Limited (EGL) to access the heat resource of the St Austell Granite, which is to the east of the Carnmenellis and the work at United Downs described in the previous section. EGL has been set up by three partners; the Eden Project, EGS Energy Ltd, and Bestec (UK) Ltd. The Eden Geothermal project is not a partner within the CRM-geothermal project, and so we do not have detailed knowledge of, or access to, the datasets being generated. The text below is therefore written in more general terms. Further information about the site, together with contact details of Eden Geothermal Ltd, can be found on their web site: https://www.edengeothermal.com/the-project/ .

As per the United Downs Deep Geothermal Power project above, the Eden Geothermal project targets another of the NNW-SSE crosscourse fracture zones, this time the 'Great Crosscourse' in the Saint Austell Granite (Figure 4.9). The surface location of this crosscourse structure was accurately located using observations of exposures when the Eden project site was a working quarry (open pit mining for the extraction of china clay), and also surface electrical resistivity tomography (ERT).

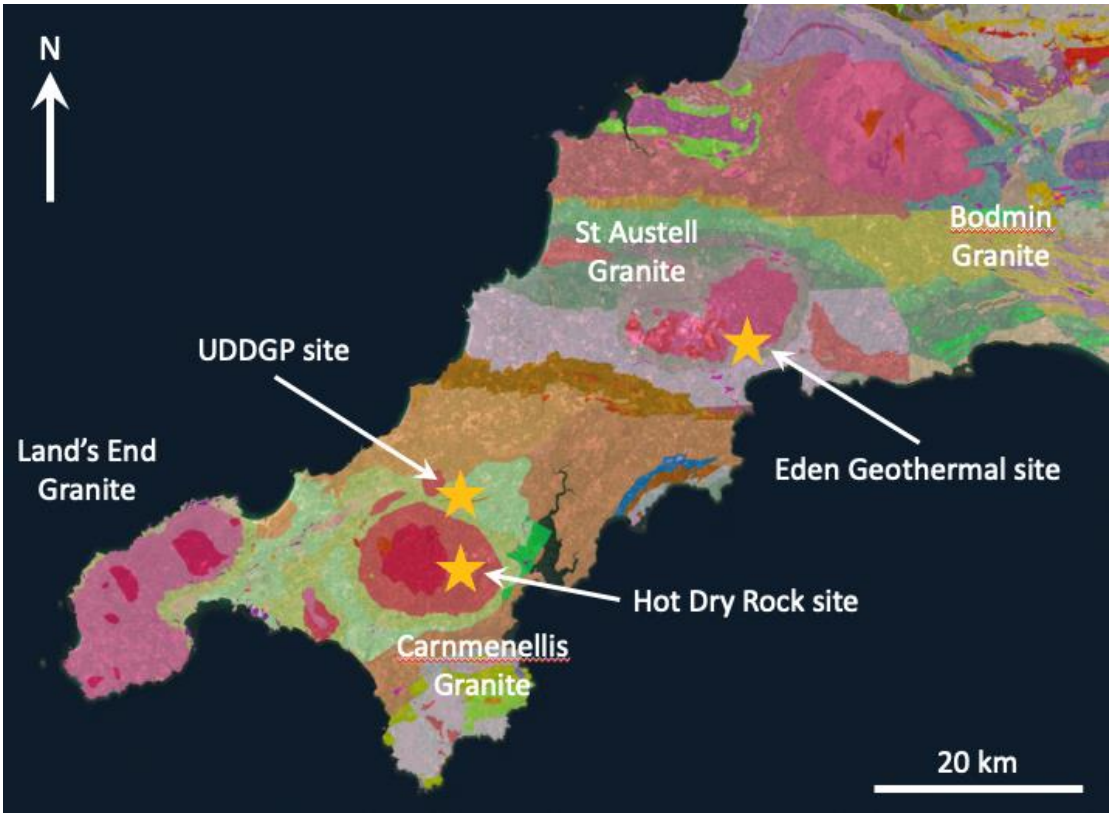

Figure 4.9: Location of the Eden geothermal project in relation to other deep geothermal sites in Cornwall (granites are pink and red, base map from BGS geological data).

The Eden geothermal site is at the northern end of the Eden Project site, and is being developed in 2 stages:

1) Drilling of an initial borehole (EG-1) to provide heat (via a downhole heat exchanger) to the biomes at the Eden project, in order to reduce use of a fossil-fuel heating system and make greenhouse gas savings.
2) Drilling of a second borehole and creation of a doublet system, in order to provide enough hot water to add a power production unit, and also hot water for a heat network to local houses.

Unlike the UDDGP project, the EG-1 borehole enters the target fracture zone though its footwall. A consequence of this is a slightly longer borehole length compared to its true vertical depth (5277 m versus 4871 m). With a length of 5277 m, EG-1 is the longest geothermal borehole in the UK – though not the deepest, see section above.

At the time of writing this report, the project is within phase (1) above:

- EG-1 is a 5277 m long deviated borehole that has been drilled to a true vertical depth of 4871 m, and completion operations have been undertaken.
- The lowermost 1417 m of the borehole have been left open, which coincides with a number of drilling fluid loss zones (i.e. potential permeable zones for geothermal fluid flow).
- Various logging operations of the borehole have been undertaken.
- Testing of the borehole is ongoing, including: mainly water injection to test permeability and develop the accessible geothermal 'reservoir', but there were also some short production tests. There was a small felt seismic event in early 2022 and this caused a pause in borehole testing. Some acidic stimulation has also been done as part of the MEET project (https://www.meet-h2020.com).
- The surface pipeline to the Eden Biomes as part of the local heat network has been installed, but the downhole heat exchanger is not yet in place.

Phase 1 continues, and the funding for Phase 2 of the project has not yet been secured.

Work within Phase 1 has produced a number of datasets, and in broad terms these are:

- Background geology of the site and its surroundings (including information from: BGS regional surveys, opencast mining plans, PhD and Masters studies by students at Camborne School of Mines [Exeter University]), as well as specific studies by Eden Geothermal Ltd.
- Site-specific investigations (including: characterisation of the drill chips, a range of borehole logs, pumping tests). Note that no drill core was recovered from the EG-1 borehole.

As far as we are aware, the short production tests have focussed on deriving water flow rates, and hence overall rock permeability. There would appear to not have been longer-term production testing and recovery of relatively undisturbed geothermal water (and gases). As such, there remains uncertainty as to the precise composition of the deep geothermal fluid beneath the Eden geothermal site. It is anticipated that longer-term production testing will be done at some point in the future, though it is possible that this could be part of the Phase 2 programme.

4.4 FLUIDS AND DISSOLVED RESOURCES

Fluids associated with both Sn-W greisen and Sn-Cu polymetallic lode mineralisation in south-west England are primarily of magmatic origin. In contrast, fluids associated with post-granite crosscourse mineralisation are associated with flow from sedimentary basins to the sides of the granite batholith. More recent waters within the crosscourses and other fractures in the granites are also associated with increasing amounts of meteoric input. It is these more modern waters that carry the dissolved resources. Here we provide a summary of information about these fluids.

4.4.1 Ancient fluids linked with ore mineralisation

Academic research in south-west England during the past 30 years has focussed on the nature of mineralising fluids, and their role in metal transport and ore deposit formation. Fluid inclusion (i.e. fluids trapped during mineral growth) studies have been invaluable in revealing the composition (salinity), temperature and in some cases the pressure of the mineralising fluids. Complimentary stable isotope studies (e.g. O, H, He and S) have also provided useful information on the source of the mineralising fluids (e.g. He signatures suggest a mantle-derived volatile component) (Shail *et al.*, 2003). Studies of shallow groundwaters (down to c. 100 m), as part of the HDR programme have provided insights into water-rock interaction over short time intervals and at shallow depths. Similar studies of deep, thermal spring waters from disused mines provide information on fluid circulation and mixing. When combined these data (e.g. shallow groundwater and mine water composition, and fluid inclusion studies) have enabled important conclusions to be drawn regarding palaeofluid circulation in both the granites and country rocks of south-west England (Smedley, *et al.*, 1989).

Broadly two dominant fluid types have been implicated in the formation of mineralisation in south-west England:

3) Moderate to high salinity ($NaCl+CO_2$), high temperature magmatic fluids that produced the granite-related mineralisation (e.g. polymetallic Sn-Cu lodes).
4) High salinity ($NaCl+CaCl_2$), lower temperature basinal fluids that formed the younger, post-magmatic mineralisation (e.g. crosscourses) (Table 4.5).

Stable isotope studies (i.e. Cl, O, H, He and S) on fluids taken from inclusions in the mineralisation have provided useful insights in to the origin of mineralising fluids. For example, isotopic studies of main stage, polymetallic lodes indicate that mineralising fluids were principally magmatic in origin, whilst fluids associated with later crosscourses are distinctly non-magmatic, having a strong sediment-derived fluid signature (Wilkinson *et al.*, 1995; Gleeson *et al.*, 1999; Banks *et al.*, 2000; Shail *et al.*, 2003).

Table 4.5: Summary of fluid inclusion data for mineralising fluids (Smith *et al.*, 1996 and Gleeson *et al.*, 2001).

Mineralisation style	Temperature	Salinity	Composition
Greisen[1]	450–350 °C	5-10 wt. %	NaCl±CO_2
Polymetallic lode (Sn-Cu)[2]	280–200 °C	3–15 wt. %	NaCl
Polymetallic lode (Pb-Zn)[2]	c.220 °C	0–5 wt. %	NaCl
Crosscourse[2]	c.130 °C	26 wt. %	NaCl±$CaCl_2$

Warm (up to 55 °C), high-salinity groundwaters have been found at depths of up to 820 m, primarily issuing from crosscourses and lodes in mines at the northern edge of the Carnmenellis granite. These flows occur in mines in both the granite and in the killas. Some of the crosscourse flows have been discharging for more than 30 years, suggesting that a large reservoir of saline, thermal water exists at depth (Smedley *et al.*, 1989). These deep spring waters 31–55 °C, mildly acidic to neutral (pH 5.4–7.7), and compositionally they are dominated by Na, Ca and Cl (Smedley *et al.*, 1989) (Table 4.6). Stable oxygen ($\delta^{18}O$) and hydrogen ($\delta^{2}D$) isotope studies indicate that these waters are not derived from seawater, but are more likely diluted palaeobrines which have flowed through crosscourse structures within the granite and killas. Their chemical and isotopic signatures also indicate mixing and dilution by circulation of local meteoric water (Alderton and Sheppard, 1977; Smedley *et al.*, 1989).

Low salinity, shallow groundwaters from within the granite and killas show considerable compositional overlap. However, slight differences can be observed in both the major cation (i.e. Ca, Mg, Na and K) and anion (i.e. HCO_3, SO_4, Cl and NO_3) contents of these waters. Granite-related shallow groundwaters are more acidic (pH 4.3–6.9) and are dominated by Na, K and Cl, whilst killas-related groundwaters are more alkaline (pH 4.9–8.0), and have compositions dominated by Ca, Mg and HCO_3. The higher overall concentration of elements (e.g. Ca, Mg, Cl, etc.) in killas-related groundwaters suggests that that the killas is more reactive, or possibly more soluble, than the granite. The abundance of minerals such as calcite, dolomite, chlorite and clays in the killas may account for these higher concentrations by dissolution and precipitation, and ion-exchange reactions. Element enrichment and depletion patterns suggest that shallow groundwater compositions are strongly controlled by lithology. For example, granite-related waters typically have higher Ba and Rb contents, which likely reflects dissolution of alkali feldspar (Smedley *et al.*, 1989; Smedley and Allen, 2004).

Table 4.6: Summary of mine water compositions (n.r., 'not reported').

Parameter	South Crofty (420 level)	South Crofty (420 level)	Wheal Jane	Clifford United
Source	Smedley *et al.*, 1989		Alderton and Sheppard, 1977	
Depth	690	690	198	448
pH	6.79	5.38	7.70	n.r.
Temperature (°C)	45.3	34.3	31.5	52
Total dissolved solids	14,099	10,454	9,934	9,189
Na	3,210	1,890	2,073	2,043
K	138	66.8	127	111
Mg	51.6	94.8	29.5	32
Ca	1,670	1,630	1,326	1,166
Cl	8,750	6,500	6,110	5,628
SO_4	107	240	118	124
HCO_3	n.r.	n.r.	23.8	n.r.

Previous studies suggest that palaeo-fluid flow in and around the Carnmenellis granite can be divided in to four main stages (Figure 4.10):

a) Expulsion of early magmatic fluids associated with the emplacement of the granite, which led to the formation of sheeted Sn-W greisens in the granite roof zone and overlying metasedimentary rocks. Hydrothermal convection of formation waters starts to occur in response to the thermal anomaly created by the granite emplacement.

b) Copper, zinc and sulfur are leached from the host rocks. Formation waters are drawn down through the granite as the system begins to cool, resulting in the deposition of Cu-Zn-sulfides in veins.

c) Main-stage, polymetallic lodes are emplaced within the granite roof zone by further expulsion of magmatic fluids.

d) Formation waters start to circulate through the granite in response to cooling of the system, resulting in the deposition of Cu-Zn-sulfides in steeply dipping fissures (Smedley, *et al.*, 1989). Post-magmatism basinal brines circulate through N-S-trending structures within the granite and killas, mixing with meteoric waters. These fluids deposited Pb-Zn-rich mineralisation within the so called crosscourse veins (Scrivener *et al.*, 1994; Gleeson *et al.*, 2000; 2001).

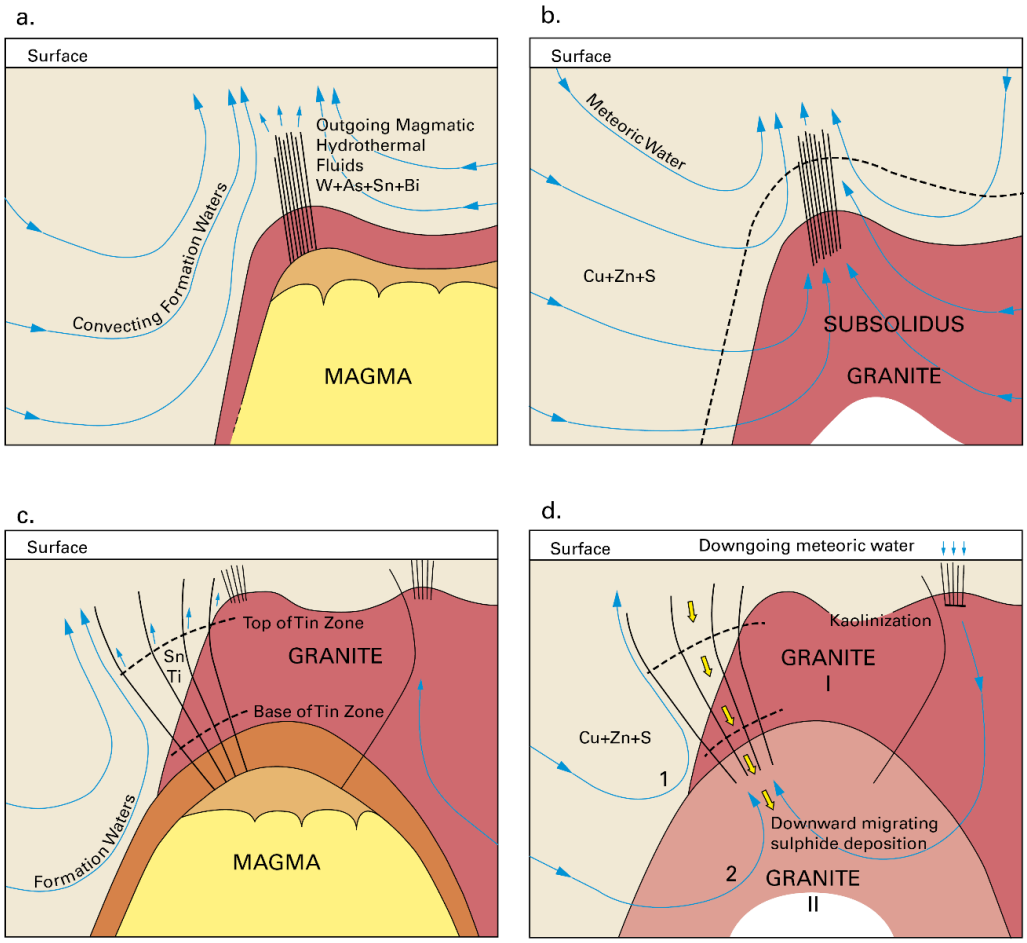

Figure 4.10: Schematic diagram illustrating fluid flow regimes in relation to emplacement of the Carnmenellis granite. (a) Expulsion of magmatic fluids forming Sn-W greisens and generation of hydrothermal convection in overlying groundwaters. (b) Leaching of metals and sulfur from the host rocks. Cooling of the system permits meteoric waters to pass down into the granite pluton. (c) Main stage, polymetallic lodes form in the roof zone of the granite pluton by expulsion of magmatic fluids. (d) Meteoric waters circulate through the granite as the system cools. Cu-Zn sulfides are deposited in a series of lodes (re-drawn after Smedley, *et al.*, 1989).

4.4.2 Present-day waters and dissolved mineral resources

The main source of information on the waters and their dissolved mineral content comes from:

- The Hot Dry Rock project (see previous sections for details)
- The United Downs Deep Geothermal Power project (UD-1 production testing)
- Intermediate depth boreholes drilled and produced by Cornish Lithium Ltd (range of depths to about 1.8 km)

The first of the above sources is summarised in Section 4.2.1 above, with the more recent work summarised in the two sections below.

4.4.2.1 Deep waters at United Downs

The recently-drilled 5 km deep UD-1 borehole went under an extended pumping (ESP) test for several days at end June/early July 2021. Whilst the test was short and the borehole infrastructure did not reach thermal equilibrium, the produced water was hot enough to boil and generate steam once at surface (Figure 4.11). The test was primarily aimed at determining the flow characteristics of the borehole. However, 19 water samples were recovered during the production operation, and analysed by the BGS as part of the GWatt project (Rochele et al., 2021) and Cornish Lithium for a range of major and trace cations and anions, plus also a range of isotopes. In summary, the water is a relatively low salinity, Na/Cl-dominated deep groundwater, and is consistent with extrapolation of data from the Hot Dry Rock project. Datasets of water chemistry, isotopic content, and gas composition exist, and at the time of writing this report are being incorporated into publications.

Some 150 m^3 of the produced water from UD-1 was recovered by Cornish Lithium Ltd and stored in large tanks, for the purpose of future testing of a range of lithium extraction technologies (Figure 4.12).

Figure 4.11: Steam rising from production equipment during testing of the UD-1 borehole at United Downs. (BGS image, ©UKRI)

Figure 4.12: Thermal image of water storage tank during the testing of the UD-1 borehole at United Downs. The level of the warm water is clearly visible inside the tank. (BGS image, ©UKRI).

4.4.2.2 Intermediate-depth waters in the United Downs area

Intermediate depth waters in the United Downs area have been evaluated during recent exploration (by Cornish Lithium Plc (CL) who have undertaken three drilling campaigns to a maximum depth of 1750 m (as of November 2022). Two boreholes at United Downs (hereafter GWDD_001 & GWDD_002) have been drilled to a depth of c. 860 m and c. 1100 m respectively. A further borehole has been drilled at Crosslanes Farm, Twelveheads (GWDD_003) to a depth of c. 1750 m (Figure 4.13). The primary focus of these drilling campaigns was to determine lithium concentrations within geothermal springs flowing through naturally fractured fault zones at depth. Test work undertaken to date has been both geochemical sampling of fluids pumped to surface, and hydraulic injection testing.

Geochemical analysis of the water pumped to surface shows similar characteristics and chemical ratios to that within the deeper geothermal fluids. The reservoir is characterised by low-salinity fluids that have a relatively high dissolved lithium component. Figure 4.14 shows the mixing series between "mature" reservoir waters that have high Cl contents, and the immature meteoric waters as described from the CL mine waters archive. An element of mine-water derived constituents can be seen in the chemical signatures of waters found proximal to massive sulphide mining territories, however these signatures disappear with depth and over the duration of the pump test. Long-term test work has shown reservoir chemistry stabilises, and interception of mature waters can be achieved after a short amount of pumping, removing the meteoric water component quickly.

Datasets with geochemical, pumping, and hydraulic characterisation of GWDD_001 & GWDD_002 will be included within the report deliverable D5.1. This includes wireline geophysics logs.

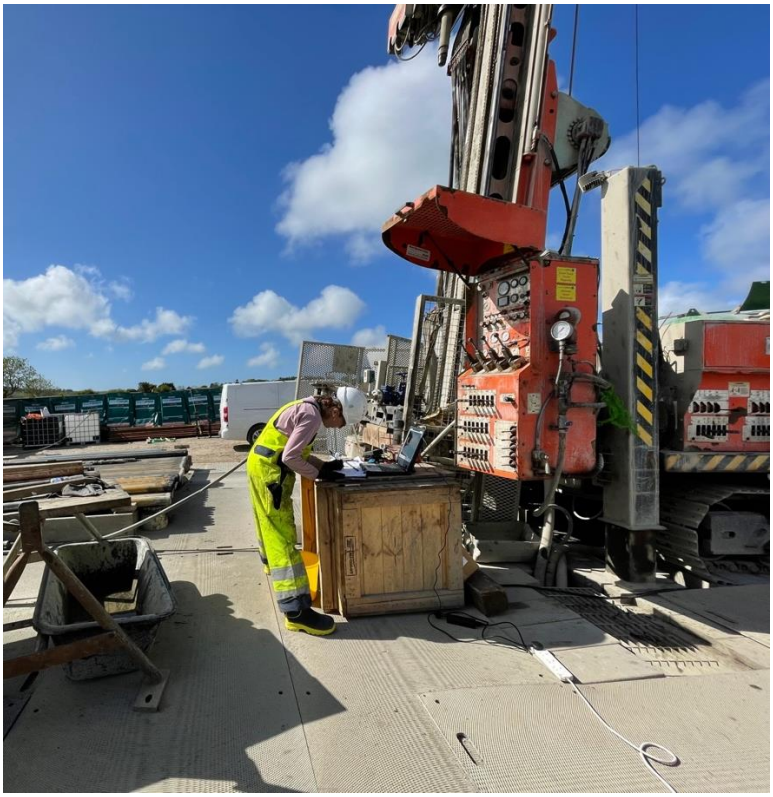

Figure 4.13: Water sampling undertaken at GWDD_003 during the summer 2022.

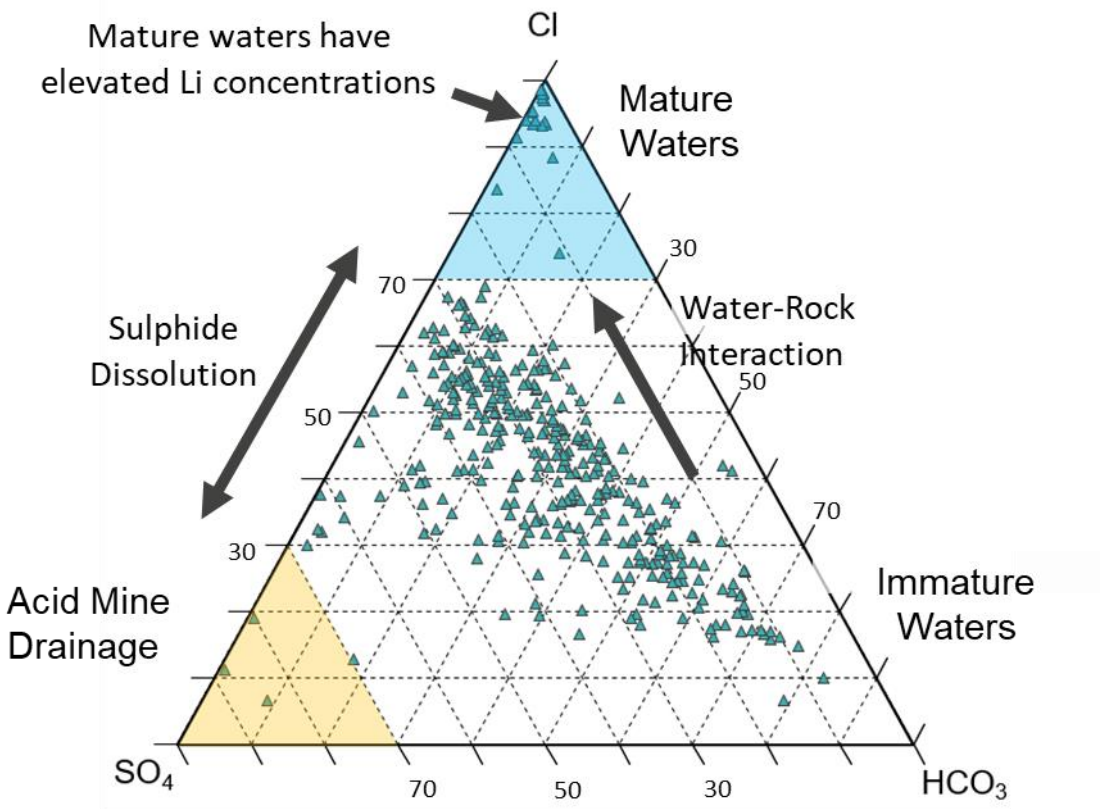

Figure 4.14: Mixing series of waters collated from CL's mine water database.

4.5 DEEP SUB-SURFACE TEMPERATURES IN SOUTH-WEST ENGLAND

4.5.1 United Kingdom overview

Between 1977 and 1994 the UK government funded an assessment of potential UK geothermal energy resources. This programme considered three main elements: (1) appraisal of heat flow; (2) potential of hot-brines from deep hyper-saline aquifers (HAS) for direct heat production; and (3) the potential of EGS, which included the HDR Programme. A catalogue of sub-surface temperatures, heat flow estimations, thermal conductivity measurements and geochemical data was compiled by BGS (Burley and Edmunds, 1978). It was subsequently updated by Burley and Gale (1982), Burley *et al.* (1984) and Rollin (1987). The findings of this work were summarised by Downing and Gray (1986a, 1986b), BGS (1988), Parker (1989, 1999) and most recently in Barker *et al*. (2000).

A heat flow map (Figure 4.15) of the UK was generated and subsequently revised (Downing and Gray, 1986a, b; Lee *et al.*, 1987; Rollin, 1995; Rollin *et al.*, 1995; and Barker *et al.*, 2000). The map shows two areas of enhanced heat flow that are associated with the radiogenic granites of south-west England (Cornwall) and the buried granites of northern England. Temperatures at 5 km depth were estimated to be as high as 180–190 °C in Cornwall, and up to 130–170 °C in northern England, but rarely exceeded 95 °C elsewhere. The average geothermal gradient is 26 °C km^{-1} but locally it can exceed ≈ 35 °C km^{-1} (Busby, 2010). The average UK heat flow is approximately 55 mWm^{-2}.

4.5.2 South-west England overview and historic data

Of specific interest to this project are the data for the south-west region of the UK, in particular Cornwall where the geothermal gradient is estimated to be highest. Barker *et al*. (2000) noted that the average heat flow in the Cornubian granites of south-west England is ≈ 120 mWm^{-2}. Heat production values for the Cornubian granites can be found in Wheildon *et al*. (1981) and Thomas-Betts *et al*. (1989). Beamish and Busby (2016) re-assessed the quality of these original data sets, and, in addition, recalculated the heat flows in accordance with our improved understanding of paleoclimate. This resulted in revised values that are higher than the original estimates, with the consequence that temperatures at depth are also greater i.e. at 5 km they range from approximately 185 °C for the Dartmoor granite to approximately 220 °C for the St Austell granite, (Figure 4.16) which is an increase of between 6 and 11 per cent. The vast majority of the temperature data comes from shallow wells (about 100 m), with additional data available from some former mines (e.g. Geevor mine at about 400 m and South Crofty at about 600 m). These estimated temperatures are based on a model that assumes constant heat production to a depth of 5 km.

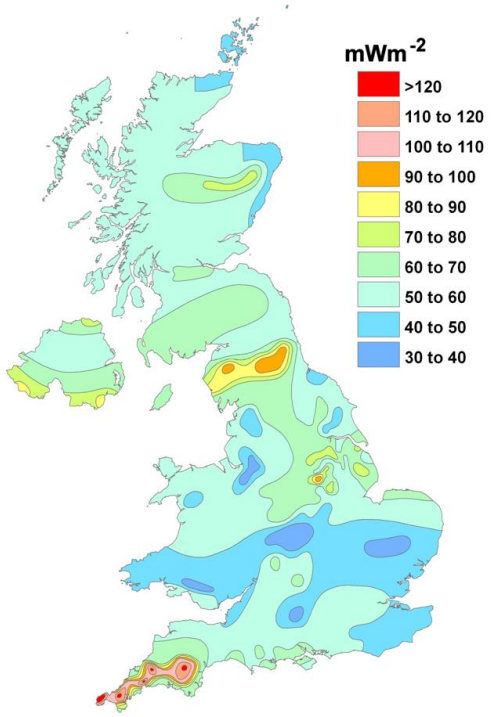

Figure 4.15: Heat flow map of the UK (after Busby, 2010).

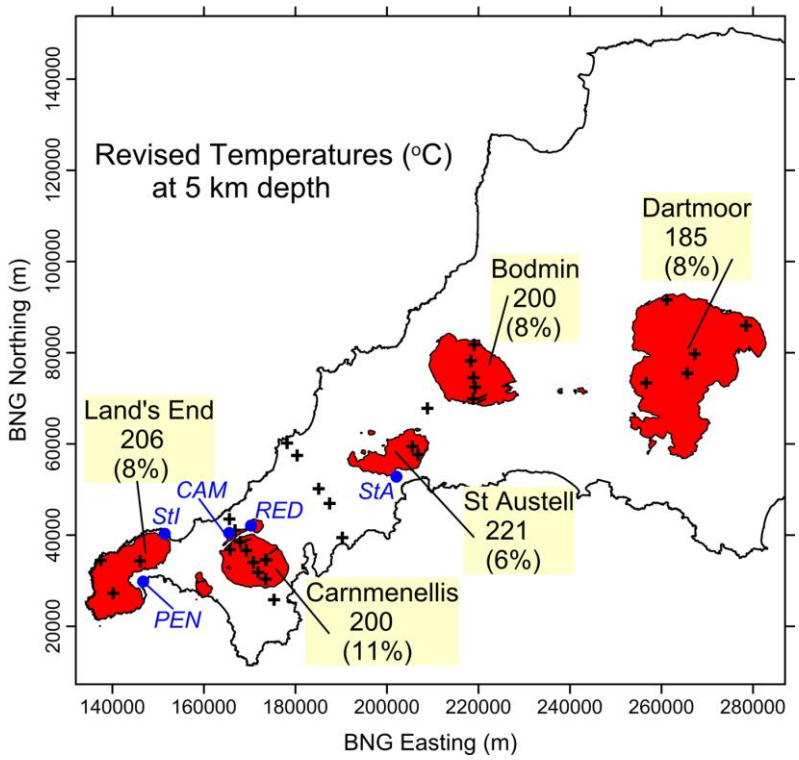

Figure 4.16: Revised estimated granite-related average temperatures (°C) at a depth of 5 km and the percentage increases (in brackets) over previously published estimates. Locations of five towns, are shown in blue; PEN = Pen zance; StI = St Ives; CAM = Camborne; RED = Redruth and; StA = St. Austell (after Busby and Beamish, 2016).

Historically, there were only very limited temperature data available from depths below 600 m, largely comprising data from the former HDR Project at Rosemanowes Quarry, near Redruth, on the Carnmenellis granite. Here three deep wells were drilled, the deepest being a 2,600 m vertical well, plus several shallow boreholes (300 m). Barker *et al*. (2000) reported that measured temperatures were about 80 °C at 2.1 km depth (in well RH12) and about 100 °C at 2.6 km (in well RH15). The revised heat flow data from Beamish and Busby (2016) gives slightly higher, estimated, subsurface temperatures of about 84 °C, and about 102 °C at 2.1 km and 2.6 km, respectively. Unfortunately, UK government funding was withdrawn from the HDR project before it could investigate conditions at 5–6 km, and it closed in 1994.

4.5.3 Recent geothermal developments

In the past 5 years, deep geothermal drilling has been undertaken at United Downs, an industrial estate just to the north of the surface expression of the Carnmenellis granite, plus also close to the Eden Project on the St Austell Granite.

The United Downs Deep Geothermal Power project (owned and managed by Geothermal Engineering Limited) targets a steeply-dipping crosscourse structure, the Porthtown Fracture Zone, in the Carnmenellis Granite. This is intercepted by the c. 5 km deep UD-1 production borehole at approximately 4.5 km, via the hanging wall. It is also intercepted by the UD-2 re-injection borehole at approximately 2.5 km, also via the hanging wall. The primary aim of the project is generation of electrical power via a binary power plant. However, some sale of heat to local businesses is anticipated (e.g. a rum distillery). The testing phase of this project is now complete, and delivery of the power plant is expected in 2023. Seven further sites for geothermal development are currently being explored by GEL, with one gaining planning permission in September 2022.

The Eden Geothermal project (owned and managed by Eden Geothermal Limited) also targets a steeply-dipping crosscourse structure, this time the Great Crosscourse, and is in the St Austell Granite. This is intercepted by the c. 4.5 km deep EG-1 borehole, this time via the footwall of the fracture zone. There is potential for a second borehole and development of a binary system, but as of late 2022 drilling of this borehole has not started. The primary aim of this project is supply of heat to the biomes at the Eden Project. However, with a second borehole and sufficient flow rates, Eden Geothermal Ltd are looking to produce some electrical power if possible.

Cornish Lithium Limited are still in exploration and development phases in terms of accessing dissolved lithium. However, if they do end up producing lithium-enriched water from their 1-2 km deep boreholes, then that would likely give rise to a thermal water source that could be used for geothermal heating purposes. This aspect is however, a subject for future studies.

In summary, a significant body of data exists from assessments of the potential geothermal energy resources in the UK, over a period spanning over four decades. South-west England, specifically Cornwall, was estimated to have the highest geothermal gradient in the UK. Temperatures at 5 km depth in the Cornubian granites are estimated to be in the range of about 185–220 °C, which has been proved at United Downs (Carnmenellis Granite). However, it is important to note that the estimates for the other granites are based on modelled heat flow and heat production, as data from depths of >600 m are very limited.

4.6 STRUCTURE AND STRESS-FIELD MEASUREMENTS

South-west England is a structurally complex region whose geological past has been dominated by Variscan tectonics. British Geological Survey mapping, academic research and seismic surveys have led to the identification of three main deformational phases associated with Variscan orogenesis. Two phases are related to crustal shortening (D_1 and D_2) whilst the third (D_3) is associated with crustal extension during orogenic collapse (Alexander and Shail, 1996; Leveridge *et al.*, 2002). The D_1 deformation event (c. 385 Ma) is characterised by:

1) Large-scale (10s km), NW-SE-trending strike-slip faults
2) A NNW-trending mineral lineation
3) E-W-trending folds.

Structures associated with the second deformation event (D_2) are similar to those formed during D_1, but D_2 structures are generally more steeply dipping. The D_3 event (c. 305–300 Ma) occurred in response to orogenic collapse and associated crustal extension. It resulted in the development of steep to gently inclined WNW-ESE-trending extensional faults (Alexander and Shail, 1996; Leveridge *et al.*, 2002). Regionally extensive NNW-SSE-trending crosscourse structures formed during the Permian in response to a period of crustal extension (Scrivener *et al.*, 1994; Shail and Alexander, 1997).

In south-west England both granite and the killas have inherently poor permeability (Heath *et al.*, 1985). Accordingly, fluid circulation in the region is largely controlled by regional-scale structures (e.g. NNW-SSE-trending faults) (Figure 4.17) and fractures (Heath *et al.*, 1985; Bromley *et al.*, 1989; Smedley *et al.*, 1989). The trend direction of these and similar structures is also picked up by automated analysis of surface and sub-sea lineaments, which reveal potentially far more NNW-SSE-trending structures (Figure 4.18) (Yeomans et al., 2019, 2021, 2022). Fractures in the granite are primarily the result of magma chamber processes, for example cooling and hydro-fracturing (caused by the movement of magmatic fluids). In contrast fractures in the killas are principally the result of granite emplacement. Local zones of high-fracture density, in both granite and killas, may also be associated with episodes of late faulting. The permeability and connectivity of these fractures, particularly at depth, remains enigmatic (Heath *et al.*, 1985), but is the focus of borehole testing activities at both United Downs and the Eden geothermal sites.

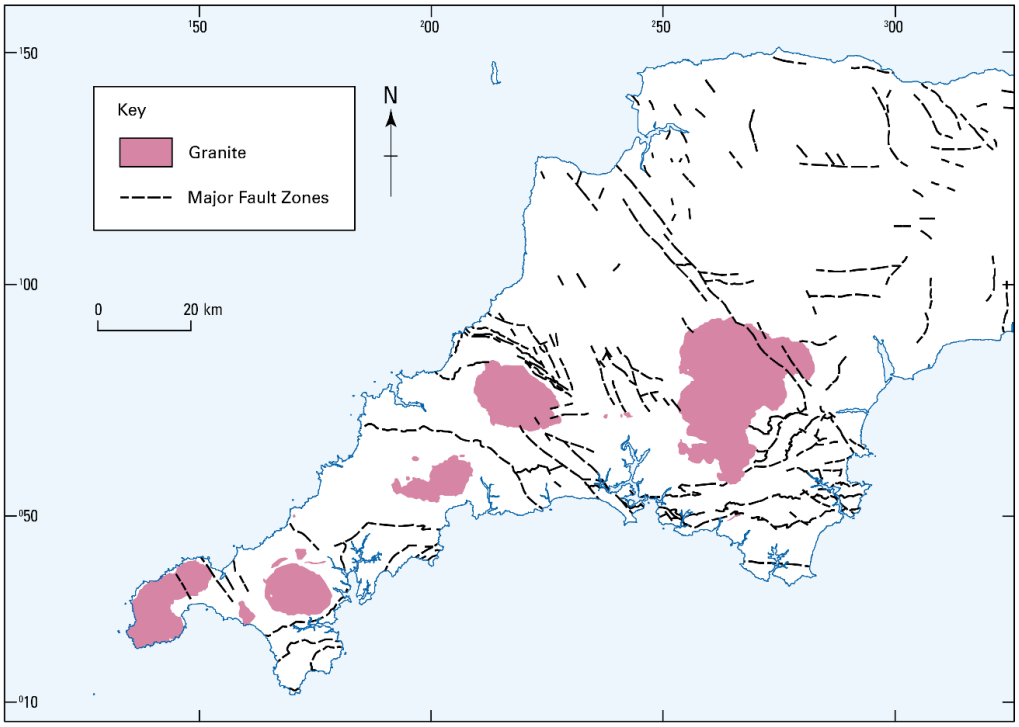

Figure 4.17: Map of the distribution of major NW-SE-trending faults and granite bodies in south-west England (drawn from BGS mapping data).

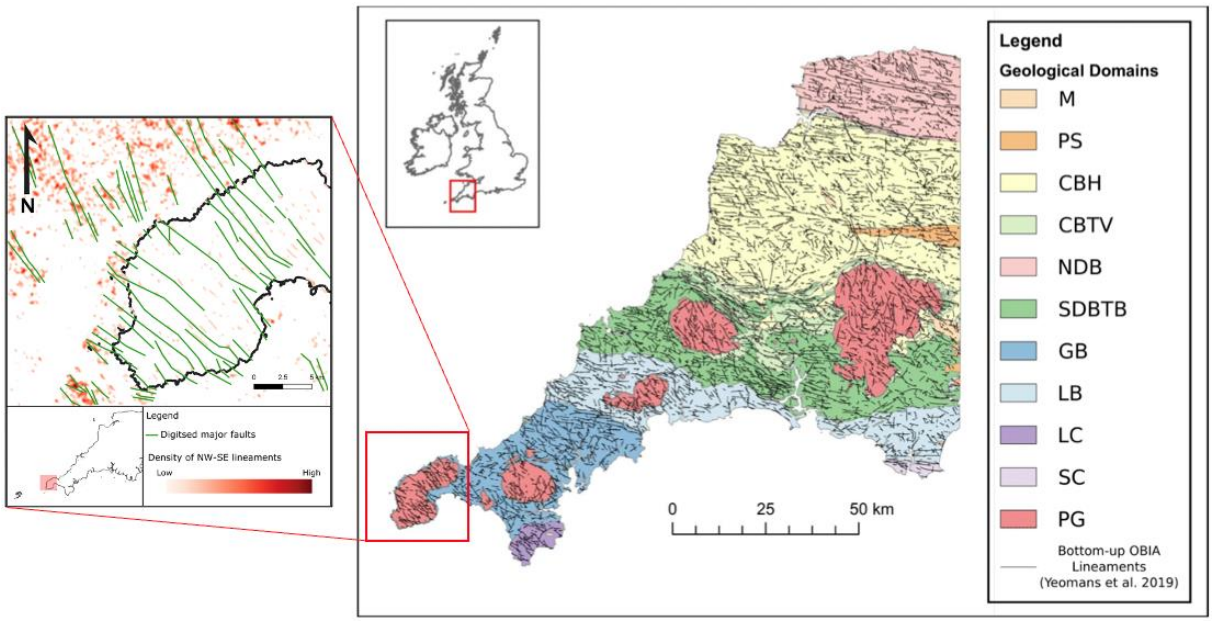

Figure 4.18: Map of the distribution of lineaments in south-west England (Yeomans et al., 2019, 2021, 2022).

A relatively small number of stress field measurements were made on the Carnmenellis granite, during the 1980s. Both hydraulic fracture tests and overcoring tests were conducted at the Rosemanowes HDR test site at depths of 0–2 km and 800 m, respectively. All of the tests were successful in achieving 'breakdowns' (i.e. the point at which the fluid pressure is high enough to fracture the rock), in only one of the tests was the hydraulic fracture fully characterised using microseismic monitoring. A series of overcoring tests were also conducted in the South Crofty mine (on the edge of the Carnmenellis granite) at a maximum depth of 790 m. A similar, but unrelated, set of stress field tests (i.e. hydraulic fracturing and overcoring) were carried out at Carwynnen quarry, also on the Carnmenellis granite. Although the hydraulic fracture tests and overcoring were conducted at much shallower levels (700 m and 34 m respectively) the two studies confirmed the presence of two joint sets in the Carnmenellis granite: one trending NNW-SSE-trending and the other ENE-WSW. The results from both studies show that the *in-situ* stress orientation is about 30° off parallel from that of the natural joint sets observed in the granite. The studies also demonstrated that maximum *in-situ* stress (σH) is approximately 70 MPa in the NNW-SSE direction, whilst the minimum *in-situ* stress (σh) is about 30 MPa in the ENE-WSW direction (Figure 4.19). It was found that stress magnitude and orientation at depth are relatively consistent across the Carnmenellis granite, and are fairly consistent with measurements from the rest of the United Kingdom. Importantly it was found that shearing along these natural joints was more likely than dilation, unless very high injection pressures were used (Pine and Batchelor, 1984; Evans, 1987; Cooling *et al.,* 1988; Haimson *et al.* 1989; Turnbridge *et al.,* 1989).

Studies linked to the United Downs Deep Geothermal Power project are also producing datasets relevant to stress information, and fracture directions/properties (e.g. Reinecher et al., 2021; and as part of the GWatt project [Haslam et al. – in prep; Baptie et al. – in prep]).

In summary, the south-west of England is a structurally complex region whose geological past has been dominated by Variscan tectonics, which resulted in at least three episodes of deformation. The permeability of rocks (i.e. granites and metasedimentary rocks) in south-west England is inherently very low, and as such faults and fractures are locally and regionally important in terms of fluid flow. In particular, the presence of large-scale, NNW-SSE-trending crosscourse structures are an important consideration for the design of any EGS system in south-west England. Initial flow tests from the UD-1 borehole provided encouraging results, indicating that the resource will sustain a 1-3MW_e binary power plant. However, greater understanding of the long-term behaviour of the reservoir will only come from sustained operation of the future power plant.

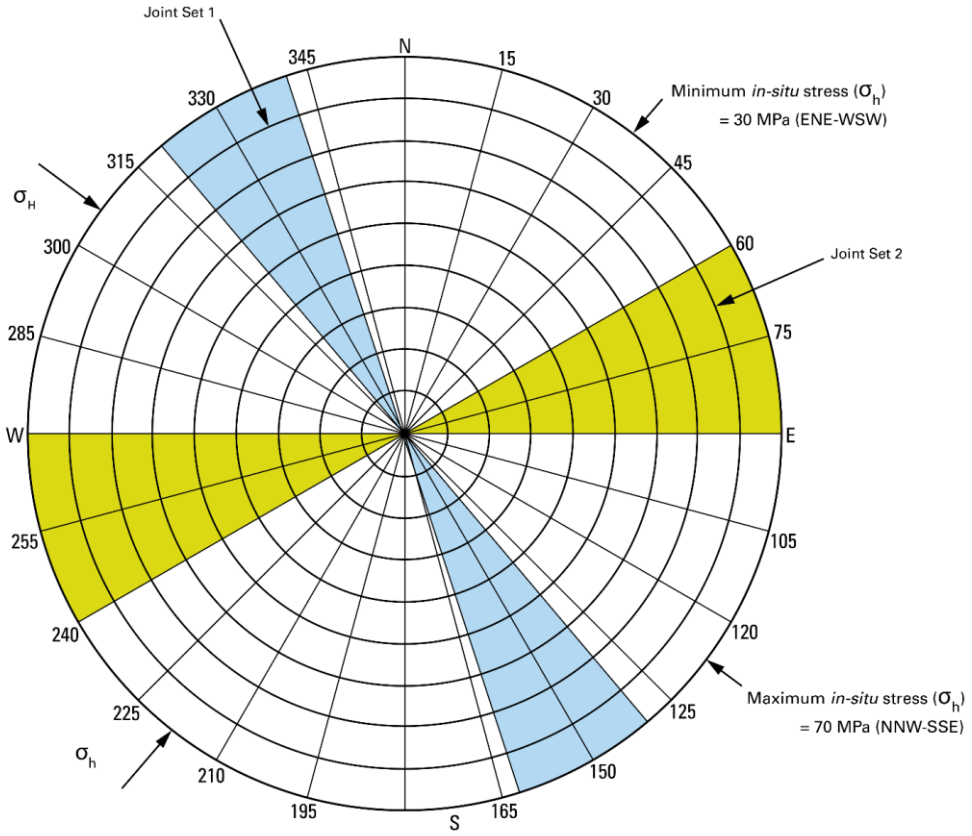

Figure 4.19: Principal stress orientation and magnitude in the Carnmenellis granite as determined by in-situ hydraulic fracture tests at the Rosemanowes HDR test site (re-drawn from Pine and Batchelor, 1984).

4.7 OTHER DATA HOLDINGS AT THE BGS

The BGS is the world's longest established national geological survey, and is the UK's premier provider of objective and authoritative geoscientific data. It has been gathering geoscience data and information about the subsurface in the UK and other countries for more than 180 years. It is a data-rich organisation with more than 500 datasets in its care, including environmental monitoring data, digital databases, physical collections (e.g. borehole core, rocks and minerals), records and archives. Importantly, a great many of these datasets are openly available, many of which provide complete, seamless UK coverage at a number of scales (Table 4.8). Certain other datasets may be subject to confidentiality clauses and/or licencing fees. Information about how to access these datasets can be found here: http://www.bgs.ac.uk/data/home.html?src=topNav.

These national datasets are available to the CRM-geothermal project and can provide a very useful starting point to assess dissolved raw material and geothermal potential in south-west England. Many of the datasets cover much of the UK, whereas others are specific to south-west England (e.g. geophysical data conducted as part of the TELLUS project, http://www.tellusgb.ac.uk/). Most of the data stored relate to surface exposures or the near-surface environment. Although, the datasets do contain much information about a large number of boreholes and mines, most do not extend below 100 m, and there is limited data below 1000 m. This places significant constraints on predictions when extrapolating the data to EGS depths (i.e. 4–6 km). The datasets are also of differing ages and levels of detail - reflecting changing national priorities over the past decades. In terms of geothermal development, much of the data are derived from a national programme of work in the 1980s and early 1990s. As a consequence, the data reflect monitoring technology and ideas at that time, and much of the data are in analogue format.

4.8 CONCLUSIONS

We describe the breadth of information available for south-west England, and relevant to the development of enhanced geothermal systems. South-west England is a geologically complex region with a long and significant history of metal mining, producing primarily tin and copper. The requirement to better understand the economic mineral potential of the region has resulted in almost 200 years of applied and academic research. These studies generated a huge volume of data that includes; geological mapping, geophysical and geochemical surveys, and numerous reports and peer-reviewed publications.

Cornwall is currently witnessing a revival in interest in geothermal exploitation, with projects focussed on both power generation and heat supply. These are producing significant amounts of data for the sites concerned (albeit that some data are currently restricted access for commercial reasons). Previous geothermal research in the region peaked between the 1970s-1990s and focussed largely on the high heat flows associated with the Cornubian granites. In 1984 a programme of work was undertaken by the BGS to assess the UK's geothermal potential. Over the same time period (1977–1984) the Camborne School of Mines was assessing the feasibility of creating HDR geothermal systems at the Rosemanowes quarry test site, on the Carnmenellis granite, Cornwall.

In summary a huge amount is known about the geology, mineralisation, fluid history and geothermal potential of south-west England. A significant body of data underpins this knowledge base, the majority of which is freely, or openly available. However, there are limitations. For example, much of this data (with the exception of a limited number of geothermal datasets – HDR, UDDGP project, Eden Geothermal), only relates to the upper 1000 m of the crust. This has significant implications regarding the accuracy of modelled conditions in an enhanced geothermal system (EGS) at greater depths. There are also 'gaps' in the data (e.g. very limited deep-geophysical data), and some datasets have not been updated since their creation several decades ago.

Table 4.7: Summary of relevant datasets held by the BGS.

Datasets	Description	Scale	Coverage	Access cost	Link
Hydrogeology					
Depth to groundwater	Spatial model showing depth (m) to the phreatic water table.	1:50,000	Great Britain	15p per km^2	http://www.bgs.ac.uk/products/hydrogeology/depthToGroundwater.html
Hydrogeological maps	Spatial model of aquifer potential based on geological formations.	1:625,000	UK	Free	http://www.bgs.ac.uk/products/hydrogeology/maps.html
Permeability	Spatial model showing flow regimes (e.g. fracture flow) and relative flow rates.	1:50,000	Great Britain	10p per km^2	http://www.bgs.ac.uk/products/hydrogeology/permeability.html
Geophysics and remote sensing					
LiDAR	High-resolution LiDAR digital terrain model (DTM) and digital surface model (DSM).	Resolution information on website	SW England	Free	http://www.tellusgb.ac.uk/data/home.html
Airborne magnetics	Airborne survey data showing variation in the magnetic field.	Resolution information on website	SW England	Free	http://www.tellusgb.ac.uk/data/airborneGeophysicalSurvey.html
Airborne radiometrics	Airborne survey data for the radioactive isotopes Th, U, and K.	Resolution information on website	SW England	Free	http://www.tellusgb.ac.uk/data/airborneGeophysicalSurvey.html
Land gravity	A database of over 165,000 gravity observations.	N.A.	Great Britain	Free	http://www.bgs.ac.uk/products/geophysics/landGravity.html
Geophysical borehole logs	An archive of geophysical downhole log data.	N.A.	Various	£30 per hole	http://www.bgs.ac.uk/products/geophysics/boreholeLogs.html

Datasets	Description	Scale	Coverage	Access cost	Link
Geology					
Geological maps	2D lithological and structural mapping (bedrock and superficial)	*1:50,000	UK	**20p per km^2	http://www.bgs.ac.uk/products/digitalmaps/DiGMapGB_50.html
UK3D	A 3D bedrock model of the UK at 1:625,000 scale	1:625,000	UK	Free	http://www.bgs.ac.uk/research/ukgeology/nationalGeologicalModel/gb3d.html
Boreholes					
Borehole database	A database of over one million records of boreholes, shafts and wells	N.A.	Great Britain	Free	http://www.bgs.ac.uk/products/onshore/SOBI.html
Borehole scans	Online access to more than one million borehole logs	N.A.	Great Britain	Free	http://www.bgs.ac.uk/data/boreholescans/home.html
Physical properties					
Rock stress	Online access to almost 1,000 rock stress measurements	N.A.	Great Britain	Free	http://mapapps.bgs.ac.uk/rockstress/home.html
Discontinuities	Spatial model of discontinuities in bedrock (e.g. fractures and faults)	1:50 000	Great Britain	**30p per km^2	http://www.bgs.ac.uk/products/groundConditions/discontinuities.html
Geochemistry					
GBASE south-west	Geochemical baseline survey of soils and stream sediments.	N.A.	SW England	Free	http://www.bgs.ac.uk/products/geochemistry/GbaseSWproducts.html
Minerals					
Britpits	A database of over 180,000 records of active/inactive mine & quarry workings	N.A.	UK	***£50 per region	http://www.bgs.ac.uk/products/minerals/BRITPITS.html

Footnotes:

* Other scales available (e.g. 1:25,000; 1:10,000; 1:625,000).

** Commercial rate. Free to use via the BGS web-based viewer: http://mapapps.bgs.ac.uk/geologyofbritain/home.html

*** The full dataset comprises fifteen regions.

4.9 REFERENCES

ALDERTON, D.H.M. and SHEPPARD, S.M.F. 1977. Chemistry and origin of thermal waters from southwest England. Institution of Mining and Metallurgy, B191-B195.

ALDERTON, D.H.M. 1993. Mineralization associated with the Cornubian Granite Batholith. 270-354 in Mineralization in the British Isles. Pattrick, R.A.D. and Polya, D.A. (Eds.). (London: Chapman and Hall).

ALEXANDER, A.C. and SHAIL, R.K. 1996. Late- to post-Variscan structures on the coast between Penzance and Pentewan, south Cornwall. Proceedings of the Ussher Society, Vol. 9, 72-78.

ANDREWS, J.N., HUSSAIN, N., FORD, D.J. and YOUNGMAN, M.J. 1989.The use of natural radioelement and radiogenic noble gas dissolution for modelling the surface area and fracture width of a Hot Dry Rock system. In Geochemistry in Relation to Hot Dry Rock Geothermal Development in Cornwall; British Geological Survey Research Report SD/89/2. Vol. 3.

ANDERSEN, J.C.Ø., STICKLAND, R.J., ROLLINSON, G.K. and SHAIL, R.K. 2016. Indium mineralisation in SW England: host paragenesis and mineralogical relations. Ore Geology Reviews, Vol. 78, 213–238.

BANKS, D.A., GLEESON, S.A. and GREEN, R. 2000. Determination of the origin of salinity in granite-related fluids: evidence from chlorine isotopes in fluid inclusions. Journal of Geochemical Exploration, 69-70, 309-312.

BARKER, J.A., DOWNING, R.A., GRAY, D.A., FINDLAY, J., KELLAWAY, G.A., PARKER, R.H. and ROLLIN, K.E. 2000. Hydrogeothermal studies in the United Kingdom. Quarterly Journal of Engineering Geology and Hydrogeology, 33, 41-58.

BEAMISH, D. and BUSBY, J. 2016. The Cornubian geothermal province: heat production and flow in SW England: estimates from boreholes and airborne gamma-ray measurements. Geothermal Energy, 4, 1-25.

BEER, K.E. and Scrivener R.C. 1982 Metalliferous mineralization. In: Geology of Devon, Durrance, E.M. and Manning, D.A.C. (Eds.), Univ Exeter, pp 117–147

BGS. 1988. Geothermal Energy in the United Kingdom: review of the British Geological Survey's Program 1984-1987. British Geological Survey, Keyworth.

BRAY, C.J., & SPOONER, E.T. 1983. Sheeted vein Sn-W mineralization and greisenization associated with economic kaolinization, Goonbarrow china clay pit, St. Austell, Cornwall, England; geologic relationships and geochronology. Economic Geology, 78(6), 1064-1089.

BRISTOW, C.M., & EXLEY, C.S. 1994. Historical and geological aspects of the china clay industry of south-west England. Transactions of the Royal Geological Society of Cornwall, 21(6), 247-314.

BROMLEY, A.V. 1989. The Cornubian Orefield. International Association of Geochemistry and Cosmochemistry, 6th International Symposium on Water–Rock Interaction, Malvern, UK, Field-Guide, Camborne School of Mines, Redruth.

BROMLEY, A.V., THOMAS, L.J., SHEPHERD, T.J. and DARBYSHIRE, D.P.F. 1989. Mineralogy and geochemistry of the Carnmenellis granite. In Geochemistry in Relation to Hot Dry Rock Geothermal Development in Cornwall; British Geological Survey Research Report SD/89/2. Vol. 5.

BROOKS, M., DOODY, J.J. & AL-RAWI, F.R.J. 1984. Major crustal reflectors beneath SW England. Journal of the Geological Society, London, 141, 97-103.

BURLEY, A.J. and EDMUNDS, W.M. 1978. Catalogue of geothermal data for the land area of the United Kingdom. Investigation of the Geothermal Potential of the UK, Department of Energy, London.

BURLEY, A.J. and GALE, I.N. 1982. Catalogue of geothermal data for the land area of the United Kingdom. First revision: August 1981. Investigation of the Geothermal Potential of the UK, Institute of Geological Sciences, Keyworth

BURLEY, A.J., EDMUNDS, W.M. and GALE, I.N. 1984. Catalogue of geothermal data for the land area of the United Kingdom. Second revision: April 1984. Investigation of the Geothermal Potential of the UK, British Geological Survey, Keyworth.

BURT, R., BURNLEY R., GILL, M. and NEILL, A. 2014. Mining in Cornwall and Devon Mines and Men. University of Exeter Press, Exeter.

BUSBY, J. 2010 Geothermal Prospects in the United Kingdom. Proceedings World Geothermal Congress, Bali Indonesia, 25-29 April 2010.

CHAPPELL, B.W. and HINE, R., 2006. The Cornubian Batholith: an example of magmatic fractionation on a crustal scale. Resource Geology, 56, 203–244.

CHEN, Y., CLARK, A.H., FARRAR, E., WASTENEYS, H.A.H.P., HODGSON, M.J. and BROMLEY, A.V. 1993. Diachronous and independent histories of plutonism and mineralization in the Cornubian batholith, southwest England. Journal of the Geological Society, London, 150, 1183-1191.

CHESLEY, J.T., HALLIDAY, A.N., SNEE, L.W., MEZGER, K., SHEPHERD, T.J. and SCRIVENER, R.C. 1993. Thermochronology of the Cornubian batholith in southwest England: implication for pluton emplacement and protracted hydrothermal mineralization. Geochimica and Cosmochimica Acta, 57, 1817-1835.

CLARK, A.H., CHEN, Y., FARRAR, E., WASTENEYS, H.A.H.P., STIMAC, J.A., HODGSON, M.J., WILLIS-RICHARDS, J. and BROMLEY, A.V. 1993. The Cornubian Sn-Cu (-As, W) metallogenetic province: product of a 30 m.y. history of discrete and concomitant anatectic, intrusive and hydrothermal events. Proceedings of the Ussher Society, 8, 112-116.

CLARK, A.H., CHEN, Y., FARRAR, E., NORTHCOTE, B., WASTENAYS, H.A.H.P, HODGSON, M.J, and BROMLEY, A. 1994. Refinement of the time/space relationships of intrusion and hydrothermal activity in the Cornubian Batholith (abstract). Proceedings of the Ussher Society, 8, 345.

CLAYTON, R.E., SCRIVENER, R.C. and STANLEY, C.J. 1990. Mineralogical and preliminary fluid inclusion studies of lead-antimony mineralisation in north Cornwall. Proceedings of the Ussher Society, 7, 258-262.

COOLING, C.M., HUDSON, J.A. and TURNBRIDGE, L.W. 1988. In situ rock stresses and their measurement in the U.K. –part II. site experiments and stress field interpretation. International Journal of Rock Mechanics and Mining Sciences & Geomechanics, Vol. 25(6), 371–382.

DANGERFIELD, J. and HAWKES, J.R. 1981. The Variscan granites of south-west England: additional information. Proceedings of the Ussher Society, 5, 116-120.

DARBYSHIRE, D.P.F. and SHEPHERD, T.J. 1994. Nd and Sr isotope constraints on the origin of the Cornubian batholith, SW England. Journal of the Geological Society, London, 151, 795-802.

DARBYSHIRE, D.P.F 1995. Late vein mineralisation in the Plymouth District NERC Isotope Geosciences Laboratory Report, No. 68.

DE LA BECHE, H.T. 1839. Report on the geology of Cornwall, Devon and West Somerset. Mem. Geol. Survey. London, Longman, Orme, Brown, Green and Longmans, 648.

DINES, H.G. 1934. The lateral extent of ore shoots in the primary depth zones of Cornwall. Transactions of the Royal Geological Society of Cornwall, 16, 279-296.

DINES, H.G. 1956. The metalliferous mining region of south-west England. Economic memoir of the Geological Survey of Great Britain.

DOMINY, S.C., CAMM, G.S., BUSSELL, M.A., SCRIVENER, R.C., and HALLS, C. 1995. A review of tin stockwork mineralization in the south west England orefield. Proceedings-Ussher Society, 8, 368-368.

DOWNING, R. A. AND GRAY, D. A. (Eds.) 1986a. Geothermal Energy – The potential in the United Kingdom. HMSO, London.

DOWNING, R. A. AND GRAY, D. A. 1986b. Geothermal resources of the United Kingdom. Journal of the Geological Society, London, 143, 499-507.

EDMUNDS, W.M., ANDREWS, J.N., BROMLEY A.V., RICHARDS, H.G., SAVAGE, D. and SMEDLEY, P.L. 1989. Application of geochemistry to Hot Dry Rock geothermal development: an overview. In Geochemistry in Relation to Hot Dry Rock Geothermal Development in Cornwall; British Geological Survey Research Report SD/89/2. Vol. 1.

EVANS, C.J. 1987. Crustal stress in the United Kingdom. Investigation of the Geothermal Potential of the UK, British Geological Survey Research Report WJ/GE/87/8.

EXLEY, C.S. & STONE, M. 1964. The granitic rocks of South-West England. In: HOSKING, K.F.G. & SHRIMPTON, G.J. (Eds.) Present view of some aspects of the geology of Cornwall, Blackford, Truro, 131-184.

EXLEY, C.S. and STONE, M. 1982. Hercynian intrusive rocks. In: SUTHERLAND, D.S. (Ed.) Igneous rocks of the British Isles, Wiley, Chichester. 287-320.

EXLEY, C.S., STONE, M. and FLOYD, P. 1983. Composition and Petrogenesis of the Cornubian Granite Batholith and post-orogenic volcanic rocks in Southwest England. In: HANCOCK, P.L. (Ed.) The Variscan foldbelt in the British Isles, Adam Hilger Ltd, Bristol. 153-177.

FLOYD, P.A., EXLEY, C.S. and STYLES, M.T. 1993. Igneous rocks of South-West England. Chapman and Hall, London.

GLEESON, S.A., WILKINSON, J.J., SHAW, H.F. and HERRINGTON, R.J. 2000. Post-magmatic hydrothermal circulation and the origin of base metal mineralization, Cornwall, UK. Journal of the Geological Society, London, 157, 589-600.

GLEESON, S.A., WILKINSON, J.J., STUART, F.M. and BANKS, D.A. 2001. The origin and evolution of base metal mineralising brines and hydrothermal fluids, South Cornwall, UK. Geochimica et Cosmochimica Acta, 65, 2067-2079.

GRANT, J., and SMITH, C. 2012. Evidence of tin and tungsten mineralisation in the Isles of Scilly. Geoscience in South-West England, 13, 65-70.

HALL, A., 1971. Greisenisation in the granite of Cligga Head, Cornwall. Proceedings of the Geologists' Association, 82(2), pp.209.

HAWKES, J.R. and DANGERFIELD, J. 1978. The Variscan granites of south-west England: a progress report. Proceedings of the Ussher Society, 4, 158-171.

HAWKES, J.R., HARRIS, P.M., DANGERFIELD, J., STRONG, G.E., DAVIES, A.E., NANCARROW, P.H.A., FRANCIS, A.D. and SMALE, C.V. 1987. The Lithium potential of the St Austell Granite. BGS Report Vol. 19, No. 4.

HAIMSON, B.C., TURNBRIDGE, L.W., LEE, M.Y. and COOLING, C.M. 1989. Measurement of rock stress using the hydraulic fracturing method in Cornwall, UK – part II. data reduction and stress calculation. International Journal of Rock Mechanics and Mining Sciences & Geomechanics, Vol. 26(5), 361–372.

HEATH, M.J. 1985. Geological control of fracture permeability in the Carnmenellis granite, Cornwall: implications for radionuclide migration. Mineralogical Magazine, Vol. 49, 233-244.

HOSKING, K.F.G. 1950. Oxidation phenomena of the Cornish lodes. Transactions of the Royal Geological Society of Cornwall, 18, 120-145.

HOSKING, K.F.G. 1951. Primary ore deposition in Cornwall. Transactions of the Royal Geological Society of Cornwall, 18, 309-356.

HOSKING, K.F.G. 1952. Cornish pegmatites and bodies with pegmatite affinity. Transactions of the Royal Geological Society of Cornwall, 18, 411-455.

HOSKING, K.F.G. 1964. Permo-Carboniferous and later primary mineralisation of Cornwall and south-west Devon. In: HOSKING, K.F.G. & SHRIMPTON, G.J. (Eds.) Present view of some aspects of the geology of Cornwall, Blackford, Truro, 201-245.

HOSKING, K.F.G. 1969. The nature of the primary tin ores of the South-West of England. In: Second technical conference on tin (Bangkok), London, International Tin Council, 3, 1155-1244.

HENWOOD, W.J. 1843. On the metalliferous deposits of Cornwall and Devon. Transactions of the Royal Geological Society of Cornwall, 5, 1-386.

JACKSON, N.J., MOORE, J.M., and RANKIN, A.H. 1977. Fluid inclusions and mineralization at Cligga Head, Cornwall, England. Journal of the Geological Society, 134(3), 343-349.

JACKSON, N.J., WILLIS-RICHARDS, J., MANNING, D.A.C. and SAMS, M.S. 1989. Evolution of the Cornubian ore field, Southwest England; Part II, Mineral deposits and ore-forming processes. Economic Geology, 84(5), 1101-1133.

LEBOUTILLIER, N.G. 2002. The tectonics of Variscan magmatism and mineralisation in South West England. Unpublished PhD thesis, University of Exeter.

LEE, M.K., BROWN, G.C., WEBB, P.C., WHEILDON, J. and ROLLIN, K.E. 1987. Heat flow, heat production and thermo-tectonic setting in mainland UK. Journal of the Geological Society, London, 144, 35-42

LEVERIDGE, B.E., HOLDER, M.T., GOODE, A.J.J., SCRIVENER, R.C., and MONKHOUSE, R.A. 1990. Geology of the country around Falmouth. Memoir of the British Geological Survey, Sheet 352 (England and Wales).

LEVERIDGE, B.E., HOLDER, M.T., GOODE, A.J.J., SCRIVENER, R.C., JONES, N.S. and MERRIMAN, R.J. 2002. Geology of the Plymouth and south-east Cornwall area. Memoir of the British Geological Survey, Sheet 348 (England and Wales).

LONDON, D. and MANNING, D.A.C. 1995. Chemical variation and significance of tourmaline from Southwest England. Economic geology, 90(3), 495-519.

MANNING, D.A.C., HILL, P.I. and HOWE, J.H. 1996. Primary lithological variation in the kaolinised St Austell Granite, Cornwall, England. Journal of the Geological Society, London, 153, 827-838.

MANNING, D., 1998. Granites and associated igneous activity. In SELWOOD, E.B., DURRANCE, E.M. and BRISTOW, C.M. (Eds.) The Geology of Cornwall and the Isles of. Scilly. Exeter (Exeter University Press), 120-135.

MÜLLER, A, and HALLS, C. 2005. Rutile – the Tin-Tungsten Host in the Intrusive Tourmaline Breccia at Wheal Remfry, SE England. In: Mineral Deposit Research: Meeting the Global Challenge (Eds.) J. MAO and F.P. BIERLEIN. Proceedings of the Eighth Biennial SGA Meeting, Beijing, China, 18th-21st August 2005, Springer, Berlin, 441-444.

PARKER, R.H. (Ed.). 1989. Hot Dry Rock Geothermal Energy, Phase 2B Final Report of the Camborne school of Mines Project. Pergamon Press.

PARKER, R. H. 1999.The Rosemanowes HDR Project 1983- 1991. Geothermics, 28, 603-615.

PHILLIPS, W. 1814. On the veins of Cornwall. Transactions of the Geological Society, First Series, 2, 110-160.

PINE, R.J. and BATCHELOR, A.S. 1984. Downward migration of shearing in jointed rocks during hydraulic injections. International Journal of Rock Mechanics and Mining Sciences & Geomechanics, Vol. 21(5), 249–263.

PRYCE, W. 1778. Mineralogia Cornubiensis. James Phillips, London, 331.

REINECKER, J., GUTMANIS, J., FOXFORD, A., COTTON, L., DALBY, C. and LAW, R. 2021. Geothermal exploration and reservoir modelling of the United Downs deep geothermal project, Cornwall (UK). Geothermics, 97, 102226, 17pp.

RICHARDS, H. G., SAVAGE, D. and SHEPHERD, T. J. 1989. Geochemical prognosis for a Hot Dry Rock system in south-west England. In Geochemistry in Relation to Hot Dry Rock Geothermal Development in Cornwall; British Geological Survey Research Report SD/89/2. Vol. 7.

RICHARDS, H. G., WILKINS, C., KAY, R. L. F. and Savage, D. 1989. Geochemical results from the Rosemanowes Hot Dry Rock system 1986–1989. In Geochemistry in Relation to Hot Dry Rock Geothermal Development in Cornwall; British Geological Survey Research Report SD/89/2. Vol. 2.

Rochelle, C., Busby, J., Kilpatrick, A., Shail, R., Yeomans, C, Eyre, M., den Hartog, S., Arnold, D., Geiger, S., Busch, A., Ledingham, P., Law, R., Carroll, C., and members of the GWatt project team 2021. Geothermal Power Generated From UK Granites (GWatt). Proceedings of the World Geothermal Congress 2020+1, Reykjavik, Iceland, April - October 2021, paper 16028, 7pp.

ROLLIN, K. E. 1987. Catalogue of geothermal data for the land area of the United Kingdom. Third revision: April 1987. Investigation of the Geothermal Potential of the UK, British Geological Survey, Keyworth

ROLLIN, K. E. 1995. A simple heat-flow quality function and appraisal of heat-flow measurements and heat-flow estimates from the UK Geothermal Catalogue. Tectonophysics, 244, 185-196.

ROLLIN, K. E., KIRBY, G. A., ROWLEY, W. J. AND BUCKLEY, D. K. 1995. Atlas of Geothermal Resources in Europe: UK Revision. Technical Report WK/95/07, British Geological Survey, Keyworth.

ROUSE, J. C., and COLEMAN, M. L., 1976. Sulfur isotope project: Mount Wellington mine, Cornwall: Inst. Geol. Sci. Stable Isotope Rept. 4 (unpublished).

SAVAGE, D., BATEMAN, K., MILODOWSKI, A., CAVE, M. R., HUGHES, C. R., GREEN, K., REEDER, S. and PEARCE, J. 1989. Experimental investigation of granite-water interaction. In Geochemistry in Relation

to Hot Dry Rock Geothermal Development in Cornwall; British Geological Survey Research Report SD/89/2. Vol. 6.

SCHWARZ, G., RIPA, M., THUNHOLM, B., SHAW, R.A., BATEMAN, K., DEADY, E., LUSTY, P., RAMALHO, E.C., MATOS, J.X., CARVALHO, J.G., PERȘA, D., MARINCEA, S., BALTREȘ, A., COSTEA, C., DUMITRAȘ, D., PREDA, G., BISEVAC, V. and FERNANDEZ, I. 2016. CHPM2030 Deliverable D1.2 - Report on data availability. CHPM2030 project, University of Miskolc, Hungary, 241pp.

SCRIVENER, R.C. 1982. Tin and related mineralization of the Dartmoor granite. Unpublished PhD thesis, University of Exeter.

SCRIVENER, R.C, LEAKE, R., LEVERIDGE, B., and SHEPERD, T. 1989. Volcanic-exhalative mineralisation in the Variscan province of SW England. In Terra Abstracts, Vol. 1, p. 125.

SCRIVENER, R.C., DARBYSHIRE, D.P.F. and SHEPHERD, T.J. 1994. Timing and significance of crosscourse mineralization in SW England. Journal of the Geological Society of London, 150, 587-590.

SCRIVENER, R.C., 2006. Cornubian Granites and Mineralisation of SW England, in BRENCHLEY, P.J., and RAWSON, P.F. (Eds.). The Geology of England and Wales, the Geological Society, 257-267.

SELWOOD, E.B., DURRANCE, E.M. and BRISTOW, C.M. (Eds.). 1998. The Geology of Cornwall and the Isles of. Scilly. Exeter (Exeter University Press), 298.

SHAIL, R. K. and ALEXANDER, A. C. 1997. Late Carboniferous to Triassic reactivation of Variscan basement in the western English Channel: evidence from onshore exposures in south Cornwall. Journal of the Geological Society, London, 154, 163-168.

SHAIL, R.K., STUART, F.M., WILKINSON, J.J. AND BOYCE, A.J. 2003. The role of post-Variscan extensional tectonics and mantle melting in the generation of the Lower Permian granites and the giant W-As-Sn-Cu-Zn-Pb orefield of SW England (extended abstract). Applied Earth Science (Transactions of the Institutions of Mining and Metallurgy: Section B), 112, 127-129.

SHAIL, R.K., and LEVERIDGE, B.E. 2009 The Rhenohercynian passive margin of SW England: Development, inversion and extensional reactivation, Comptes Rendus Geoscience, Vol. 341, pages 140-155.

SHAIL, R.K. 2014. Regional geological evolution. In: SHAIL, R.K., ANDERSEN, J.O., SIMONS, B. and WILLIAMSON, B. (Eds.) EUROGRANITES 2014 – Granites and mineralisation of SW England. Unpublished field excursion guidebook, University of Exeter, Penryn, 147 pp.

SHAIL, R.K., ANDERSEN, J.O, SCRIVENER, R.C., WILLIAMSON, B., HALLS, C., MÜLLER, A., SIMONS, B., and ROLLINSON, G. 2014. Mineralisation. In: SHAIL, R.K., ANDERSEN, J.O., SIMONS, B. and WILLIAMSON, B. (Eds.) EUROGRANITES 2014 – Granites and mineralisation of SW England. Unpublished field excursion guidebook, University of Exeter, Penryn, 147 pp.

SHAIL, R.K., SCRIVENER, R.C., SIMONS, B., MÜLLER, A., ANDERSEN, J., WILLIAMSON, B., HALLS, C. and HUGHES, S. 2014. Early Permian post-Variscan magmatism. In: SHAIL, R.K., ANDERSEN, J.O., SIMONS, B. and WILLIAMSON, B. (Eds.) EUROGRANITES 2014 – Granites and mineralisation of SW England. Unpublished field excursion guidebook, University of Exeter, Penryn, 147 pp.

SHAW, R.A., DEADY, E., BATEMAN, K. and LUSTY, P., 2016. CHPM2030 Deliverable D1.2 - Report on data availability: South-West England. CHPM2030 project, University of Miskolc, Hungary, 59pp.

SHEPPARD, S.M.F. 1977. The Cornubian batholith, SW England: D/H and 18O/16O studies of kaolinite and other alteration minerals. Journal of the Geological Society, 133(6), 573-591.

Simons, B.J., Shail, R.K. and Andersen, J.C.O. 2016. The Petrogenesis of the Early Permian Variscan granites of the Cornubian Batholith - lower plate post-collisional peraluminous magmatism in the Rhenohercynian Zone of SW England. Lithos, 3928. 10.1016/j.lithos.2016.05.010

SMEDLEY P. L., BROMLEY A. V., SHEPHERD T. J., EDMUNDS, W. M., and KAY R. L. F. 1989. Fluid circulation in the Carnmenellis granite: Hydrogeological, hydrogeochemical, and palaeofluid evidence. In Geochemistry in Relation to Hot Dry Rock Geothermal Development in Cornwall; British Geological Survey Research Report SD/89/2. Vol. 4.

SMEDLEY, P.L. and ALLEN, D. 2004. Baseline report series 16: The granites of south-west England. British Geological Survey Commissioned Report CR/04/255.

SMITH, M., BANKS, D.A., YARDLEY, B.W.D., and BOYCE, A. 1996. Fluid inclusion and stable isotope constraints on the genesis of the Cligga Head Sn-W deposit, SW England. European Journal of Mineralogy, 8, 961-974.

STANLEY, C.J., CRIDDLE, A.J. and LLOYD, D. 1990. Precious and base metal selenide mineralization at Hope's Nose, Torquay, Devon. Mineralogical Magazine, 54 (376), 485-493.

STONE, M. and EXLEY, C.S. 1985. High heat production granites of south-west England and their associated mineralisation: a review. In: HALLS, C. (Ed.) High heat production (HHP) granites, hydrothermal circulation and ore genesis. Institution of Mining and Metallurgy, London, 571-593.

STONE, M. 1995. The main Dartmoor granites: Petrogenesis and comparisons with the Carnmenellis and Isles of Scilly granites. Proceedings of the Ussher Society, 8, 379-384.

STONE, M. 1997. A geochemical dichotomy in the Cornubian batholith. Proceedings of the Ussher Society, 9, 206-210.

STONE, M. 2000a. The early Cornubian plutons: a geochemical study, comparisons and some implications. Geoscience in south-west England, 10, 37-41.

STONE, M. 2000b. Petrogenetic implications from biotite compositional variations in the Cornubian granite batholith. Mineralogical Magazine, 64, 729-735.

SULLIVAN, R.E., SHAIL, R.K. and HUGHES, S.P. 2013. The tectonics of early stage Cornubian batholith construction and mineralisation as viewed from the NW margin of the Isles of Scilly pluton (abstract). Geoscience in south-west England, 13, 246.

TAYLOR, G K, 2007. Pluton shapes in the Cornubian Batholith: new perspectives from gravity modelling. Journal of the Geological Society, London, Vol. 164, 525–528.

THOMAS-BETTS, A., WHEILDON, J. and SAMS, M.S. 1989. Further heat flow measurement and geothermal modelling in the vicinity of Carnmenellis granite. CSM Geothermal Energy Project. Report ETSU-G-137-P16, p. 1–113.

TURNBRIDGE, L.W., COOLING, C.M. and HAIMSON, B.C. 1989. Measurement of rock stress using the hydraulic fracturing method in Cornwall, UK – part I. field measurements. International Journal of Rock Mechanics and Mining Sciences & Geomechanics, Vol. 26(5), 351–360.

WHEILDON, J., FRANCIS, M. F., ELLIS, J. R. L. and THOMAS-BETTS, A. 1981. Investigation of the SW England thermal anomaly zone. CEC Final Report, Contract No 097-76 EGUK, 568-78-1 EGUK, p. 1–410.

WILKINSON, J.J., JENKIN, G.R.T., FALLICK, A.E. and FOSTER, R.P. 1995. Oxygen and hydrogen isotopic evolution of Variscan crustal fluids, south Cornwall, U.K. Chemical Geology, 123, 239-254.

WILLIAMSON, B J, STANLEY, C J, and WILKINSON, JJ. 1997. Implications from inclusions in topaz for greisenisation and mineralisation in the Hensbarrow topaz granite, Cornwall, England. Contributions to Mineralogy and Petrology, 127, 119-128.

WILLIAMSON, B.J., SPRATT, J., ADAMS, J.T., TINDLE, A.G. & STANLEY, C.J. 2000. Geochemical constraints from zoned hydrothermal tourmalines on fluid evolution and Sn mineralization: an example from fault breccias at Roche, SW England. Journal of Petrology, 41, 1439-1453.

WILLIS-RICHARDS, J. and JACKSON, N.J. 1989. Evolution of the Cornubian Ore Field, Southwest England: Part I. Batholith Modelling and Ore Distribution. Economic Geology, 84, 1078-1100.

WOLF MINERAL LTD. 2015. Drakelands Mine. Wolf Minerals web page accessed: October 2016 [http://www.wolfminerals.com.au/irm/content/drakelands-mine.aspx?RID=324]

Yeomans, C.M., Middleton, M., Shail, R.K., Grebby, S. and Paul A.J. Lusty, P.A.J. 2019. Integrated object-based image analysis for semi-automated geological lineament detection in southwest England. Computers and Geosciences, 123, 137-148.

Yeomans, C.M., Claridge, H., Hudson, A.J.L., Shail, R.K., Willems, C., Eyre, M. and Harker, C. 2022. A single multi-scale and multi-sourced semi-automated lineament detection technique for detailed structural mapping with applications to geothermal energy exploration. Quarterly Journal of Engineering Geology and Hydrogeology, https://doi.org/10.1144/qjegh2022-051

Yeomans, C.M., Shail, R.K. ansd Eyre, M. 2021. The importance of tectonic inheritance and reactivation in geothermal energy exploration for EGS resources in SW England. Proceedings of the World Geothermal Congress 2020+1, Reykjavik, Iceland, April - October 2021, paper 11099, 11pp.

5 SALINE WATER IN SEDIMENTARY BASINS: NORTHERN GERMANY

Author:
Simona Regenspurg
Helmholtz Centre Potsdam, German Center of Geosciences, GFZ, Germany

5.1 SEDIMENTARY BASINS

5.1.1 Geological background

Sedimentary Basins are defined as depressions of the Earth´s crust caused by subsidence, where sediments have accommodated over long time periods forming thick layers of sedimentary rocks. Those that are experiencing recent subsidence and still receiving sediments are referred to as active sedimentary basins. Subsidence on a regional scale is often caused by tectonic stretching of the earth's crust, where different types of tectonic basins can be distinguished in different plate tectonic scenarios, such as back-arc basins (subduction), pull-apart basins, and rift valleys (divergence).

The layout of a sedimentary basins depends on the formation mechanism. Simple tectonic stretching tends to produce elongated structures, pull-apart basins and basins formed by thermal subsidence can also have more rounded shapes. The fill of the basins are predominantly sediments and sedimentary rocks, but also volcanic effusion, dyke rocks and pyroclastic sediments can form the fill of the basin.

The rate of bedrock subsidence is typically on the order of millimeters per year and generally increases from the edge to the center of a sedimentary basin. The thickness of the basin fill usually decreases from the basin center to the edges. Basin formation caused by tectonics are characterized by so-called basin edge faults, where especially the filling is relatively sharply separated against the peripheral bedrock. In the course of the geological history of a sedimentary basin, its deposit centers can shift, which is reflected in fluctuating thicknesses of strata of different ages in different regions of the basin. The extent to which the subsidence is expressed morphologically in an active sedimentary basin depends on the amount of deposited sediment per unit time (sedimentation rate).

The sediment is almost always brought into the basin from the surrounding elevated areas exposed to erosion by flowing water, i.e. rivers and streams as well as ocean currents. In certain areas of a sedimentary basin characterized by relatively steep relief, mass movements such as suspension or debris flows are also important for sediment transport or deposition. With high subsidence rates, the height of the basin often drops below sea level, and the sea then usually penetrates into the corresponding region, particularly at continental margins. Sedimentary basins are therefore often sea basins with marine sedimentation. With lower subsidence rates or a very remote location, sedimentation is more likely to occur in lakes and alluvial plains. In sea or lake basins in tropical climates, the in-situ precipitation of calcium carbonate or relatively easily soluble salts (evaporites) often plays an important role in sedimentation.

The layers that were first deposited in a sedimentary basin get deeper and deeper with continued subsidence, are pressed together by the weight of layers that are subsequently deposited (compaction) and are transformed into sedimentary rocks such as sandstone or claystone in the long term (diagenesis). In continental sedimentary basins, the younger (upper) layers of gravel and other loose material often contain important reservoirs of groundwater that can be used for drinking water production. In the course of subsidence, the remains of dead plants (including algae) accumulated in the subsidence area and were successively covered by layers of gravel, sand and clay. Where this occurred in the absence of air, coal, oil and natural gas formed from the organic residues. The coalification or thermal ripening of the remains is promoted by the further sinking of the sedimentary basin, continuous deposition and the increasing temperature of the subsoil. Examples of sedimentary Basins in mid-Europe are: The North German Basin, NGB (Poland, Danmark, North Sea, Germany, The

Netherlands), the Upper Rhine Graben (France; Germany, Switzerland), the Vienna Basin (Austria), the Molasse Basin (Germany, Austria, Switzerland), the Pannonian Basin (Austrai, Hungary), and the Parisian Basin (France).

Extraction of raw materials from geothermal fluids has already been considered and tested for the brines from the Upper Rhine Valley (a continental sedimentary basin in a rift valley). At several geothermal sites (e.g. Insheim, Bruchsal) methods of lithium extraction are being investigated, both within research projects (e.g. the German national funded research project UnLimited, with the research site Bruchsal or the EU project EugeLi) and within purely commercial attempts by Vulcan Energy Resources, who are currently studying this at the Insheim Geothermal site. In contrast to those projects, we focus our investigation within the CRM-geothermal project, on the potential for all critical raw materials. In the following, their occurrence is presented for the North German Basin as an example of a sedimentary basin in Europe.

5.1.2 The North German Basin

Location: The North German Basin is a rift basin located in west and central Europe. As part or sub-basin of the Southern Permian Basin it stretches in a north-south direction from the Southern Baltic Sea and North Sea across northern Germany to the German Mittelgebirge (low mountain range), and in an east-west direction from Poland to the Netherlands (Figure 5.1).

Geological Formation: The basin fill is composed of Permian to Cenozoic sediments that can reach a thickness of up to 10–12 kilometers. The evolution was largely influenced by several stages of rifting, subsidence, and salt tectonic events. Basin formation started with an initial rifting period in the late Carboniferous (295-285 Ma) associated with the Variscian Orogenesis. This initiated an intensive Volcanism (in the Permian) resulting in the formation of partly km thick volcanic rock layers in several eruption periods. During the following phase of main subsidence, a rapid accumulation of sediments from the Upper Rotliegend to the Bunter period (Permian to Triassic) occurred. A second phase of North to South rifting from 252 to 200 Ma (Triassic-Early Jurassic) was initiated by the break-up of the super-continent Pangea causing a east-west extension. This event not only resulted in the formation of the Triassic grabens, but also initiated salt tectonics. Another phase of subsidence followed until a doming phase during the Middle-Late Jurassic centered in the region of the North Sea (Middle Jurassic erosional unconformity) that caused the erosion of of Upper Triassic and Lower Jurassic strata. A third rifting phase eventually took place in the Late Jurassic (157-155 Ma) that resulted in the detachment of the Zechstein evaporites also affecting the migration of natural gas and oil formation that formed from organic-rich mudstones from the Kimmeridge Clay Formation (Jurassic, marine; Alrichs et al., 2020). Figure 5.1 shows part of the NGB area and profile in NW-SW direction that points out the various thick, sedimentary layers that increase in thickness towards the Basin center.

Figure 5.1 also shows the fault structures and the Zechstein salt doming. The major challenge for exploration of all geothermal projects in the region of the NGB are the salt tectonics. Diapirs and pillows of Zechstein salt (several layers of limestone, gypsum, sodium chloride and potassium chloride) are distributed across the NGB (Figure 5.2). The Zechstein is a lithographical group within the Permian geological period that sedimented between 260 and 250 Million years ago. It begins with the deposition of copper-containing shale (Kupferschiefer). (As the name suggests the Kupferschiefer yields large amounts of copper and was mined for that since medieval times at many locations in Germany and Poland). The Zechstein Sea, transgressed from the north, left behind up to seven cycles with partly siliciclastic, partly carbonate, partly evaporitic sediments (Werra, Staßfurt, Leine, Aller, Ohre, Friesland and Fulda). A cycle consists of mudstone, overlaid by limestone or dolomite and above that a sequence of anhydrite, halite, and potash. During later uplift of the salt the overlaying formations were tilted, twisted and thinned thus making it often difficult to predict the exact thickness and occurrence of expected formations for geothermal exploration purposes.

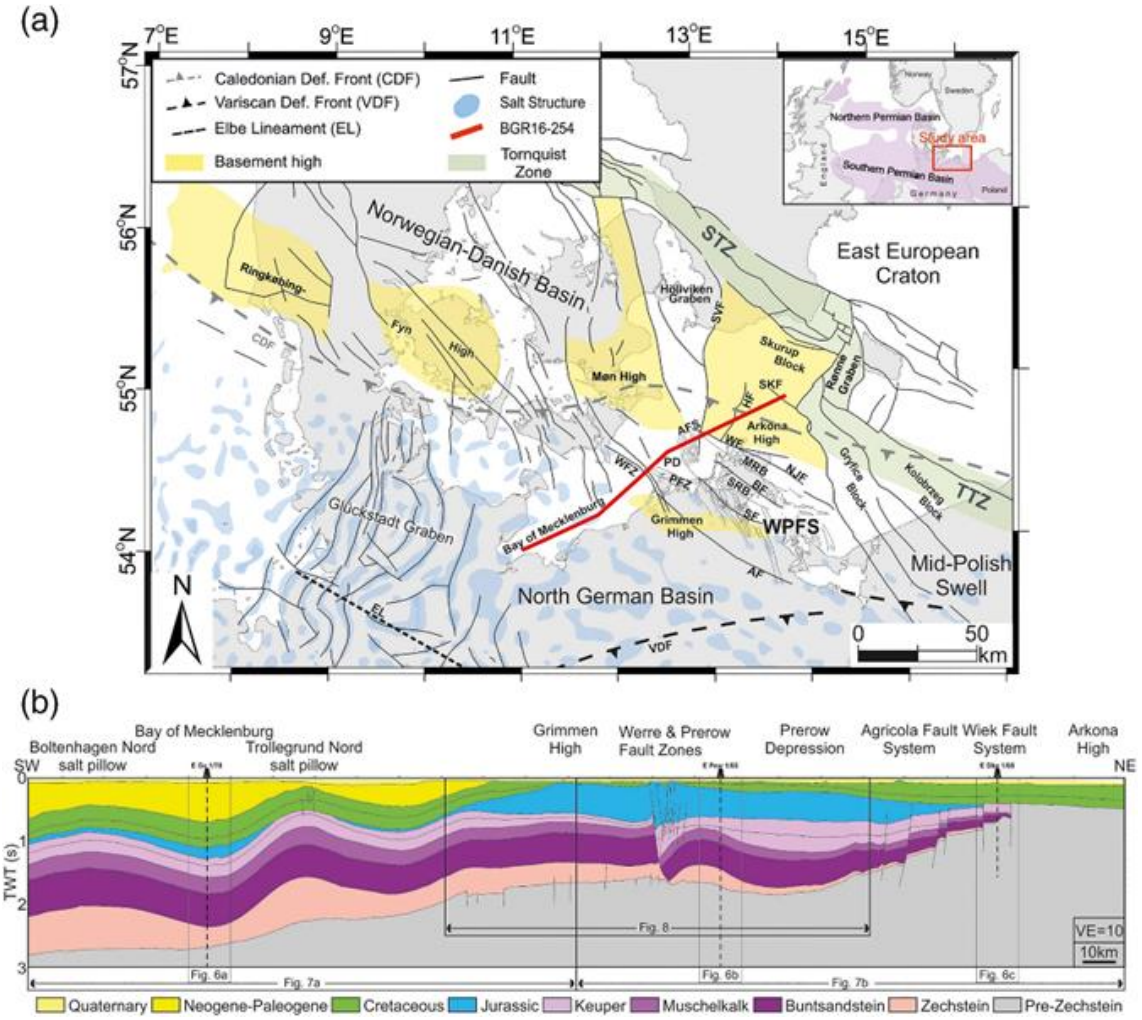

Figure 5.1: Tectonic map of the North German Basin (a) and geological cross section along profile BGR16 -254 (b) from Alrichs et al. (2020).

Details to Fig. 5.1 a: Tectonic map of the North German Basin including major geological structures (based on Vejbaek & Britze, 1994; Schlüter et al., 1997; Baldschuhn et al., 2001; Pharaoh et al., 2010; Al Hseinat & Hübscher, 2017; Seidel et al., 2018; Mazur et al., 2020). Inset shows approximate outline of the northern and southern Permian Basin. Red line marks position of profile BGR16-254 analyzed in this study. AF = Anklam Fault; AFS = Agricola Fault System; BF = Bergen Fault; CDF = Caledonian Deformation Front; EL = Elbe Lineament; HF = Hiddensee Fault; MRB = Middle Rügen Block; NJF = Nord Jasmund Fault; PD = Prerow Depression; PFZ = Prerow Fault Zone; SF = Strelasund Fault; SKF = Skurup Fault; SRB = South Rügen Block; STZ = Sorgenfrei-Tornquist Zone; SVF = Svedala Fault; TTZ = Tornquist-Teisseyre Zone; VDF = Variscan Deformation Front; WFZ = Werre Fault Zone; WF = Wiek Fault; WPFS = Western Pomeranian Fault System. (b) Condensed geological cross section along profile BGR16-254 analyzed in this study, showing main structures and stratigraphic features. Seismic data acquired during cruise MSM52 (Hübscher et al., 2016).

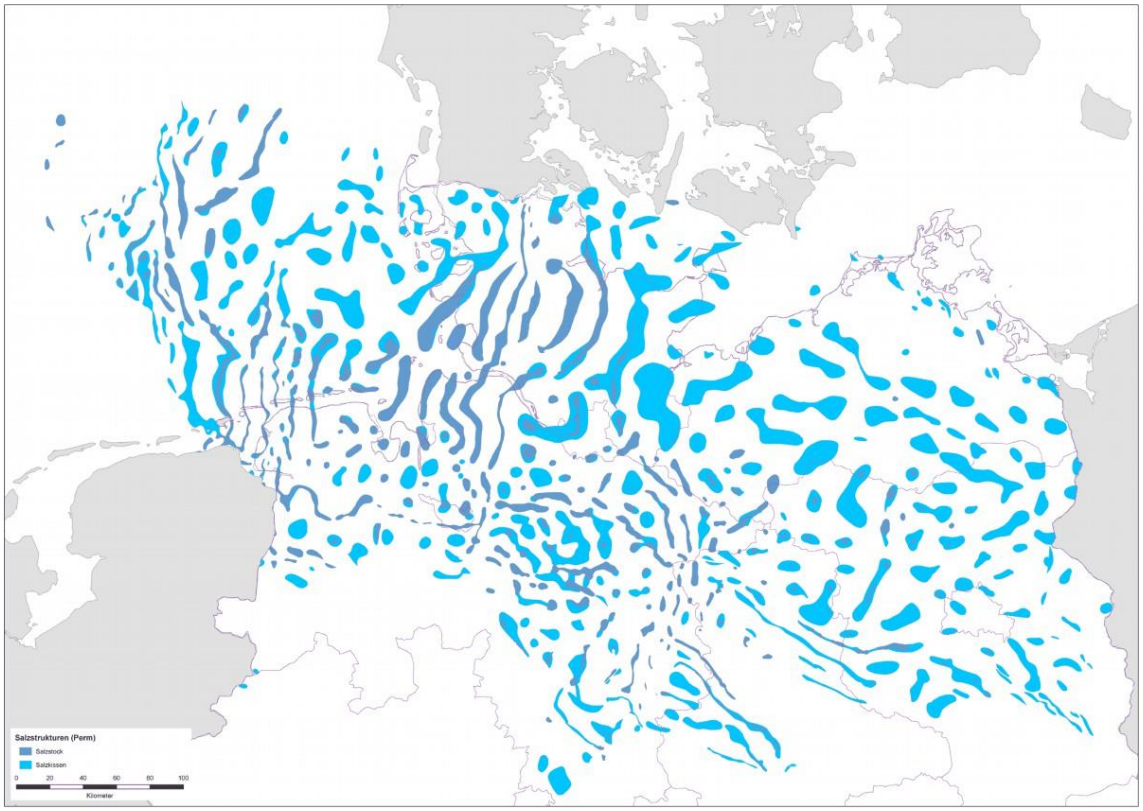

Figure 5.2: BGR Salt structures in the North German Basin: https://www.bgr.bund.de/DE/Themen/Endlagerung/Bilder/Salzstruk_NDtl_p.html?view=render

5.2 GEOTHERMAL EXPLORATION AND EXPLOITATION

Sedimentary Basins can have large economic importance since they often host natural gas, oil, salt, and coal. In some areas, and under specific conditions, metal ores may also occur.

For mining geothermal heat, formations of high permeability and ideally good thermal properties are required. The various geological formations in sedimentary basins allow the utilization of different formations for different purposes. In the North German Basin, the following formations have been considered and explored so far for geothermal purposes: Rotliegend sandstones and underlying Permo-Carboniferous Volcanic rocks, Bunter sandstone, Muschelkalk (limestone), Upper Keuper (various sandstones), Jurassic Hettang sandstone.

1. Rotliegend formation and underlying volcanic rocks:

These formations, also explored and used for oil and gas wells (e.g. in the German Altmark region), and typically occur at 3-5 km depth. At those depths, temperatures are above 100 °C and geothermal fluids can serve for both heat and electricity production. Intense research has been performed for over 20 years at the geothermal research site in Groß Schönebeck (GrSk; located 50 km NE of Berlin). Due to the promising content of CRM in the GrSk fluid, this side will be described in more detail below.

Groß Schönebeck geothermal research platform: In 1990/91, the GrSk 3/90 borehole was drilled down to a depth of 4240m (MD) for natural gas exploration into sandstones and volcanic rocks of the Rotliegend. In 2003 the hole was deepened to 4309m (MD) serving later as an injection well for the well dublet. The GrSk 4/05 borehole was drilled in 2006, also reaching the Rotliegend volcanic rocks at a depth of 4400 m (MD). It was later used as a production well (Zimmermann and Moeck, 2008). Due to the low-permeability of the sandstones and volcanic rocks they were subject to research on EGS (Enhanced Geothermal Systems). For this purpose, gel proppant fracs and other

stimulation measures were applied to increase the productivity of the reservoir (Zimmermann and Reinicke, 2010). However, after an initial increase in the productivity to a PI (productivity index) of 14 m^3/h*MPa, the productivity strongly decreased during circulation tests. The most likely reason was due to massive scaling in the production well, that was clogged for few hundred metres by native copper and other scales. Although the materials were removed from the well by a work-over procedure, the PI was still low (quantified by a N_2 lift test in 2014). Therefore, the wells were closed, and remain so (Blöcher et al., 2016).

Reservoir Rocks: The reservoir rocks of the GrSk3/90 and GrSk 4/05 boreholes are sandstones and volcanic rocks of the Rotliegend that are characterized by a large lithological heterogeneity with siltstones, sandstones, conglomerates and volcanic rocks (Rockel and Hurter, 2000). The sandstone complex is 146m thick and extends from 4085-4231m. It mainly consists of reddish-brown, fine sandstone, partly also medium-sized sandstone. More precisely, these are lithoclast-bearing arenites (Huenges and Wolfgramm 2004). They have an effective porosity of 8-10 % and a permeability of up to 16.5 mD (Zimmermann and Reinicke, 2010). The complex is irregularly interrupted by layers or benches of siltstone and mudstone. These layers and benches have a thickness in the centimeter to decimeter range. In the depth range 4211-4231m several thin, weakly calcareous fine conglomerate banks occur consisting of porphyrites, quartz, sandstone, siltstone and mudstone (Rockel and Hurter 2000). The volcanic rocks that occur from 4231 m were previously classified as andesites (Rockel and Hurter, 2000) or dacite (Regenspurg et al., 2016).

Fluids: The fluids from the Groß Schönebeck wells have a high salinity of about 265 g/L total dissolved solids and are classified as Na-Ca-Cl fluids. The gas/water volume ratio is 1:1 to 2:1. The aqueous phase consists mainly of dissolved $CaCl_2$ and NaCl, these two compounds make up about 98% of the salinity. In addition, the fluids are highly corrosive due to their high chloride concentrations. The gas phase consists of about 85-90 vol% nitrogen and 10-15 vol% methane (Regenspurg et al., 2015). The fluids were mainly derived from the evaporation of meteoric water (primary fluid) and halite solution (secondary fluid). A geochemical differentiation of fluids from different rock formations is not possible, since the sediments represent weathering products of the volcanic rocks and thus have a similar mineralogical composition. In addition, the units might be connected hydraulically by faults. However, mixing with Zechstein fluids or younger meteoric water was ruled out based on isotopic analysis (Regenspurg et al., 2016). A commercial geothermal project targeting the Rotliegend formation is currently developed in Munster, Lower Saxony, where the Rotliegend at 5 km depth will be used for heat provision.

2. Bunter Sandstone (Buntsandstein):

The Bunter sandstone occurs in Brandenburg at depth between few hundred to nearly 4000 m. correspondingly the temperature range is variable ,but it can reach up to 130 °C in the NW of Brandenburg (Figure 5.3).

Due to the ideal temperature conditions, it is currently most intensely explored formation for geothermal heat provision in the North German area. Research projects for the Bunter in northern Germany have been performed in Hanover (2 Sites: Buchholz and Horstberg). However, so far, no commercial project has been established. In the city of Berlin several wells have been drilled in into the Bunter in the area of Spandau (West of Berlin), where a gas storage was operated until recently, however all wells are closed and now sealed. Information of rocks and fluids have been collected over the years by the operating company, the Berliner Erdgasspeicher (BES). The main energy provider of the city of Potsdam (Brandenburg) is also intensively working on geothermal projects to allow geothermal heat provision for the population in Potsdam. Seismic monitoring has already been performed, and a decision taken to drill down into the Bunter formation to access 60-85 °C water.

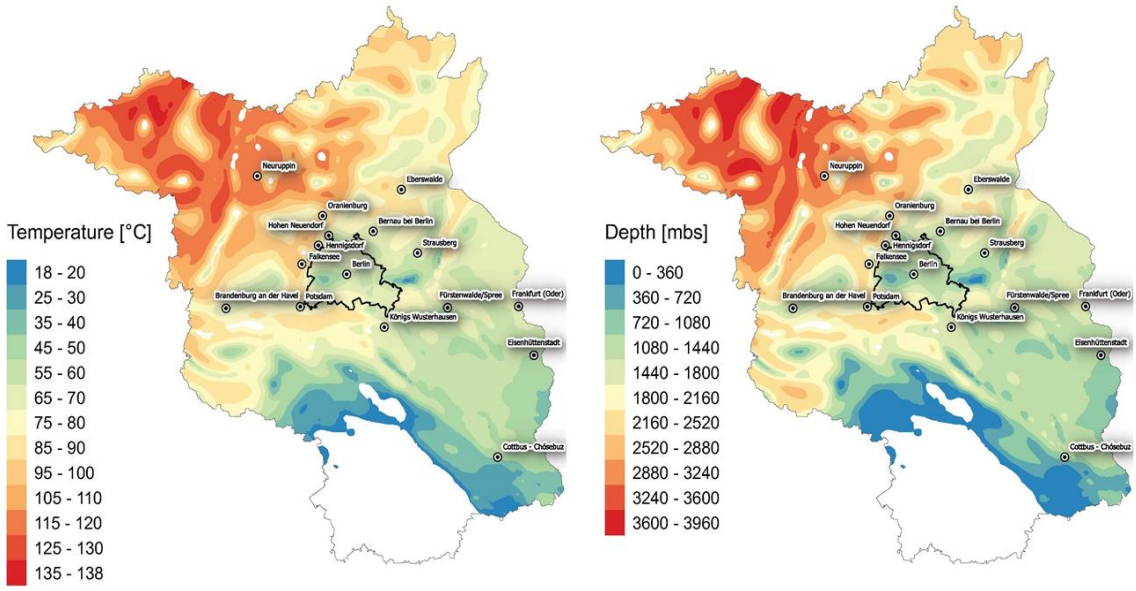

Figure 5.3: Frick et al. (2022) Distribution of the depth and temperatures of the Bunter formation in Brandenburg (Germany).

3. Muschelkalk formation:

Similar to the Bunter, the overlaying Muschelkalk could provide sufficient permeability and temperature for either heat production or storage. Research has been done in Berlin Spandau, where the Muschelkalk was used as an injection horizon for the brine that was produced from the Bunter during gas extraction. The Muschelkalk is a predominantly carbonatic formation. The oolithic limestone of the Schaumkalk sub-formation is of high porosity, but its permeability is only sufficiently high for geothermal purposes in fractured areas. An outcrop of the Muschelkalk exists in the East of Berlin, where in Rüdersdorf the limestone has been mined for a long time for the construction and cement industry. So far there are no data on fluid chemistry of the Muschelkalk in the North German Basin available. However, recent hydraulic tests performed in Spandau (not yet published), reveal a seawater salinity.

4. Upper Keuper (Exter or Rhät):

The Rhätkeuper is the key geological horizon for most geothermal projects in the North German Basis (Neustadt-Glewe, Waren, Neubrandenburg; Hamburg Wilhelmsburg, Schwerin). The formation consists of sandstones (with the Triletes, Contorta, Postera sub formations) that formed within the alluvial fans draining as deltas from the North into the center of the basin. Within the Northern channels the thickness and permeability of the sands is highest (Figure 5.4) and decreases towards the South. Therefore, in the Berlin-Brandenburg areas, the Upper Keuper is less thick. However, a research well drilled in the Center of Berlin targeting the Exter formation for ATES showed that the thickness of 8 m would be sufficient for operating an ATES system (Regenspurg et al., 2020).

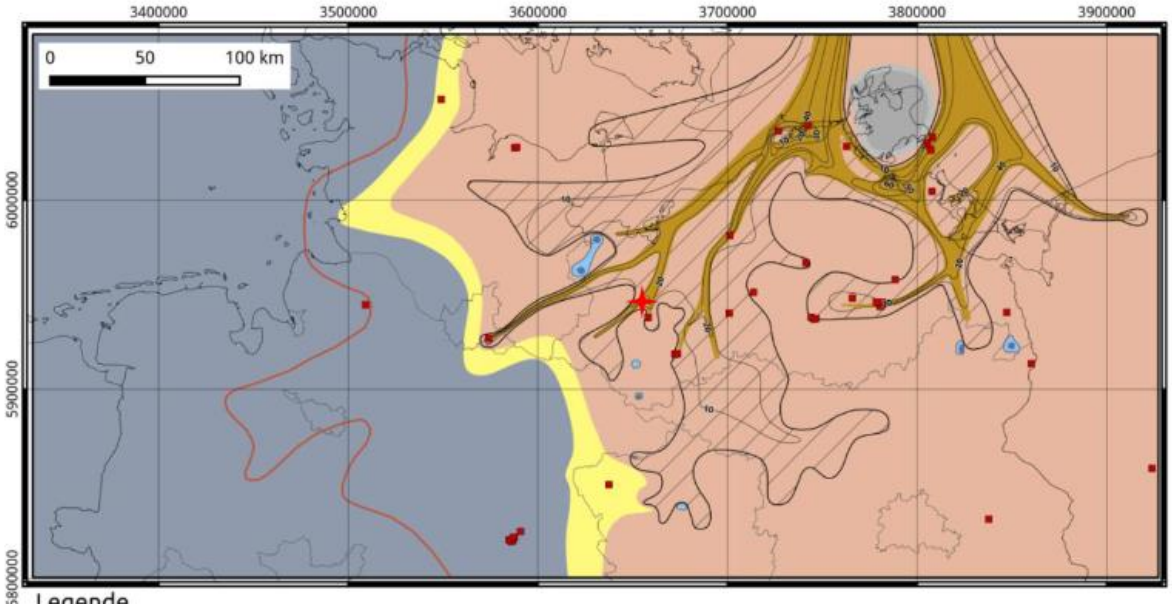

Figure 5.4: Distribution of various sediments in Northern Germany: the alluvial fans and channels (brown) with lacustrine playas (blue), clayish playas (bright red), siliciclasic sediments near the ancient coast (yellow), and marine sediments in dark grey. Investigated drill core are marked as red dots (Wolfgramm et al., 2019).

5. Jurassic Hettang

In 1999 a new heat supply and storage system for the Berlin parliament building was installed. Here an aquifer thermal energy storage (ATES) system was constructed that targeted the Jurassic Hettang as a reservoir for storing heat coming from a combined heat and power plant. Two wells were drilled into the Jurassic Hettang that was found at a depth of roughly 300 m, a relatively homogenous, little consolidated sandstone (Rockel et al., 1999; Müller & Regenspurg, 2014). The fluid salinity (NaCl-type) was below that of sea water. Leaching of minerals from the Hetang sandstone was investigated by Müller et al. (2017). They showed a pyrite content that could cause the release of Fe and potential other heavy metals into the aquifer upon oxidation. Currently a second ATES site is drilled in the East of Berlin (Adlershof) into the same formation.

Geological formations above the Jurassic are generally not considered for geothermal exploitation due to lower temperatures and potential conflict with drinking water aquifers.

5.3 FLUIDS AND DISSOLVED RESOURCES

Due to the old age, great depths but also of the often extremely arid deposit conditions with high evaporation rates of the sedimentary basin fluids, generally the salt content in the fluids is very high. An exception are fluids from the South German Molasse Basin that have salinity below 1 g/TDS (total dissolved solids). Most other sedimentary fluids are marked by salinities between 20 and 300 g/L TDS. Table 5.1 summarizes the depths and temperatures of three sedimentary basin fluids in Germany: The North German Basin (NGB), South German Molasse Basin (SMB), and Upper Rhine Graben URG) and gives also the strontium (Sr) and lithium (Li) content of those fluids. Strontium and lithium are of the few CRM that are relatively frequently measured (as part of standard analysis) in geothermal fluids.

It is clear from the data in Table 5.1 that the CRMs Li and Sr hardly occur in the low salinity fluids from the SMB, whereas in the Upper Rhine Graben and the NGB these concentrations can reach several hundred g/L. The highest concentrastions of both Li and Sr were measured in the Rotliegend formation of the URG. The highest lithium content was found in the Groß Schönebeck geothermal fluid and the highest strontium in the Bunter of the Hanover Horstberg formation (1950 mg/L) followed by Groß

Schönebeck (1900 mg/L; Table 5.1). However, both sites are marked by extremely high salinities of the fluids and suffered from enormous clogging of the wells that eventually led to closing of well operation (Hesshaus et al., Regenspurg et al., 2015).

Table 5.1: Li and Sr content of various geothermal fluids as collected in the North German Basin (NGB), Upper Rhine Graben (URG), South German Molasse Basin (SMB) (Table modified from N. Pogarell (2021))

Geothermal site/ well	Reservoir rock	Latitude	Longitude	Depth [m]	T [°C]	Li [mg/L]	Sr [mg/L]	Reference
Groß Schönebeck GrSk 3/90	NGB Rotliegend	52,491900	13,361200	4235	150	240	1900	*www.geothermperform.eu
Groß Schönebeck GrSk 4/05		52,903588	13,601572			212	1650	*www.geothermperform.eu
Neubrandenburg Gt N1-6	NGB Upper Keuper	53,553990	13,247660	1200	55 sample	106		https://doi.org/10.1016/S0043-1354(97)00252-2
Neuruppin SolNn		52,925540	12,816200				44	*www.geothermperform.eu
Waren Müritz GtWa	NGB Upper Keuper	53,507780	12,701180				148	*www.geothermperform.eu
Neustadt-Glewe Gt NG 1/88	NGB Contorta Sandstein	53,370120	11,586180		99	10	440	https://gfzpublic.gfz-potsdam.de/rest/items/item_8482_3/component/file_10082/content
Horstberg Z1	NGB Middle Bunter	52,903352	10,327991		90	182	1950	*BGR
Groß Buchholz Gt1 (Genesys)	NGB Middle Bunter	52,405382	9,826342		160	4,2	350,5	*BGR
Dreilingen Z1	NGB Rotliegend	52,906709	10,339628	4509-4513		80		Niedersächsisches Landesamt für Bodenforschung Hannover; print
Hamburg-Allermöhe 1	NGB sandstone	53,467796	10,114614	3201-3276	125.4		324	www.geotis.de
Bad Urach 3	URG Rotliegend	48,506982	9,373198	3320-4444	170	44.5	111	https://doi.org/10.1111/gfl.12186
Bad Urach 3		48,506982	9,373198	3270	139.5		80	https://doi.org/10.1111/gfl.12186
Insheim Gt 1/2	URG,Bunter, Muschelkalk granite	49,153720	8,153700		165	168	456	Hydrochemical database Hessen
Landau Gt La 1	URG Bunter	49,185600	8,122510		155	179	430	
Bühl	URG Bunter	48,698401	8,131255	2402	122	41.2	485	www.geotis.de

Geothermal site/well	Reservoir rock	Latitude	Longitude	Depth [m]	T [°C]	Li [mg/L]	Sr [mg/L]	Reference
Bruchsal Gb1	URG Bunter	49,135625	8,581102		120	166	324	https://doi.org/10.1016/0016-7037(93)90387-C
Bruchsal Gb2	URG Bunter	49,125540	8,5675140	2542	120	159	391	Hydrochemical database Hessen
Wald-kraiburg Th 1	SMB Malm	48,201326	12,420315		98,4 Probe 108	0.8		https://www.univie.ac.at/ajes/archive/volume_109_1/goldbrunner_vasvari_ajes_109_1.pdf
Unter-haching Gt 1	SMB Malm	48,057078	11,597516	2526-2788	122	0.232	1.61	www.geotis.de
Unterhaching Gt 2	SMB Malm	48,056099	11,641217	2418-2790	122	0.14	0.54	www.geotis.de
Pullach Th 1a	SMB Malm	48,067709	11,525761	2208-2727	105	1.08	9.37	www.geotis.de
Pullach Th 2		48,067697	11,525868	2357-2870	105	0.07	8.88	www.geotis.de
Simbach-Braunau (am Inn) Th 1	SMB Malm	48,257168	13,010513	1389-1501	81		0.63	www.geotis.de
Unterschleiß-heim Th 1/2	SMB Malm	48,260109	11,591494	1121-1527	nm	0.77	0.52	www.geotis.de

Other CRM are typically not measured in the fluids. An exception here is the Groß Schönebeck geothermal fluid, where most trace elements were measured as well. Here specifically zinc and copper can be mentioned that reach concentrations similar to lithium (about 200 mg/L; Regenspurg et al., 2015). The high metal content is explained by the close vicinity and connection of the Rotliegend fluids with the underlying Permocarboniferous volcanic rocks since most metal enrichments (heavy elements) are connected to magmatism and often to volcanism.

5.4 CONCLUSIONS

The saline fluids of sedimentary Basins can be strongly enriched with lithium and strontium. Other CRM probably only occur if there is a vicinity/hydraulic contact of the sedimentary formation with a magmatic rock (volcanic or plutonic) that yield increased amounts of CRM.

The exploration for lithium in the NGB is already being investigated in both commercial and research activities. A recent study by Goldberg et al. (2022) evaluates the chances for an economic Li production from geothermal systems in Germany. They also consider the challenges and costs in lithium extraction and potential formation of scales in various types of geothermal fluids. They conclude that from nine producing geothermal wells in Germany and France (NGB and URG) with an optimistic production scenario (90 % efficiency of extraction, constant Li concentration, 100 % use of the fluid a maximum of

7200t/a lithium carbonate could be produced (Goldberg et al., 2022). However, specifically the extraction technology represents an enormous challenge.

For other CRM, both extraction technologies and knowledge on their occurrence is still missing. The aim of the CRM project is therefore to close this gap. Within the project time, a better overview on the occurrence of various CRM in the different geological formations in the NGB as well as plans for optimized extraction technologies will be developed.

5.5 REFERENCES

Ahlrichs, N., Hübscher, C., Noack, V., Schnabel, M., Damm, V. and Krawczyk, C.M., 2020. Structural evolution at the northeast North German Basin margin: From initial Triassic salt movement to Late Cretaceous-Cenozoic remobilization. Tectonics, 39(7), p.e2019TC005927.

Blöcher, G., Reinsch, T., Henninges, J., Milsch, H., Regenspurg, S., Kummerow, J., Francke, H., Kranz, S., Saadat, A., Zimmermann, G. and Huenges, E., 2016. Hydraulic history and current state of the deep geothermal reservoir Groß Schönebeck. Geothermics, 63, pp.27-43.

Goldberg, V., Nitschke, F. and Kluge, T., 2022. Herausforderungen und Chancen für die Lithiumgewinnung aus geothermalen Systemen in Deutschland–Teil 2: Potenziale und Produktionsszenarien in Deutschland. Grundwasser, pp.1-15.

Hesshaus, A., Houben, G. and Kringel, R., 2013. Halite clogging in a deep geothermal well–Geochemical and isotopic characterisation of salt origin. Physics and Chemistry of the Earth, Parts A/B/C, 64, pp.127-139.

Huenges, E.; Wolfgramm, M. (Hg.) (2004): Sandsteine im In-situ-Geothermielabor Groß Schönebeck. Reservoircharakterisierung, Stimulation, Hydraulik und Nutzungskonzepte. Scientific Technical Report STR04/03. Geoforschungszentrum Potsdam in der Helmholtz-Gemeinschaft. Online verfügbar unter https://gfzpublic.gfz-potsdam.de/rest/items/item_8626_4/component/file_8625/content#page=172.

Frick, M., Kranz, S., Norden, B., Bruhn, D. and Fuchs, S., 2022. Geothermal Resources and ATES Potential of Mesozoic Reservoirs in the North German Basin. Energies, 15(6), p.1980.

Müller, D. and Regenspurg, S., 2014. Geochemical characterization of the lower Jurassic Aquifer in Berlin (Germany) for aquifer thermal energy storage applications. Energy Procedia, 59, pp.285-292.

Müller, D.R., Friedland, G. and Regenspurg, S., 2017. An improved sequential extraction method to determine element mobility in pyrite-bearing siliciclastic rocks. International Journal of Environmental Analytical Chemistry, 97(2), pp.168-188.

Pogarell, N. (2021) Gewinnung von Lithium und Strontium aus Thermalwässern -Auslaugung von permischen Sandsteinen und Vulkaniten (Groß Schönebeck, Deutschland). Bachelor thesis, Freie Universität Berlin.

Regenspurg, S., Feldbusch, E., Byrne, J., Deon, F., Driba, D.L., Henninges, J., Kappler, A., Naumann, R., Reinsch, T. and Schubert, C., 2015. Mineral precipitation during production of geothermal fluid from a Permian Rotliegend reservoir. Geothermics, 54, pp.122-135.

Regenspurg, S., Feldbusch, E., Norden, B. and Tichomirowa, M., 2016. Fluid-rock interactions in a geothermal Rotliegend/Permo-Carboniferous reservoir (north German basin). Applied Geochemistry, 69, pp.12-27.

Regenspurg, S., Alawi, M., Norden, B., Vieth-Hillebrand, A., Bloecher, G., Kranz, S., Scheytt, T., Horn, F., Burckhardt, O., Rach, O. and Saadat, A., 2020. Effect of cold and hot water injection on the chemical and microbial composition of an aquifer and implication for its use as an aquifer thermal energy storage. Geothermics, 84, p.101747.

Rockel, W., Brandt, W. and Seibt, P., 1999. Ein mesozoischer Aquifer im Zentrum Berlins als saisonaler Wärmespeicher für Parlamentsbauten. Brandenburgische geowiss Beitr, 6, pp.91-101.

Rockel, W.; Hurter, S. (2000): Tiefe Altbohrungen als Beitrag zur Nutzbarmachung klüftig - poröser Speichergesteine (geologische Grundlagen): Groß Schönebeck. Online verfügbar unter

https://www.researchgate.net/publication/267545418_Tiefe_Altbohrungen_als_Beitrag_zur_Nutzbarmachung_kluftig_-_poroser_Speichergesteine_geologische_Grundlagen_Gross_Schonebeck.

Wolfgramm, M., Thiem, S., Buse, C., Hoffmann, F., Tilsen, R., Rüdiger, R., (2019). Geothermie Schwerin-Lankow - ein Leuchtturmprojekt. Beitrag "Der Geothermiekongress DGK 2019" München, 19. – 21. November 2019.

Zimmermann G., Moeck, I. (2008): Geothermie Forschungsbohrung in Groß Schönebeck – von der Planung bis zur Stimulation. In: Brandenburgische Geowissenschaftliche Beiträge, S. 155–164. Online verfügbar unter https://lbgr.brandenburg.de/media_fast/4055/1-2_08_Zimmermann_155-164.pdf.

Zimmermann, G., Reinicke, A. (2010): Hydraulic stimulation of a deep sandstone reser-voir to develop an Enhanced Geothermal System: Laboratory and field experiments. In: Geother-mics 39 (1), S. 70–77. DOI: 10.1016/j.geothermics.2009.12.003

6 ALKALINE GEOTHERMAL AREA

Authors:
Michael Bau
Constructor (formerly Jacobs) University Bremen, Germany
Bettina Strauch, Martin Zimmer
GFZ German Research Centre for Geosciences, Germany

6.1 GEOLOGICAL BACKGROUND

The East African Rift System (EARS) extends from the Red Sea – Afar triple junction in the north to Malawi and Mozambique in the south, the western branch to Rwanda and the southwestern branch to Botswana. Initiated around 45 Ma ago, it is characterized by crustal movement and volcanic activity. One or more mantle plumes led to the formation of ~1000 km scale dynamic uplifts. The plateau uplift caused extensional stresses in the plate that were locally released through faulting and thinning to create the East African rift valleys (e.g. Stamps et al., 2018). There exists a close association between doming, rifting and alkaline magmatism/doming.

The volcano-tectonic history can be described as follows:

- The Early to Middle Miocene is characterized by early uplift and outpouring of alkali basalts and nephelinites.
- The Upper Miocene is characterized by doming of about 300 m and downwarping at future rift shoulders and fissure eruptions with more basalts and phonolites.
- The Pliocene is characterized by off-rift volcanism and further doming of about 1400 m, accompanied by the main rifting and graben faulting with deposition of trachytes on the rift floor (Southern Kenya Rift), and more basaltic volcanism.
- The Quaternary is characterized by major graben faulting, by caldera volcanoes in the axial zone of the rift, and by basalt phonolite volcanism in off-rift volcanoes (beginning in the Upper Pliocene).

The Kenya rift contains the largest accumulation of peralkaline salic lavas association, which are mildly alkaline and comprised of transitional basalts, trachytes, and occasional Kenya-type phonolites, pantellerites, and comendites (Baker & Wohlenberg, 1971; Baker et al., 1977; Macdonald et al., 1987; Saemundsson, 2010).

Pyroclastics, such as tuffs, agglomerates and ashes are also commonly associated with both large and central type off-axis volcanoes as well as with numerous central volcanic cones that characterize the rift floor. Also associated with the rifting and volcanics were relatively minor alkaline plutons, which resulted in the carbonatite-bearing complexes such as the Rangwe-Homa intrusive complex in the lake Victoria region (Le Bas, 1987; Mathu & Davies, 1996)

6.2 GEOTHERMAL EXPLORATION AND EXPLOITATION

The volcanic activity and hence the geothermal potential are the highest in the northeastern part of the EARS (Djibouti, Ethiopia, Kenya, Tanzania), where the geothermal potential of has long been recognized (e.g. geothermal exploration in Ethiopia started in 1969; Pürchel et al., 2013). Zemedkun (2018) estimated that the EARS geothermal resources are more than 20 GW, however, currently it is only utilized in Kenya (676 MW_e) and Ethiopia (7.5 MW_e; Zemedkun, 2018).

Among the countries in the East African rift, Kenya appears to be the most advanced in exploiting geothermal resources for power generation, but other countries in the rift also developing their geothermal resources, are Ethiopia, Djibouti, Tanzania, Mozambique, and Rwanda. The focus of geothermal exploration in Kenya has been in the central Kenya rift. This started already around 1956

with two wells drilled in Olkaria Kenya to a depth of 1035 m, which obtained temperatures up to 235 °C. Currently there are over two hundred deep wells at various depths <3000 m.

6.3 FLUIDS AND DISSOLVED RESOURCES

Very little emphasis has been placed upon the potential enrichment of critical metals in the geothermal waters in the EARS. Volcanic rocks in the EARS can vary from normal basalts (e.g. Rungwe Volcaninc Complex; Dávalos-Elizondo et al., 2021) to silicic trachytes (e.g. Kenya Rift Valley; Karingithi et al., 2010). Typical for rift magmatism, alkaline volcanics are widespread, with the most prominent example being natrocarbonatitic Oldoinyo Lengai volcano in the northern Tanzania. The major solute chemistry of these alkaline fluids is relatively well characterized (Awaleh et al., 2020; Dávalos-Elizondo et al., 2021; Karingithi et al., 2010; Pürschel et al., 2013). Many of the hot springs have alkaline pH, up to c. 10 and are typically Na-HCO_3 or Na-Cl type waters with high fluoride content (Awaleh et al., 2020; Dávalos-Elizondo et al., 2021). The high alkalinity is due the degassing of magmatic CO_2 and the subsequent chemical weathering of the surrounding rocks (e.g., $2KAlSi_3O_8 + 2CO_2 + 3H_2O$ ó $Al_2Si_2O_5(OH)_4 + 2K^+ + 2HCO_3^- + 4SiO_2$; Pürschel et al., 2013).

Rare Earth Elements: To the best of our knowledge, there has been only a handful of studies presenting data for rare earth elements (REE) from alkaline fluids from the EARS (Dekov et al., 2014, 2021). Indication for the REE content in alkaline geothermal fluids could be taken from the hyperalkaline Lake Abhè, located at the border between Ethiopia and Djibouti, which is fed by numerous hot springs. Dekov et al. (2014) has presented REE data from the hot spring, cold spring and the Lake water, where the ∑REE were 0.079, 0.601 and 1.745 ppb, respectively. Interestingly, both hot and cold spring showed a similar flat shale-normalized REE pattern, whereas the lake shows a strongly heavy REE-enriched pattern. A recent study by Dekov et al. (2021) on Lake Asal with neutral pH from the central part of Djibouti, showed significantly lower REE concentrations, suggesting that pH and alkalinity in the fluids could play an important role for keeping the REE in the solution. This is supported by some recent experimental work highlighting the role of alkalis and alkalinity in REE-ore forming processes (Anenburg et al., 2020; Louvel et al., 2022). Anenburg et al. (2020) has shown that not only the anion composition of the fluids is important for REE mobility, but also the alkali concentration. They emphasise that Na and K concentration are crucial for effective heavy REE transport in hydrothermal fluids associated with carbonatites. Moreover, a recent study by Louvel et al. (2022) highlighted the role of carbonate complexation in enhancing hydrothermal transport of REE. This has been also described in natural settings. Singh et al. (2022), for example, described elevated concentration and enhanced solubility of alkali-REE-carbonate(hydroxyl) complexes in fluid inclusions from fluorite. These conditions would be also applicable to the EARS, especially to geothermal fluids percolating through alkaline and carbonatitic rocks. The latter are well known to be an important REE resource.

Helium: In 2017, He was identified as a critical raw material by the European Commission on the basis of growing concern that existing reserves could not meet the required demands. Helium is mainly produced as a byproduct of natural gas in the USA, Qatar, Algeria and Russia. However, He production from geothermal sources is not profitable yet at current world market prices.

The predominant ^4He isotope is formed from the alpha decay of U and Th. A potential He source rock must therefore have high U and Th concentrations and be relatively ancient; both requirements are met by the Tanzanian Precambrian basement rocks. For this reason, the Tanzanian craton has been selected as a target area for sampling gas from hot springs. During a field campaign in September 2022, thirteen gas samples were collected from hot springs and alkaline lakes and were analyzed for their gas chemical and isotopic composition. Samples were collected from the Tanzanian craton and, for comparison, also from surrounding volcanic and rift regions. The preliminary results show CO_2-rich and N_2-rich gases. The N_2-rich gases with crustal properties are characterized by high He concentrations occasionally above 6 vol%, whereas the CO_2-dominated volcanic gases with Earth mantle signatures show only small amounts of He.

6.4 DEEP SUB-SURFACE TEMPERATURES IN EAST AFRICA

The East African rift has a high geothermal gradient estimated at >200 °C/km (Wheildon et al., 1994), and is accompanied by significant magmatic activity due to the shallow lithosphere boundary. Exploration and development of geothermal energy along the Kenya Rift System has provided insights into surface and subsurface temperature profiles. Ground surface and steam temperature in the north Kenya Rift are on average about 80 °C and may extend to a maximum of 96 °C, which is approximately the local boiling point (Spink, 1945). While in the Central Kenya rift region within the Olkaria geothermal field, the vertical temperature gradient above the reservoirs is about 400 °C/km, a steam zone with temperatures of 240 °C is encountered at 600-800 m deep (Bodvarsson et al., 1987). Higher temperatures (>400 °C) occur deeper than 2000 m (Karingithi, 2000), whereas in the southern Kenya rift, the vertical temperature gradients along the profiles are lower and estimated to range between 70 °C/km and 112 °C/km (Githiri et al., 2012).

6.5 STRUCTURE AND STRESS-FIELD MEASUREMENTS

The East African Rift extends over 3000 km through the African continent and is characterized by a series of fault-bounded basins and volcanic centres stretching through the rift in a roughly NS direction. The EARS separates the Nubian subplate to the west from the Somalian subplate to the east. Beginning in the Afar triple junction, it crosses the Ethiopian highland, forms the Gregory Rift in Kenya and disperses in northern Tanzania after Lake Natron, forming the Eastern Rift Branch. The Western Rift Branch starts in southern Sudan and runs through the rift valley lakes (including Lake Tanganyika and Lake Malawi) to Mozambique. Fault kinematics, GPS velocities and transform fault and spreading rate data reveal that the Somali plate is composed of microplates plates (Victoria, Rovuma and Lwandle) (Saria et al., 2014; Stamps et al., 2008; Stamps et al., 2015).

Observations of the divergence between the Somalian and Nubian plates, along the East African Rift System (EARS), stand among the recent progresses in plate boundary kinematics. Saria et al. (2014) indicate a slow, clockwise rotation of the Somalian plate with respect to Nubia about a pole located offshore South Africa. Rates of relative motion along the EARS increase from south to north, with maximum opening rates of 6 mm/yr at the Afar triple junction.

The EARS is affected by stresses with a general E–W orientation of horizontal principal extension (S_{hmin}), while the Nubian plate is affected by E–W horizontal principal compression (S_{Hmax}). Most of the rift basins that surround the Tanzanian craton display S_{hmin} orientations roughly orthogonal to their trend, two dominant normal fault trends of S_{hmin} exist: WNW–ESE extension in the north-western segments of the EARS and in the South-western regions and ENE–WSW extension in the central part of the Western Rift Branch, the southern extremity of the Eastern Rift Branch, the southernmost rift segment and the continental margin(Delvaux & Barth, 2010) .

The extension zones along the volcanotectonic axis record protracted normal faulting, dyke intrusion, hydrothermal activity and frequent, low-magnitude seismicity (Ibs-von Seht et al., 2001; Mulwa et al., 2014; Tongue et al., 1994).

6.6 REFERENCES

Anenburg, M., Mavrogenes, J. A., Frigo, C., & Wall, F. (2020). Rare earth element mobility in and around carbonatites controlled by sodium, potassium, and silica. Science Advances, 6(41), eabb6570. https://doi.org/10.1126/sciadv.abb6570

Awaleh, M. O., Boschetti, T., Adaneh, A. E., Daoud, M. A., Ahmed, M. M., Dabar, O. A., Soubaneh, Y. D., Kawalieh, A. D., & Kadieh, I. H. (2020). Hydrochemistry and multi-isotope study of the waters from Hanlé-Gaggadé grabens (Republic of Djibouti, East African Rift System): A low-enthalpy

geothermal resource from a transboundary aquifer. Geothermics 86, 101805. https://doi.org/10.1016/j.geothermics.2020.101805

Baker, B., & Wohlenberg, J. (1971). Structure and evolution of the Kenya rift valley. Nature, 229(5286), 538-542. doi:10.1038/229538a0

Baker, B. H., Goles, G. G., Leeman, W. P., & Lindstrom, M. M. (1977). Geochemistry and petrogenesis of a basalt-benmoreite-trachyte suite from the southern part of the Gregory Rift, Kenya. Contributions to Mineralogy and Petrology, 64(3), 303-332.

Bodvarsson, G. S., Pruess, K., Stefansson, V., Bjornsson, S., & Ojiambo, S. B. (1987). East Olkaria Geothermal Field, Kenya: 1. History match with production and pressure decline data. Journal of Geophysical Research: Solid Earth, 92(B1), 521-539.

Dávalos-Elizondo, E., Atekwana, E. A., Atekwana, E. A., Tsokonombwe, G., & Laó-Dávila, D. A. (2021). Medium to low enthalpy geothermal reservoirs estimated from geothermometry and mixing models of hot springs along the Malawi Rift Zone. Geothermics, 89, 101963. https://doi.org/10.1016/j.geothermics.2020.101963

Dekov, V. M., Egueh, N. M., Kamenov, G. D., Bayon, G., Lalonde, S. V., Schmidt, M., Liebetrau, V., Munnik, F., Fouquet, Y., Tanimizu, M., Awaleh, M. O., Guirreh, I., & Le Gall, B. (2014). Hydrothermal carbonate chimneys from a continental rift (Afar Rift): Mineralogy, geochemistry, and mode of formation. Chemical Geology, 387, 87–100. https://doi.org/10.1016/j.chemgeo.2014.08.019

Dekov, V. M., Guéguen, B., Yamanaka, T., Moussa, N., Okumura, T., Bayon, G., Liebetrau, V., Yoshimura, T., Kamenov, G., Araoka, D., Makita, H., & Sutton, J. (2021). When a mid-ocean ridge encroaches a continent: Seafloor-type hydrothermal activity in Lake Asal (Afar Rift). Chemical Geology, 568, 120126. https://doi.org/10.1016/j.chemgeo.2021.120126

Delvaux, D., & Barth, A. (2010). African stress pattern from formal inversion of focal mechanism data. Tectonophysics, 482(1), 105-128. doi:https://doi.org/10.1016/j.tecto.2009.05.009

Githiri, J., Patel, J., Barongo, J., & Karanja, P. (2012). Spectral analysis of ground magnetic data in Magadi area, Southern Kenya Rift. Tanzania Journal of Science, 38(1), 1-14.

Ibs-von Seht, M., Blumenstein, S., Wagner, R., Hollnack, D., & Wohlenberg, J. (2001). Seismicity, seismotectonics and crustal structure of the southern Kenya Rift—new data from the Lake Magadi area. Geophysical Journal International, 146(2), 439-453.

Karingithi, C. W. (2000). Geochemical characteristics of the Greater Olkaria geothermal field, Kenya: United Nations University.

Karingithi, C. W., Arnórsson, S., & Grönvold, K. (2010). Processes controlling aquifer fluid compositions in the Olkaria geothermal system, Kenya. Journal Volcanology Geothermal Research 196, 57–76. https://doi.org/10.1016/j.jvolgeores.2010.07.008

Louvel, M., Etschmann, B., Guan, Q., Testemale, D., & Brugger, J. (2022). Carbonate complexation enhances hydrothermal transport of rare earth elements in alkaline fluids. Nature Communications, 13(1), Article 1. https://doi.org/10.1038/s41467-022-28943-z

Le Bas, M. (1987). Nephelinites and carbonatites. Geological Society, London, Special Publications, 30(1), 53-83.

Macdonald, R., Davies, G., Bliss, C., Leat, P., Bailey, D., & Smith, R. (1987). Geochemistry of High-silica Peralkaline Rhyolites, Naivasha, Kenya Rift Valley. Journal of Petrology, 28(6), 979-1008. doi:10.1093/petrology/28.6.979

Mathu, E. M., & Davies, T. (1996). Geology and the environment in Kenya. Journal of African Earth Sciences, 23(4), 511-539.

Mulwa, J. K., Kimata, F., Suzuki, S., & Kuria, Z. N. (2014). The seismicity in Kenya (East Africa) for the period 1906–2010: A review. Journal of African Earth Sciences, 89, 72-78.

Pürschel, M., Gloaguen, R., & Stadler, S. (2013). Geothermal activities in the Main Ethiopian Rift: Hydrogeochemical characterization of geothermal waters and geothermometry applications (Dofan-Fantale, Gergede-Sodere, Aluto-Langano). Geothermics, 47, 1–12. https://doi.org/10.1016/j.geothermics.2013.01.00

Saemundsson, K. (2010). East African Rift System–An Overview. Short Course V on Exploration for Geothermal Resources, organized by UNU-GTP, GDC and KenGen, at Lake Bogoria and Lake Naivasha, Kenya, 29.

Saria, E., Calais, E., Stamps, D., Delvaux, D., & Hartnady, C. (2014). Present-day kinematics of the East African Rift. Journal of Geophysical Research: Solid Earth, 119(4), 3584-3600.

Singh, T., Upadhyay, D., Patel, A. K., & Mishra, B. (2022). High MREE-HREE solubility in a carbonatite-derived hydrothermal fluid: Evidence from fluorite-hosted fluid inclusions in the Amba Dongar carbonatite complex, India. Chemical Geology, 613, 121162. https://doi.org/10.1016/j.chemgeo.2022.121162

Spink, P. (1945). Thermal activity in the eastern Rift Valley. The Geographical Journal, 105(5/6), 197-207.

Stamps, D. S., Calais, E., Saria, E., Hartnady, C., Nocquet, J. M., Ebinger, C. J., & Fernandes, R. M. (2008). A kinematic model for the East African Rift. Geophysical Research Letters, 35(5).

Stamps, D. S., Iaffaldano, G., & Calais, E. (2015). Role of mantle flow in Nubia-Somalia plate divergence. Geophysical Research Letters, 42(2), 290-296. doi:https://doi.org/10.1002/2014GL062515

Tongue, J., Maguire, P., & Burton, P. (1994). An earthquake study in the Lake Baringo basin of the central Kenya Rift. Tectonophysics, 236(1-4), 151-164.

Wheildon, J., Morgan, P., Williamson, K., Evans, T., & Swanberg, C. (1994). Heat flow in the Kenya rift zone. Tectonophysics, 236(1-4), 131-149.

Zemedkun, M., 2018. Geothermal outlook in East African and contribution of UNIGTP in capacity building. In: Proceedings of the 40th Anniversary Workshop of UNUGTP. Reykjavik, Iceland

7 METAMORPHOSED FLYSCH: SEFERİHİSAR, TURKEY

Authors:
Alper Baba, Tolga Ayzit
Izmir Institute of Technology, Türkiye

7.1 GEOLOGICAL BACKGROUND

The Seferihisar site is located in the west of the Anatolian Plateau, approximately 50 km southwest of İzmir city center, Türkiye. The Anatolian plateau presents a rich metallogenetic spectrum, primarily in relation to the Alpine Himalayan orogeny. The ore occurrence in Anatolia has been associated with superimposed expansion (Middle Eocene) and compressional (Late Cretaceous) magmatism in the Bitlis-Zagros (south) and Pontides (north) subduction zones (Figure 7.1; Şengör and Yılmaz, 1981; Leman and Staude, 2002). Especially considering the high heat flow value and low Curie point depth (CPD) of western Anatolia, the potential for mineral extraction in geothermal fields draws attention.

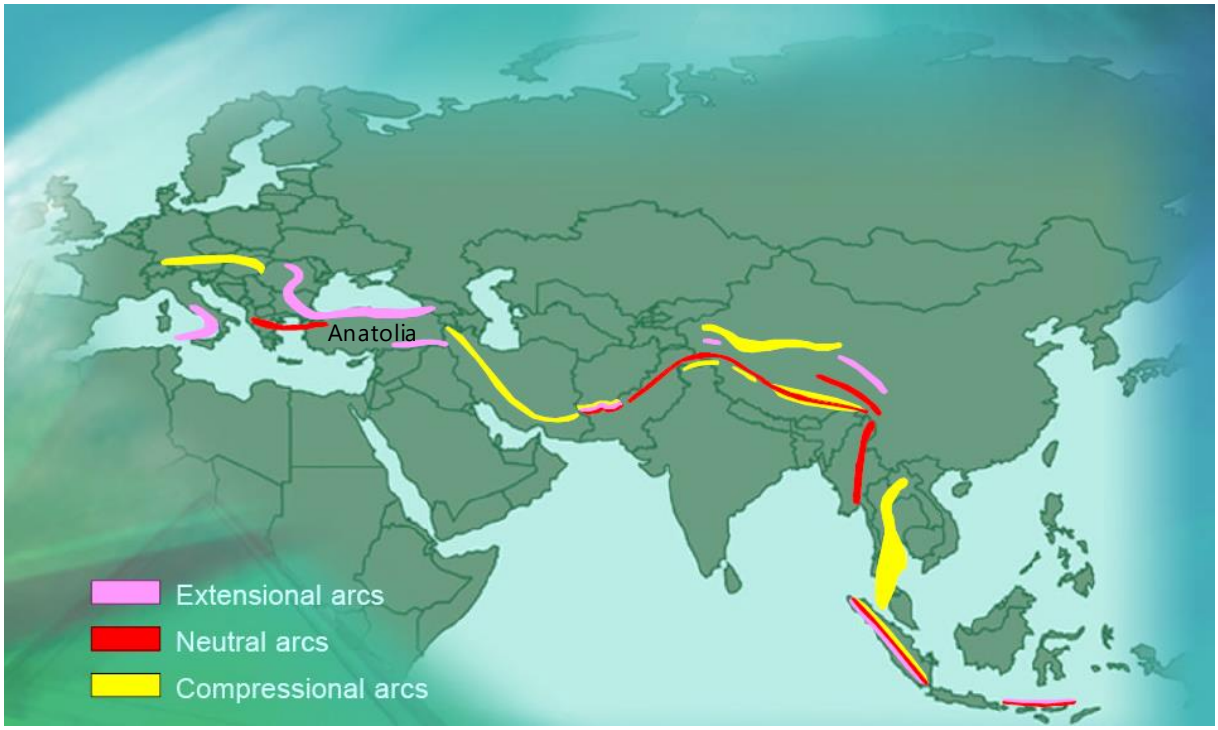

Figure 7.1: Global distribution of principal Tethyan Arcs (Modified from Şengör and Yılmaz, 1981; Leaman and Staude, 2002).

The Seferihisar site is within the scope of a sedimentary and high enthalpy area where the geothermal gradient is high due to the increased salinity of its fluids and the bedrocks are sedimentary areas (sandstone, mudstone, shale).

Seferihisar geothermal field is located within the Bornova Flysch Zone (BFZ) which consists of deformed Maastrichtian–Paleocene greywacke and shale with Mesozoic limestone and ophiolite blocks and is approximately 60 km wide and 225 km long in the northeast direction (Okay et al., 2012; Okay and Siyako, 1993). The BFZ is a regional olistostrome-melanbetween the northwest İzmir-Ankara Sutureorthwest and the Menderes Massif in the southeast (Figure 7.2).

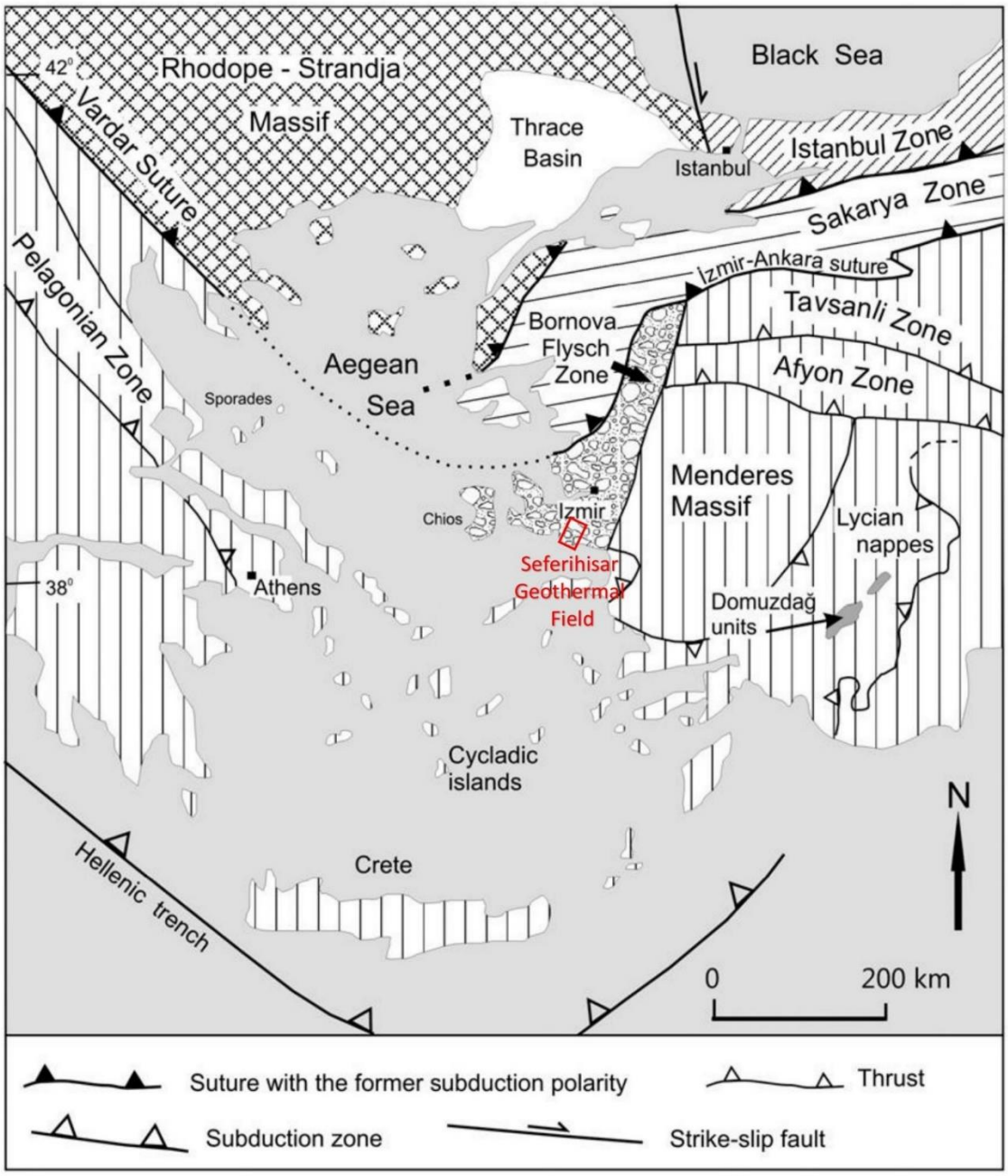

Figure 7.2: Tectonic map of the Aegean region showing the setting of the Bornova Flysch Zone and Seferihisar Geothermal Field (Modified from Okay and Tüysüz, 1999; Okay et al., 2012).

7.1.1 The regional tectonics of west Anatolia

Western Anatolia comprises two main tectonic terranes which names are the Pontides and the Anatolides-Taurides. The collision of the European and African plates during the closure of the Tethys Ocean in the Mesozoic/ early Cenozoic led to the amalgamation of these two units and resulted in the İzmir- Ankara Suture Zone (Okay and Tüysüz, 1999; Okay, 2008; Sharp and Robertson, 2006; Voudouris and Melfos, 2014; Yiğit, 2009). Western Anatolia is one of the active seismic regions where orogenic compression follows continental expansion (Dewey and Şengör, 1979; Şengör and Yılmaz, 1981; Jackson and McKenzie, 1984; Şengör et al., 1985; Eyidoğan and Jackson, 1985; Şengör, 1987; Seyitoğlu and Scott, 1991; Bozkurt, 2001a).

Crustal extension in western Anatolia began in the early Miocene with N-S to NE-SW extension, exposing the Menderes Massif and the Cycladic metamorphic complex which consists mainly of high-pressure-low temperature metamorphites (Hinsbergen, 2010; Göktaş and Çakmakoğlu, 2017). The BFZ may have acted as a transfer zone between these two centres of extension. Mid- to late-Miocene N-S extension, creating numerous volcano sedimentary basin across western Anatolia (i.e., Cumaovası basin), is cut by later wrench extension and strike-slip faults in the Pliocene (Uzel and Sözbilir, 2008; Uzel et al., 2012; Uzel et al., 2013; Hinsbergen, 2010).

7.1.2 Mineralisation in the vicinity of Bornova Flysch Zone

The metal-rich area is a component of the Western Tethyan orogen, which is made up of a number of Cretaceous through Cenozoic magmatic belts that extend over 3500 km from Slovakia to Iran and continue east into the Central and Eastern Tethyan orogen. The magmatic belts in Türkiye are generally younger to the south, ranging from Cretaceous to Paleogene arc magmatism connected to subduction in the Pontides to Neogene magmatism related to post-collision extension in central and western Anatolia created by slab-roll back. (Eldorado Gold Corporation, 2019; Jolivet et al., 2015b). Late Cretaceous to Late Miocene intrusive rocks of western Anatolia have compositions ranging from calc-alkaline granites to granodiorites and monzogranites to syenogranites and have a subduction-related origin (Delaloye and Bingol, 2000). In contrast, in eastern Anatolia, volcanic activity started in Late Miocene with basic and intermediate alkaline rocks and continued with widespread calc-alkaline volcanism during the Pliocene. During the Late Pliocene to Quaternary alkaline volcanism dominated in both areas of Anatolia (Yilmaz, 1990).

The Western Tethyan Metallogenic Belt in Anatolia hosts numerous hydrothermal mineral deposits which are structurally-controlled epithermal, porphyry and base metal deposits formed along detachment faults and SW to NE trending grabens and faults and their intersections during Neogene tectonic denudation in the Menderes Massif region (Figure 7.3; Ayzit, 2015; Gessner et al., 2017; Menant et al., 2018). The ore deposits occurring in Seferihisar Horst are hosted by flysch, which exhibits sub-green facies features, intercalated mudstone, fine-grained sandstone, limestone and marly sandstone. (Boucher, 2016). Locally, segments of marly sandstone and limestone are interbedded with lenses of ophiolitic basalt (spilite) and serpentinite that range in thickness from tens to hundreds of meters. The Bornova Flysch in the Seferihisar Horst is not fossiliferous, however other stratigraphically related sequences of the flysch have a wealth of faunal records that give age limits. In these, an Upper Cretaceous to Lower Paleocene siliciclastic sequence is overlain by ophiolitic sequences of spilite and serpentinite that are composed of Upper Jurassic to Lower Cretaceous pelagic limestone. Throughout the whole Seferihisar Horst, the flysch sequence bedding dip directions form a broad, asymmetric NE-trending (Okay and Altıner, 2007).

The Neogene sequence associated with mineralization in Seferihisar Horst forms rhyolite intrusions and hornfels zone rocks. Intrusions are, depending on the sub-volcanic magmatism, commonly showing porphyritic texture, yellowish-white, hard and angled fractures. Borsi et al., (1972) reported the Late Miocene for rhyolite rocks in the region. Rhyolite dikes crop out highly silicified as well as fresh intrusions. Distribution of the rhyolite dikes may be associated with a shallow stock. In the region where Au, Ag, Pb, Zn, Cu, Fe and Mn paragenesis is known, pyrite, chalcopyrite, sphalerite and galena sulphide ore minerals were observed in order of abundance (Ayzit, 2015). The mineralized areas in Seferihisar Horst are associated with subvolcanic rhyolite dykes along NE-SW and NW-SE tectonic lines in İzmir Flysch.

Geothermal activities in the Seferihisar area have been known since ancient times tracing back to the Roman period. People once used the thermal waters in this area for bathing and washing purposes. Travertine walls were created by thermal waters carved their way along historic aqueducts. There are many natural geothermal springs with temperatures between 36-72 °C in the region (Parlaktuna et al., 2010; Tarcan and Gemici, 2003; Eşder and Siimsek,1975, 1977; Filiz, 1982; Eşder et al., 1983; Yımazer,

1984; Canbolat, 1986; Eşder, 1990; Filiz and Tarcan, 1993; Eşder et al., 1995; Filiz et al., 1997; Conrad et al., 1997; Tarcan et al., 1999; Yılmazer, 2001).

While it is known that there are about 10 natural springs in the area of the field and with new points determined after the Samos earthquake, there are more than 40 wells that are used for different purposes or that are idle. Some wells in the field were drilled more than 30 years ago and are not currently used and rehabilitation is not possible due to corrosion of well equipment. New wells were drilled for the RSC geothermal power plant, which started operating in the region in 2020 (Baba et al., 2022). In general, the temperature of the wellhead drilled around the Tuzla fault zone (TFZ) varies in the range of 90-153 °C. (Parlaktuna et al., 2010; Tarcan and Gemici, 2003; Baba et al., 2022). In the wells drilled for electricity generation, a maximum base temperature of 207 °C was reached at a depth of 2100 meters. İzmir Geothermal Energy Industry and Trade. A.Ş. leased some of its Cumalı and Doğanbey geothermal resources to RSC Elektrik Company for electricity generation in 2016. The installed power of the power plant is 12 MW_e and its annual production is approximately 96 GWh. (Baba et al., 2022).

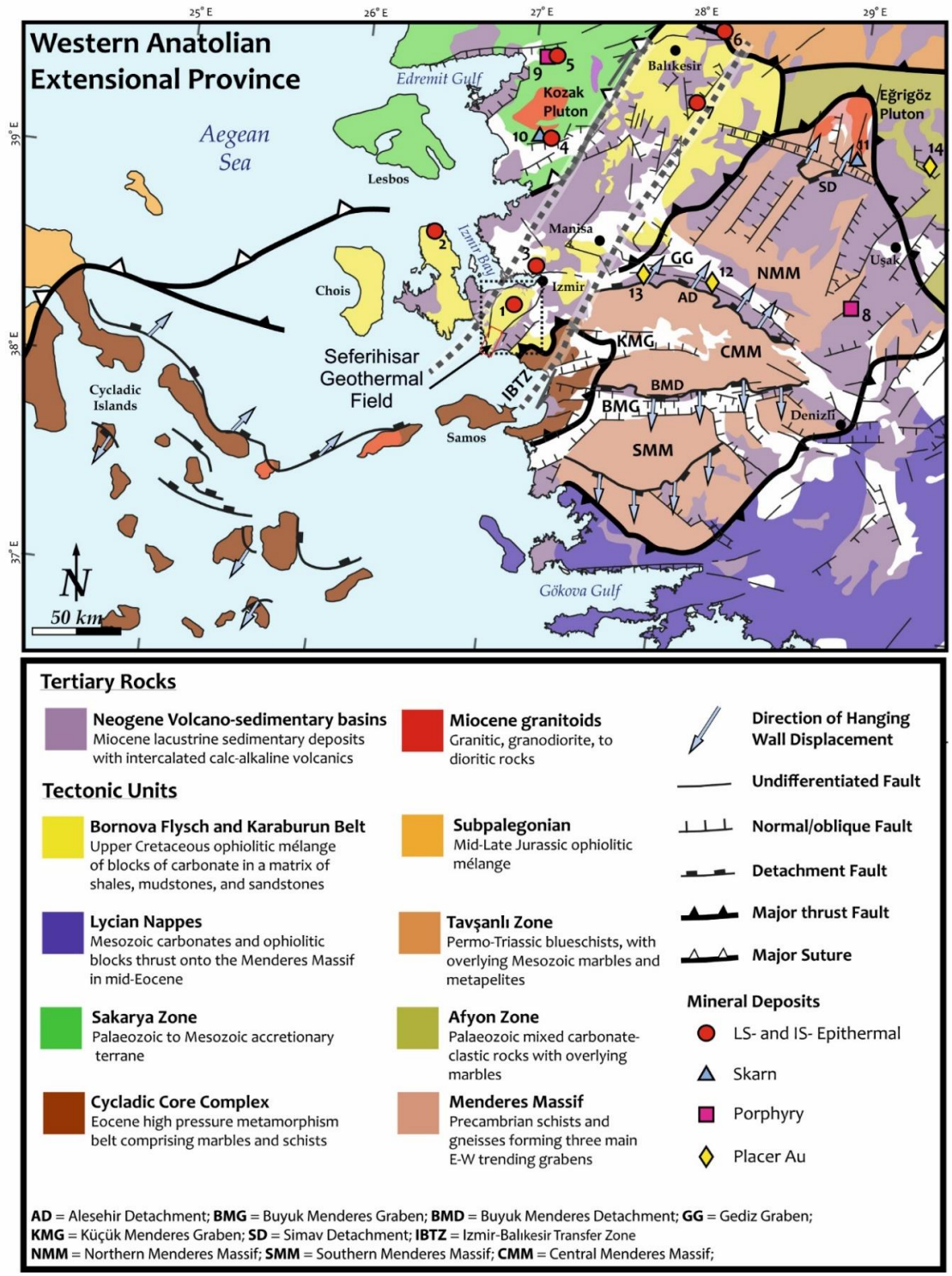

Figure 7.3: Simplified Tectonic Map of the Western Anatolian Extensional Province and Locations of Mineral Deposits (Combined with Ayzit, 2015; Boucher, 2016; Sözbilir et al., 2011; Uzel et al., 2013; Yiğit, 2006, 2009; Okay, 1989, 2008; Sharp and Robertson, 2006; Hinsbergen, 2010; Gessner et al., 2013). 1 = Efemçukuru (Au); 2 = Kalecik (Hg); 3 = Arapdağ (Au, Ag, Pb, Sb); 4 = Ovacık (Au, Ag); 5 = Küçükdere (Au); 6 = Balya (Au, Ag, Pb, Zn); 7 = Sındırgı (Au, Ag); 8 = Kışladağ (Au); 9 = Tepeoba (Cu, Mo, Au); 10 = Ayazmant (Fe, Cu); 11 = Kalkan (Fe); 12 = Pactolus (modern day Gediz) River (historic Au); 13 = Irlamaz-Manisa (Au); 14 = Sart (Au)1 = Efemçukuru (Au); 2 = Kalecik (Hg); 3 = Arapdağ (Au, Ag, Pb, Sb); 4 = Ovacık (Au, Ag); 5 = Küçükdere (Au); 6 = Balya (Au, Ag, Pb, Zn); 7 = Sındırgı (Au, Ag); 8 = Kışladağ (Au); 9 = Tepeoba (Cu, Mo, Au); 10 = Ayazmant (Fe, Cu); 11 = Kalkan (Fe); 12 = Pactolus (modern day Gediz) River (historic Au); 13 = Irlamaz-Manisa (Au); 14 = Sart (Au)

Geothermal studies have been carried out since 1970 in the Cumaovası basin, where the Seferihisar geothermal field is located (Eşder and Şimsek, 1975). There are different geothermal areas from the Seferihisar geothermal field in the east and northeast of the NE-trending right-lateral strike-slip Tuzla Fault, which controls the basin structure and morphology of the region. The geothermal resources in the Seferihisar district are distributed around Cumalı, Karakoç, Doğanbey and Orhanlı.

Candan et al. (1997) suggested that the Late Cretaceous high-pressure metamorphics cropping out in the Seferihisar geothermal area are the extension of the Cycladic Zone in Türkiye, and it has been reported in the literature in this way in recent studies (Figure 7.4). The Cycladic metamorphics consist of an uninterrupted series of Triassic-Upper Cretaceous aged sediments (platform type marbles with transitional contacts on mica-schists and metavolcanites and metaconglomerates within them) and a possible Upper Cretaceous aged overlying Cycladic metamorphics. It consists of two tectonic slices of metaolistostrom (high-pressure rocks, serpentinite and marble blocks in a pelitic matrix) (Göktaş, 2019). This unit is also overlain by the Upper Cretaceous-Paleocene-aged Bornova Flysch, which is also overlain by a tectonic thrust (Koralay et al., 2011).

Eşder and Şimşek (1975) and Aksoy et al. (2008b) stated that the limestone, metasandstone, serpentinite and splitic lavas belonging to the metamorphosed Bornova flysch are semi-permeable and form the geothermal reservoir rock (Figure 7.5). The permeability of the Bornova flysch zone is generally secondary, resulting from faults, fractures, alternation of metasandstones and volcanic intrusion. While the thickness of the reservoir rock was reported to be around 1500 m in the north of Seferihisar horst (Şalk et al. 1999), the thickness of the reservoir rock was reported to be several hundred meters according to the well logs in the Seferihisar geothermal field (Eşder and Şimşek, 1977; Öngür, 2001).

7.2 FLUIDS AND DISSOLVED RESOURCES

7.2.1 Ancient fluids linked with ore mineralisation

Efemçukuru hosts the most important mineralization in the Seferihisar horst, which is described above. The fluid inclusion data from Efemçukuru show a wide variation in T_h between 200 and 300 °C and a range in salinity between almost zero and 9 eq. wt.% NaCl. There is no discernible variation in T_h, with the higher salinities being more prevalent in depth (Table 7.1; Oyman et al., 2003).

It is only possible to truly assess the O and D isotope systematics of hydrothermal fluids in conjunction with other information, such as fluid inclusion measures, petrography, and, most crucially, field relations (Pirajno, 2009). However, the D and O isotopic data for the ore fluids obtained from quartz and clay samples indicate varying degrees of $\delta^{18}O_{water}$ enrichment relative to the meteoric water path (Oyman, 2019). The stable isotope study of the Ovacık mineralization area, which also developed due to low sulfidation, was conducted by Yılmaz et al. 2007.

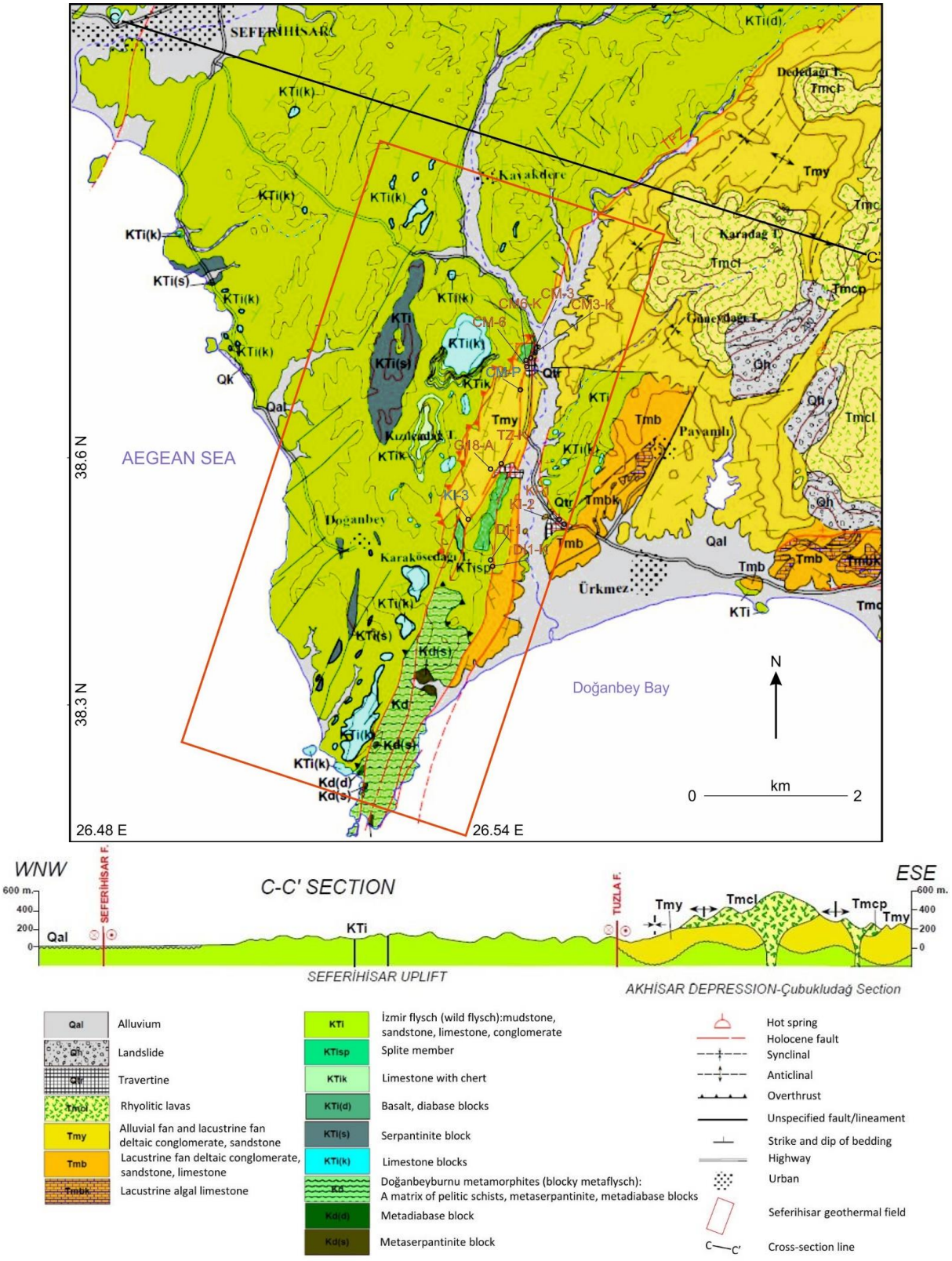

Figure 7.4: Geological map (with sample locations) and cross-section of Seferihisar geothermal field (Modified from Göktaş and Çakmakoğlu, 2017; Uzel and Sözbilir, 2008)

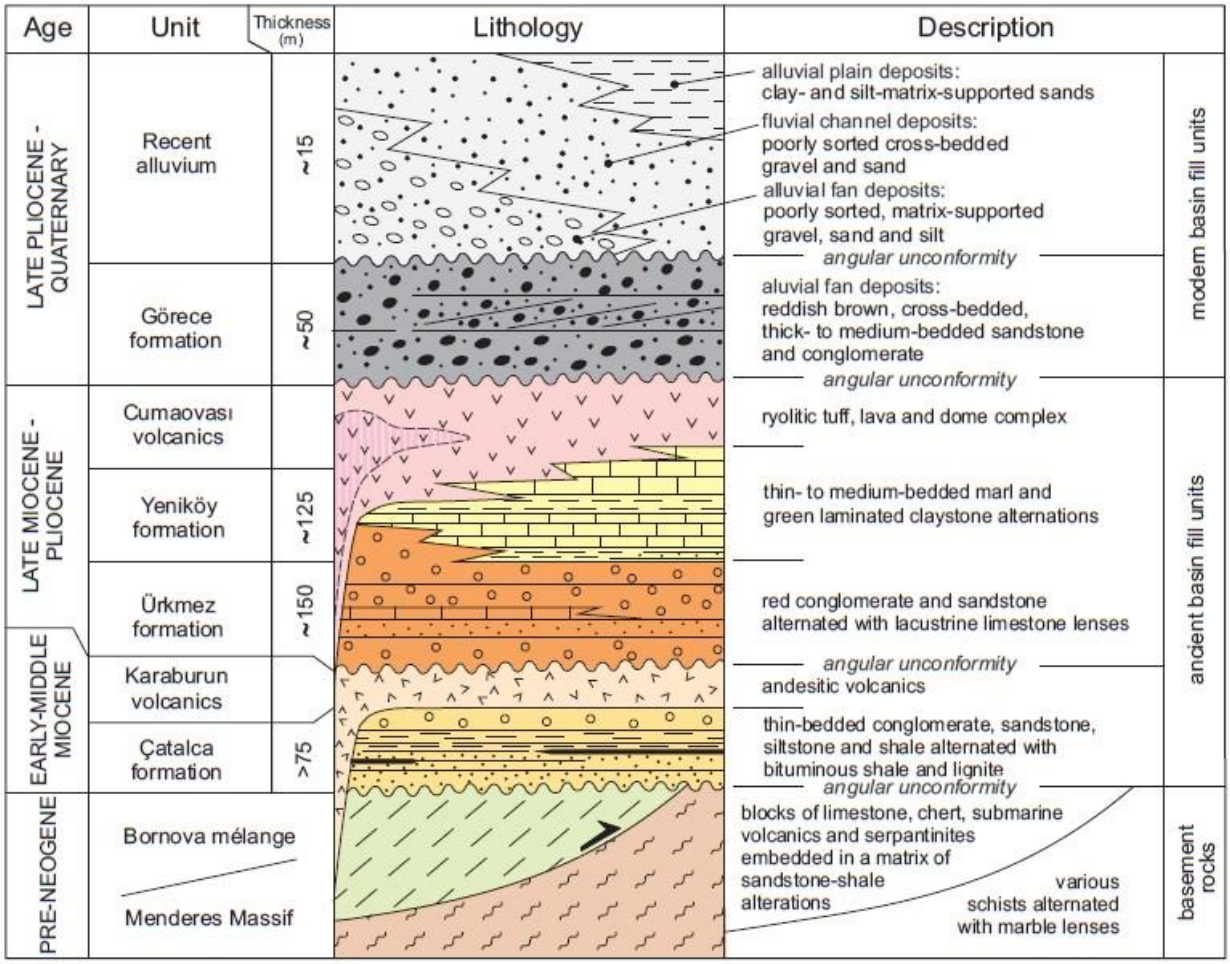

Figure 7.5: Generalized columnar section through the Seferihisar Geothermal Field (Uzel and Sözbilir, 2008).

Table 7.1: Selected fluid inclusion data for the epithermal mineralization around BFZ. All inclusions types are primary (simplified from Oyman, 2019).

Deposits	T_h (°C)		T_h (°C) average	Salinity (wt % NaCL)		Salinity average	$T_{m\ first}$	Minerals	Reference
Efemçukuru (Au)	174	328	243	0.2	9.9	-	-	Quartz	Oyman et al. (2003)
	185	224	211	2.1	4	-	-	Sphalerite	
Ovacık (Au, Ag)	148	298	187	0.7	2.1	1.4	-	Quartz	Yılmaz et al. (2007)
Sındırgı (Au, Ag)	150	395	250	0.2	4.8	1.8	−20 to −33	Quartz	Yılmaz et al. (2013)

7.2.2 Present-day waters and dissolved mineral resources

Hydrological, hydrogechemical, isotope (WB, 2021; Baba and Sözbilir, 2012; Baba et al., 2022; Bulut, 2013; Özgür et al., 2017; Kaya, 2019), alteration (Akar, 2012), numerical modeling (Magri et al., 2018) investigations of surface and underground waters in the Seferihisar geothermal area have been continuing since the 1960s.

In this section, in order to better understand the geochemical characteristics of the field, a summary is given of the report data commissioned by İzmir Geothermal Energy Industry Trade Inc. (2008). Some (*) sample locations and data were used from Tarcan and Gemici (2003) within the scope of the report (Table 7.2).

Table 7.2: Information on water samples (locations in Fig 4.) collected from the Seferihisar geothermal field (Modified from Tarcan and Gemici, 2003; IGEI, 2008; Aydın et al., 2022).

Field	Sample No	Sample Type	Well Depth (m)	T (C^0)	Ion Line-up	Hydro-geochemical Facies	pH	µS/cm	B (mg/l)	Li (mg/l)
Cumalı	CM-3	Drilling	341	153	$Cl>HCO_3>SO_4$ $Na+K>Ca>Mg$	Na+K - Cl	7.8	33600	17.5	13.4
Cumalı	CM3-K	Hot spring	-	72	$Cl>HCO_3>SO_4$ $Na+K>Ca>Mg$	Na+K - Cl	7.4	31000	16	12.2
Cumalı	CM-6	Drilling	284	148	$Cl>HCO_3>SO_4$ $Na+K>Ca>Mg$	Na+K - Cl	7.6	31900	16.2	-
*Cumalı	CM-6-K	Hot spring	-	66	$Cl>HCO_3>SO_4$ $Na+K>Ca>Mg$	Na+K - Cl	7.5	31900	16.2	12.2
*Cumalı	CM-P	Cold water	-	17	$HCO_3>Cl>SO_4$ $Ca>Mg>Na+K$	Ca-HCO3	7.9	521	0.02	-
Doğanbey	DI-1	Drilling	350	78	$Cl>HCO_3>SO_4$ $Na+K>Ca>Mg$	Na+K - Cl	7.5	13700	10.6	-
*Doğanbey	DI-1-K	Hot spring	-	68	$Cl>HCO_3>SO_4$ $Na+K>Ca>Mg$	Na+K - Cl	7.8	13000	11	4.1
*Karakoç	KI-1	Hot spring	-	59	$Cl>HCO_3>SO_4$ $Na+K>Ca>Mg$	Na+K - Cl	7.7	7580	9.7	4.1
*Karakoç	KI-2	Pond	-	59	$Cl>HCO_3>SO_4$ $Na+K>Ca>Mg$	Na+K - Cl	7.8	7910	10.4	4.1
*Karakoç	KI-3	Cold water	-	17	$HCO_3>Cl>SO_4$ $Mg>Na+K>Ca$	$Mg-HCO_3$	7.8	1720	0.63	-
*Tuzla	TZ-K	Pond	-	65	$Cl>HCO_3>SO_4$ $Na+K>Ca>Mg$	Na+K - Cl	7.4	35400	13.8	9.6
Tuzla	G18-A	Drilling	301	109	$Cl>SO_4>HCO_3$ $Na+K>Ca>Mg$	Na+K - Cl	7.3	33900	11.5	-

The Seferihisar Geothermal Field was examined in 4 different areas, namely Cumalı, Doğanbey, Karakoç and Tuzla within the scope of the report.

The dominant anion of Cumalı, Doğanbey, Karakoç, Tuzla hot waters is Cl and the dominant cations by Na+K. In this context, hot waters are (Na+K)-Cl facies. Cold waters collected from Cumalı and Karakoç fields are Ca-Mg-HCO_3 waters; While Cumalı cold water has typical Ca-HCO_3 feature, Karakoç cold water (since none of the cations is above 50%) is in the group of mixed waters.

In the Schoeller diagram, hot water samples present profiles characterized by increases in Na+K and Cl contents, while cold water profiles shown with dashed lines (although they have high Cl contents) reach the highest values in HCO_3 and Ca-Mg contents (Figure 7.6).

Hot waters form groups at the Na+K and Cl corners of the Piper diagram. The 2 water samples in positions contrary to this group are cold waters. Another parameter shown in the Piper diagram is the Total Dissolved Solid Contents (TDS) of the waters. In the diagram, in which TDS contents are reflected in proportion to the diameter of the circles, Cumalı and Karakoç hot waters come to the fore with their very high TDS values (Figure 7.6).

Since the most determinant parameters about the origin of the waters forming the geothermal system are the stable oxygen and hydrogen isotope compositions of the water molecules, the isotope

compositions of the waters are shown in Figure 7.7 by the $\delta^{18}O$ - δD diagram. The compositions of Global Meteoric Water Line, Mediterranean Meteoric Water Line, Standard Mean Sea Water (SMOW) and Aegean Sea Water are also shown on the diagram.

The average annual precipitation in İzmir is 700 mm, and more than 50% of the annual precipitation falls in winter, 40-45% in spring and autumn, and 2-4% in summer. Seferihisar waters are located close to the Global Meteoric Water Line (KMSD). This indicates that the hot and cold waters in the Seferihisar geothermal area are mainly meteoric waters. While the waters of the Karakoç and Doğanbey fields and the cold water of the Cumalı field are located just above the mentioned KMSD line, the hot waters of the Cumalı and Tuzla fields deviate towards the right of the KMSD (slightly higher $\delta^{18}O$ values).

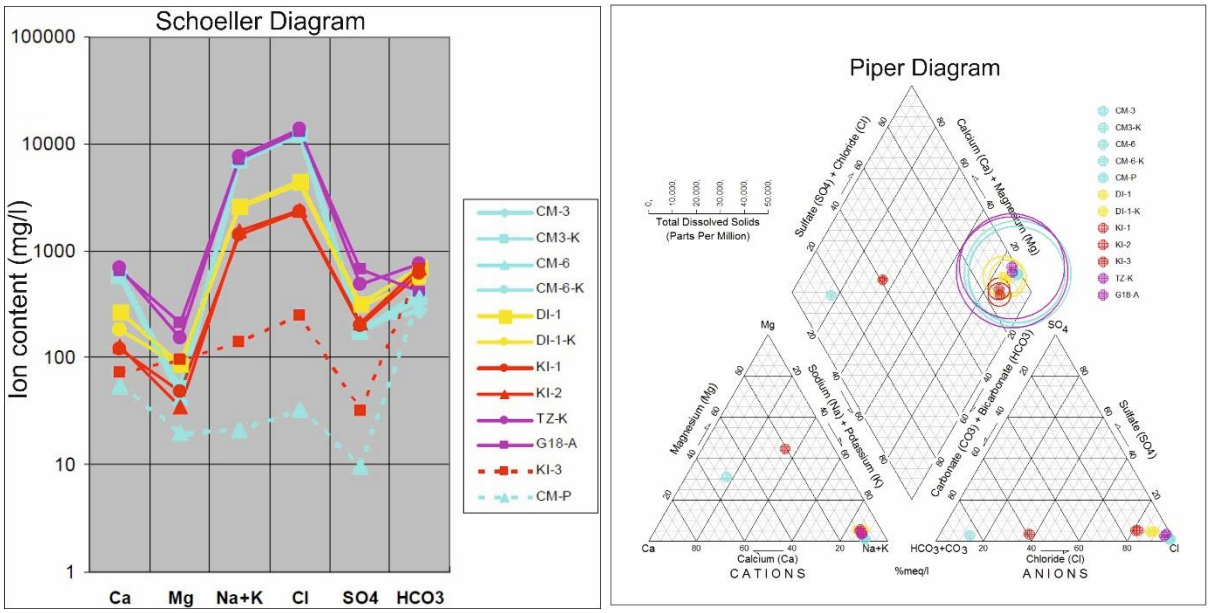

Figure 7.6: Schoeller diagram (left) and Piper diagram (right) of the waters in the Seferihisar geothermal field (IGEI, 2008).

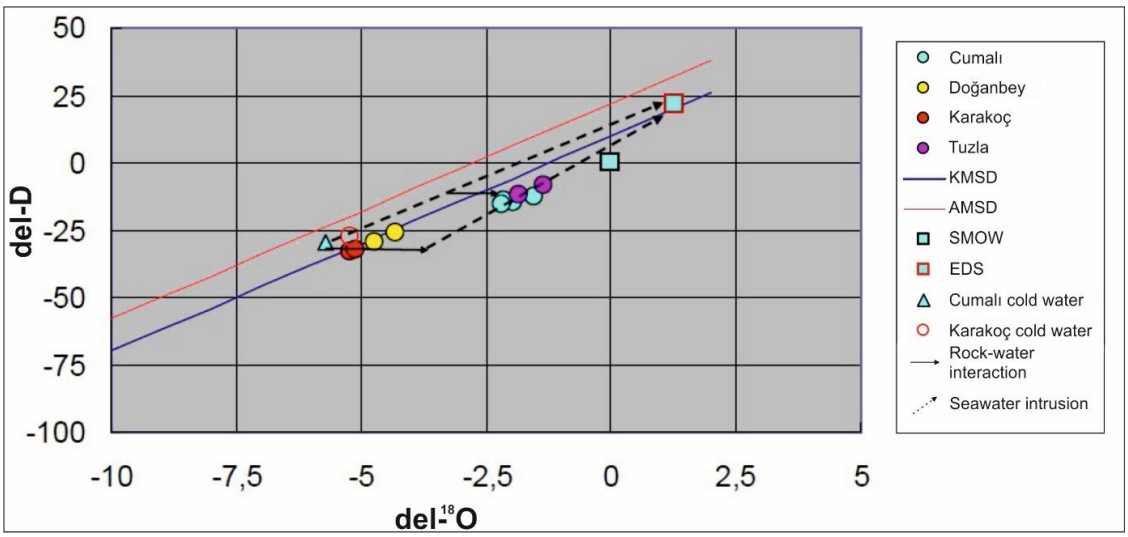

Figure 7.7: Stable isotope (δ18O - δD) diagram of Seferihisar geothermal field waters (IGEI, 2008). [KMSD: Global Meteoric Water Line (Craig, 1961), AMSD: Mediterranean Meteoric Water Actually (IAEA, 1981), SMOW: Standard Average Seawater, EDS: Aegean Seawater (Conrad et al., 1997)].

In general, $\delta^{18}O$ values, which increase while δD values remain constant, are indicative of the rock-water interaction that develops with the effect of temperature. In this context, it is understood that the waters of Cumalı and Tuzla fields are exposed to higher rock-water interaction than the waters of Karakoç and Doğanbey fields. In addition, when the cold waters, hot waters and Aegean Sea water compositions of the Seferihisar geothermal area are considered together, it is seen that the seawater mixture is also effective in the current isotope composition of the hot waters, apart from the rock-water interaction.

As part of the rock-water interaction, all of the waters in the Seferihisar geothermal field are saturated with calcite and aragonite with $CaCO_3$ composition, magnesite with $MgCO_3$ composition and dolomite with $CaMg(CO_3)_2$ composition. Therefore, there is a potential for scaling to develop with the precipitation of Ca- and/or Mg-CO_3 during production in the fields. The flow rates of the hot springs in the field were approximately 50 L/s, and the flow rates of the wells were measured as 100 L/s (WB, 2022).

The highest reservoir temperatures were obtained in the Cumalı region (excluding Na/K and K-Mg geothermometers). Silica geothermometer results were found to be more reliable than cation geothermometer results, as the regions were affected by seawater intrusion. In addition, the immature water class of the fluids except for Cumalı and Doğanbey Tuzla also supports this seawater intrusion situation. For this reason, K-Mg and silica geothermometer results for Cumalı and Doğanbey regions are more reliable and show reservoir temperatures of 170-200 °C.

Finally, the potential assessment of lithium extraction from geothermal reservoirs in the region was made by Aydın, 2022 et al. using the Monte Carlo method. The maximum dissolved Li values were found to be 13.4 mg/l, while the highest Li values were observed in the samples taken from the points on the Tuzla Fault Zone. The proven Li reserve geothermal reservoir at Seferihisar is expected to be 583 tons. Li reserves are estimated to be 1269 and 2325 tons, respectively (Aydın et al., 2022).

7.3 DEEP SUB-SURFACE TEMPERATURES IN WEST ANATOLIA

Determining the heat flow in western Anatolia has significant implications for a wide range of issues, including studies of the current extensional tectonic activity in the area and assessments of its geothermal resources. Numerous researchers have been examining heat movement, geothermal gradient, and temperature distributions at various depths since 1968 (Erentöz and Ternek 1968; Çermak et al., 1977; Tezcan, 1979; Ünalan and Öngür, 1979; İlkışık, 1992; Mıhçakan and Öcal, 1998; Karat and Aydın, 2004; Korkmaz, 2010; Tezel et al., 2013; Akın et al., 2014; Aydın et al., 2019).

Gradient data of western Anatolia were calculated using shallow (100-150 m) and deep well (1000-4500 m) temperature data of Mıhçakan et al., 2006 and Korkmaz, 2010. According to interpolation (IDW) data, virtually the entire Bornova flysch zone, particularly the Seferihisar horst, where the Seferihisar geothermal field is situated, has a high gradient value (Figure 7.8).

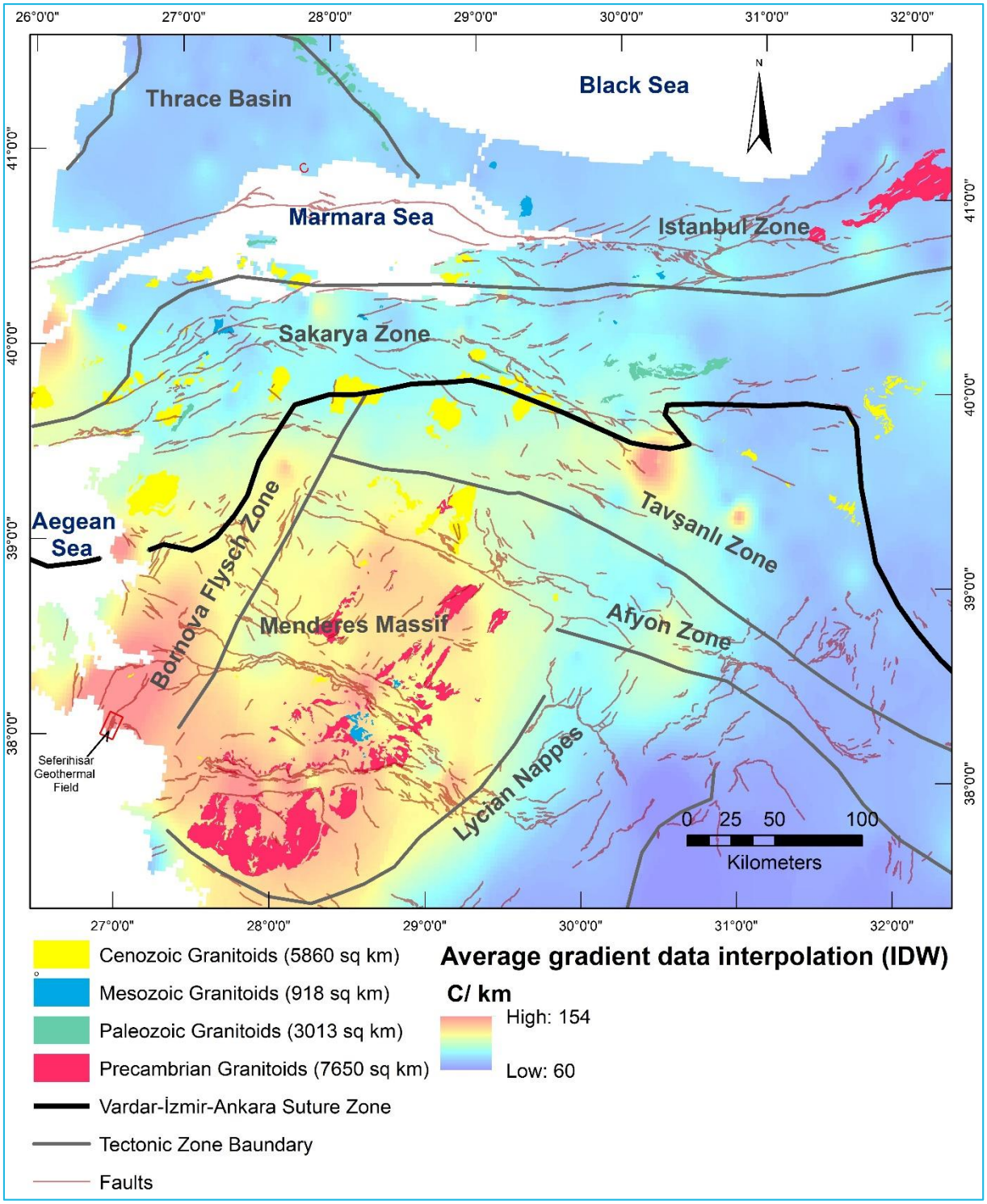

Figure 7.8: Granitoid intrusives distribution in the west Anatolian-Aegean extensional region and average of shallow (between 100 - 150 m) and deep (between 1000 - 4500 m) wells gradient data interpolation map (modified from Ayzit et al., 2022 and Chandrasekharam et al., 2022).

In addition, considering the western Anatolian curie point depth (CPD) studies (Figure 7.9; Ateş et al., 2005; Aydın et al., 2005) it is seen that it is compatible with the calculated gradient data. Curie point depth map figured out from aeromagnetic survey The MT (Magneto Telluric) survey identifies a conductive layer beneath western Anatolia at a depth of 10 km, which corresponds to the Curie point depth and suggests the zone of crustal melting in this region. In addition to CPD studies, seismic

(Sözbilir et al., 2009), magnetic (Bakak et al., 2015), gravity (Drahor et al., 1999) geophysical surveys were also conducted in the region.

Considering the high gradient and low CPD values, it becomes inevitable to evaluate the enhanced (enginereed) geothermal system potential of radiogenic granitoids in western Anatolia. Due to its availability anywhere on Earth, Enhanced Geothermal Systems projects are becoming more and more important (Chandrasekharam and Baba, 2021; 2022). High radiogenic granitoids have a very low carbon footprint and can produce a significant quantity of energy (Baba and Chandrasekharam, 2022). Such radiogenic granitoids can produce 79 × 10^6 kWh of power per cubic meter (Somerville et al., 1994).

When the radiogenic heat flow values of radiogenic granitoids in western Anatolia are calculated using the equations of Rybach (1976) and Lachenbruch (1968), it reveals the enormous energy potential (Chandrasekharam et al., 2022). The production of food, heating and cooling can be supported by this energy. Radiogenic granitoids in Western Anatolia have enormous geothermal potential that will make Türkiye energy, food, and water independent nation (Figure 7.8; Chandrasekharam et al., 2022).

7.4 STRUCTURE AND STRESS-FIELD MEASUREMENTS

The region where the Seferihisar horst is located is symbolized by faults formed by the deformation, N-S expansion versus E-W compression, which affected the Middle Miocene to the present day. Within this tectonic framework, the more dominant and taller NE and NW trending structures are strike-slip, the E-W trending ones are normal faults and are known to have been the source of major earthquakes resulting in surface rupture in the Holocene. The right-lateral strike-slip Tuzla and Seferihisar faults are the most important active faults (Emre and Barka, 2000; Sözbilir, 2000; Sözbilir et al., 2005; 2008; Emre et al., 2005; 2006; Göktaş, 2011;2019; Emre and Özalp, 2011).

In some articles, the phrase Orhanlı Fault Zone is used instead of Tuzla Fault Zone (Genç et al., 2001; Uzel and Sözbilir, 2008; Uzel, 2013).

Tuzla Fault Zone is the most noticeable structure in the area south of İzmir city and serves as the western boundary of the Cumaovası basin. The Seferihisar Horst is constrained to the east by the TFZ. Between İzmir Bay in the north and Doğanbey Bay in the south, it can be followed for around 45 km. Numerous dextral fault segments that mostly run NE-SW are part of the fault zone. Dextral strike-slip is the predominant action along the slip surfaces. However, there is some structural and geomorphological proof of an earlier sinistral strike-slip motion (Figure 7.10; Table 7.3; Uzel and Sözbilir, 2008, Uzel, 2013).

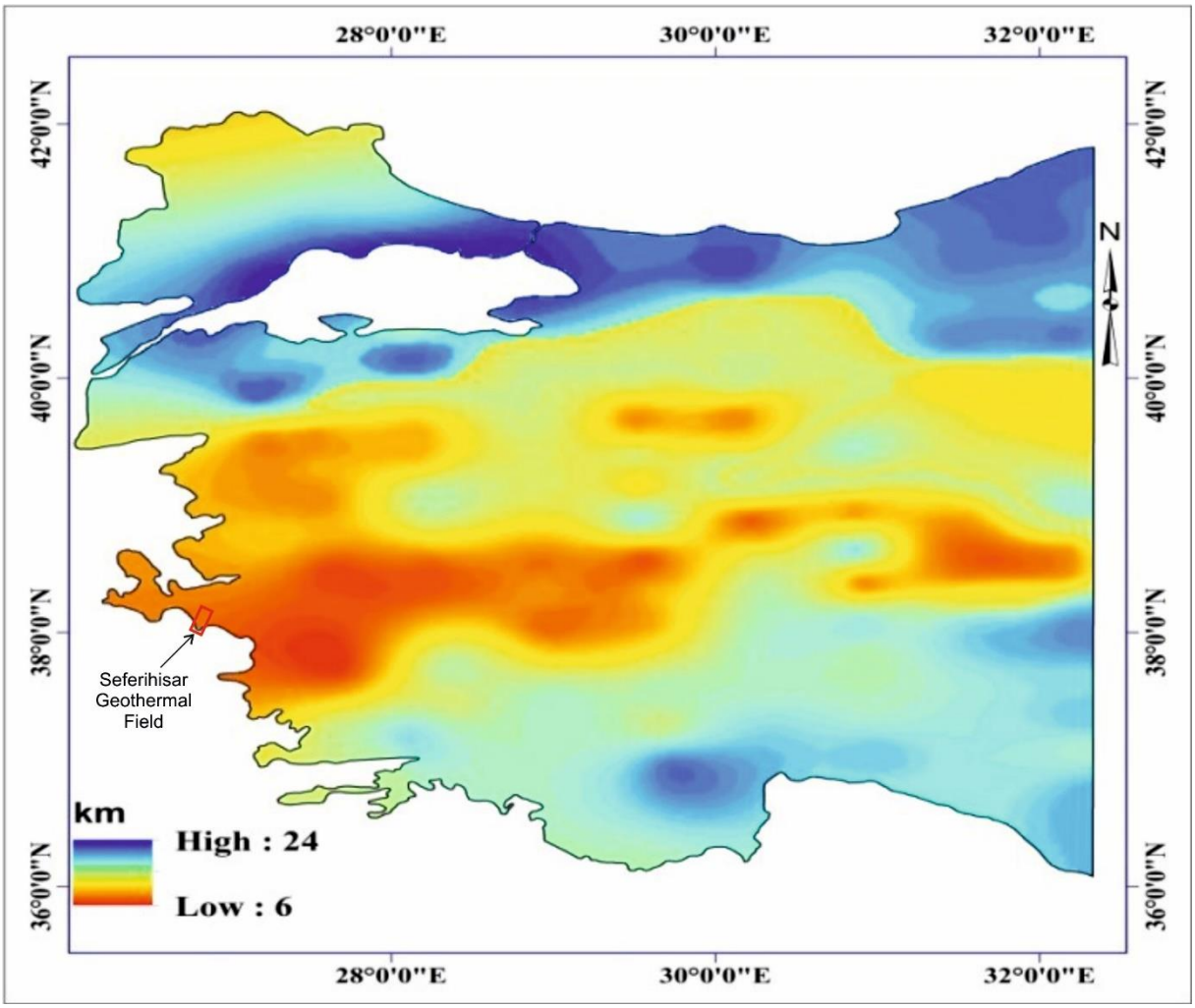

Figure 7.9: Curie point depth map of Western Anatolia (modified from Chandrasekharam et al., 2022; Ateş et al., 2005; Aydın et al., 2005).

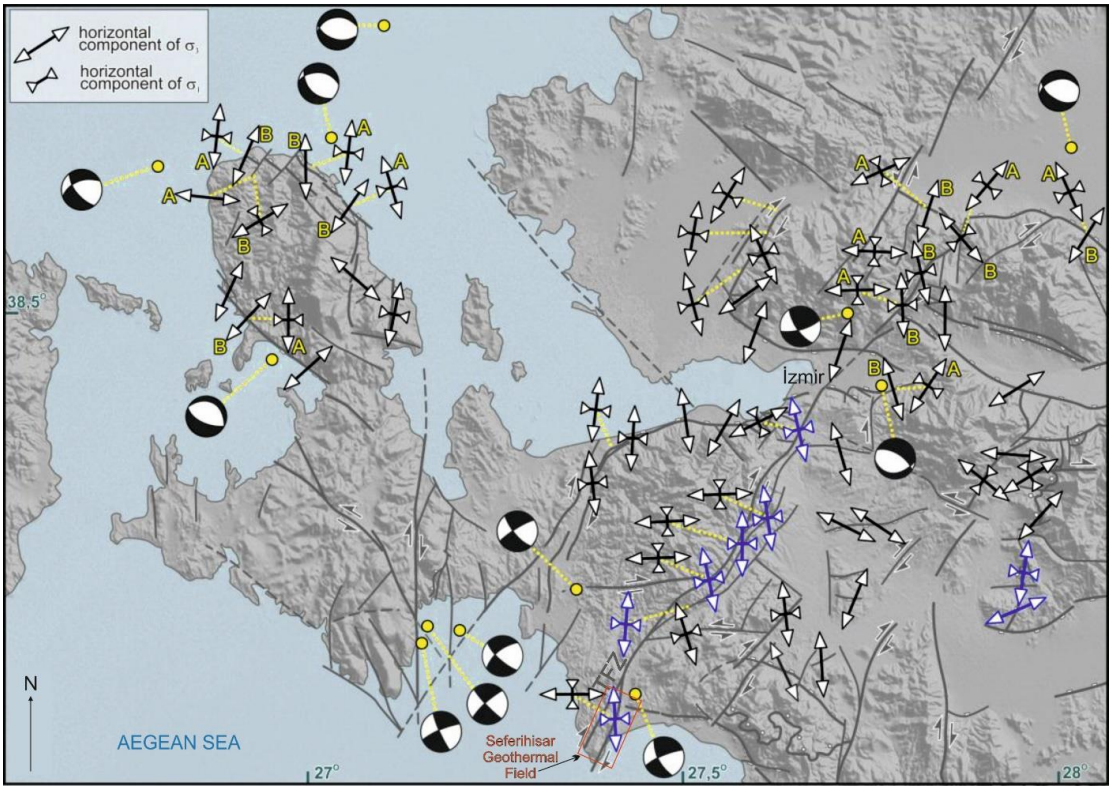

Figure 7.10: Maximum and minimum strain axes directions. Miocene faulting along the Tuzla Fault Zone (TFZ) is indicated by blue arrows (Phase 1). The older (younger) faulting on reactivated fault planes is denoted by the letters A (B). The big earthquakes' focal mechanism (Modified from Uzel, 2013; Tan, 2008).

Table 7.3: Palaeostress tensors with 6 fault slip data for Tuzla Fault Zone (Uzel and Sözbilir, 2008). Φ; ratio of stress magnitude difference [Φ = (σ2 − σ3) / (σ1 − σ3)].

Principle stress axes (dip^0/ plunge^0)			Φ
σ 1	σ 2	σ 3	
163/17	276/53	062/32	0.613
257/06	014/77	166/11	0.315
360/23	162/66	267/06	0.716
260/40	098/48	001/09	0.651
185/05	291/72	094/17	0.565
278/39	095/51	187/07	0.626
355/15	206/72	088/09	0.336
267/22	063/66	173/09	0.579
358/04	261/64	090/26	0.434
265/17	096/73	356/03	0.212
355/15	206/72	088/09	0.336
258/11	066/78	167/02	0.821
275/14	086/76	185/02	0.688
259/03	154/77	350/12	0.516
106/07	350/74	198/15	0.715

Along sections of the TFZ, it is possible to see typical tectonic features such as fault scarps, systematically deflected stream channels and ridges, and shutter ridges. The early sinistral offsets are

thought to be later overprinted by dextral offsets based on their morphological and structural characteristics. Additionally, a number of hot springs are found in the fault zone's central region, suggesting that the fault zone serves as an efficient conduit for the geothermal field. This suggests that nearby hot springs are linked to active faults (Uzel and Sözbilir, 2008; Uzel, 2013).

Stress and displacement studies are frequently carried out since the region shows active tectonic features (Figure 7.11; Özdemir et al., 2021; Havazlı and Özener, 2021; Özener et al., 2013; Demirtaş, 2015; Timur, 2017; Timur and Sındırgı, 2006).

As a result of the observations made in the geothermal fields around Seferihisar after the earthquake and tsunami in Samos Island (30 October 2020), new resource formations were found in the Karakoç and Cumalı geothermal fields located in the southeast of Seferihisar. In these geothermal fields located on the Tuzla Fault, new geothermal resource formation, mud and gas outflows were observed after the earthquake. The temperature of these water outlets was measured at 97 °C (Sözbilir et al., 2020; Baba et al., 2022).

7.5 CONCLUSIONS

This report provides geological information about western Anatolia, especially the Seferihisar geothermal field, and many references where you can find detailed information. Thanks to many mining (especially gold) and industrial raw material activities carried out in the region for a long time, besides mineralization and geochemistry studies, structural and stress direction studies have been carried out as it contains active tectonic lines along the W-E and NE-SW directions.

In addition, there are many hydrogeological and isotope studies to investigate the source and potential of thermal waters used by civilizations for many years. Deep geophysical (via MT) and geotechnical studies have been started to investigate the potential of enhanced (engineered) geothermal systems, especially owing to the presence of radiogenic granites and thin crustal thickness that western Anatolia hosts.

Seferihisar field is a field that has attracted a lot of attention in recent years in terms of geothermal. The only geothermal power plant in İzmir is located in Seferihisar. In this field, there is a high resource for direct use applications that can be beneficial and economical for the region, such as applications integrated with existing electricity production, heating-cooling, greenhouse cultivation and thermal tourism, as well as brine mining potential.

The CRM-geothermal project will allow more comprehensive geochemical analyses and modelling (considering geology, temperature and pressure), and will enable us to perform environmentally friendly metal extraction in an efficient way, as well as clean energy.

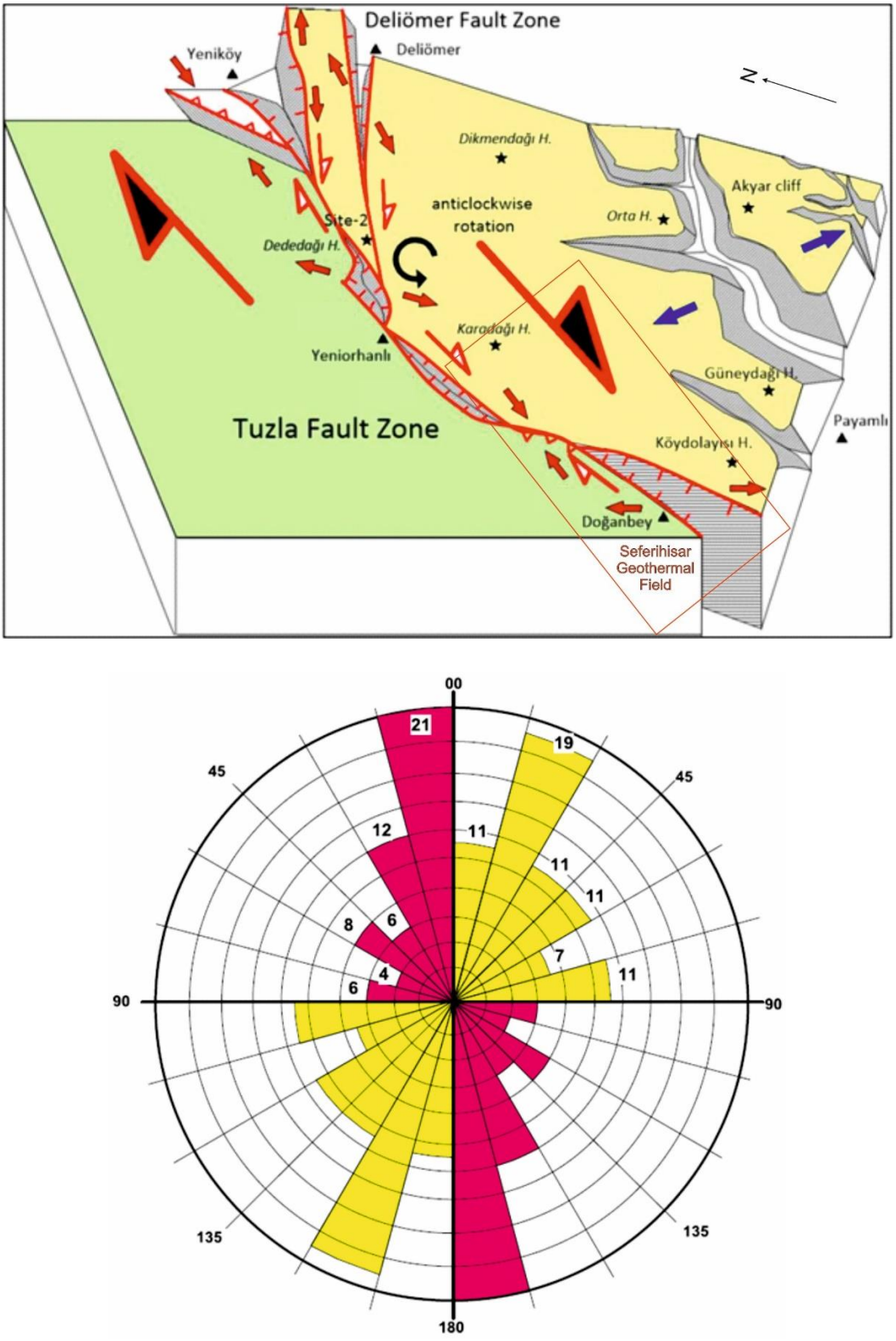

Figure 7.11: Top: Controlling the geothermal system are the Tuzla Fault Zone's fault geometry and its left- and right-turn areas, opening areas, intersection zones, and tear areas (modified from Özdemir et al., 2021). Bottom: Principal stress orientation results obtained by measuring tectonic fracture traces at 127 points in total, as a result of observations made at 231 stops at the borders of Seferihisar horst (Demirtaş, 2015).

7.6 REFERENCES

Akar, A. T. 2012. Modeling of fluid flow in Seferihisar and Balçova geothermal fields and surrounding aquifers, PhD Thesis, DEU, (in Turkish).

Akartuna, M. 1962. On the geology of İzmir-Torbalı-Seferihisar-Urla district. MTA Bul., 59, 1-18.

Akin, U., Ulugergerli, E. and Kutlu, S. 2014. The assessment of the geothermal potential of Turkey by means of heat flow estimation. Bull. Min. Res. Exp.149, 201-210.

Aksoy, N., Şimşek, C. ve Gündüz, O. 2008b. Groundwater contamination mechanism in a geothermal field: A case study of Balçova, Turkey. Journal of Contaminant Hydrogeology, 103, (1-2), 13-28.

Ateş, A., Bilim, F., And Buyuksarac, A. 2005. Curie point depth investigation of Central Anatolian Turkey, Pure Appl. Geophys. 162, 357–371.

Aydin, H., Sengun, R., Hakkidir, F. T. 2022. Potential Assessment of Lithium Extraction from Geothermal Reservoirs. PROCEEDINGS, 47th Workshop on Geothermal Reservoir Engineering, Stanford University, Stanford, California, February 7-9, SGP-TR-223

Aydin, I., Karat,H. I. and Cak, A.K. 2005. Curie-point depth map of Turkey. Geophy. J. Inter. 162, 633-640, doi: 10.1111/j.1365-246X.2005.02617. x.

Aydın, Ü., Şen, P., Özmen, Ö., Şen, E. 2019. Petrological and geochemical features of Biga Peninsula granitoids, NW Anatolia, Turkey. Bull. Min. Res. Exp. 160, 81-115.

Ayzit, T. 2015. The Intermediate Sulfidation Mineralization Around Çamtepe Village (Menderes-İzmir) And Investigation of the Alteration Data, (unpublished)

Ayzit, T., Chandrasekharam, D., Baba, Alper. 2022. A sustainable clean energy source for mitigating CO2 emissions in the west Anatolian-Aegean extensional region. 14th of the International Conference on Hydroscience and Engineering, ICHEE 2022: Proceeding book, 81-84.

Ayzit, T., Chandrasekharam, D., Baba, A. 2022. Salihli Granitoid, Menderes Massif, Western Anatolia: A Sustainable Clean Energy Source for Mitigating CO2 Emissions. Springer Nat. 272–283.

Baba, A. and Chandrasekharam, D. 2022. Geothermal Resources for sustainable development: Case study: Turkey. Inter, J. Energy Res. 1-18. DoI: 10.1002/er.7778.

Baba, A., Sözbilir, H. 2012. Source of arsenic-based on geological and hydrogeochemical properties of geothermal systems in Western Turkey, Chemical Geology, 334:364-377.

Baba, A., Sözbilir, H., Demir, M., Akkurt, G., Özşen, A., Şener, F., Hancıoğlu, E., Uzelli, T. 2022. İzmir ilindeki jeotermal kaynaklarin potansiyeli, kullanim alanlari, Ekonomik ve çevresel etkilerinin belirlenmesi araştırması, İZKA report, (in Turkish).

Bakak, Ö., Özel, E., Ergün, M. 2015. Geothermal potential of the Sığacık Gulf (Seferihisar) and preliminary investigations with seismic and magnetic surveys. Energy Procedia 76: 230-239

Borsi, J., Ferrara, G., Innocenti, F., Mazzuoli, R., 1972. Geochronology and petrology of recent volcanicsin the eastern Aegean Sea (West Anatolia andLesbos Island). Bulletin of Volcanology 36, 473–496

Boucher, K. 2016. The structural and fluid evolution of the Efemçukuru epithermal gold deposit, western Turkey: M.Sc thesis, Vancouver, BC, Canada, The University of British Columbia, 466p.

Bozkurt, E. 2001a. Neotectonics of Turkey – a synthesis Geodinamica Acta. 14, 3-30.

Bulut, M. 2013. A new medium to high enthalpy geothermal field in aegean region (Akyar Menderes-Seferihisar-Izmir, Western Anatolia, Turkey, Bulletin of MTA. 147:153-167.

Candan, O., Oberhänsli, R., Ölsner, F. ve Dürr, St. 1997. Blueschist relics in the Mesozoic cover series of the Menderes Massif and correlations with Samos Island, Cyclades. Schweiz Mineral. Petrol. Mitt., 77, 95-97.

Canbolat, A. 1986. Seferihisar jeotermal sondajlar| bitirme raporlar| (Tuzla 1, G-2A, G-3, G3A, G12A, G17A (in Turkish). MTA rap. J143, Izmir.

Cermak, V., Hurting, E. 1977. Preliminary Heat Flow Map of Europe, IASPET Internal Heat Flow Commission, Geophys. Inst. Czech. Acad. Sci., Praha, Central Earth Phys. Inst., Acad. Sci. of the GDR, Potsdam.

Chandrasekharam, D., Baba, A. 2021. High heat generating granites of Kestanbol: Future Enhanced Geothermal System (EGS) province in Western Anatolia. Turkish J. Earth Science.

Chandrasekharam, D., Baba, A. and Ayzit, T. 2022. High radiogenic granites of western Anatolia for EGS: A review. In (Eds) D. Chandrasekharam and A. Baba. "EGS: the future energy road ahead" CRC Press, UK. (under publication. Expected date of release: 2023).

Chandrasekharam, D. and Baba, A. 2022. Carbon dioxide emissions mitigation strategy through Enhanced Geothermal systems: western Anatolia, Turkey. Environ. Earth Sci. 81, 235. doi.org/10.1007/s12665-022-10345-5.

Conrad, M.A., Hipfel, B., Satır, M. 1997. Chemical and stable isotopic characteristics of thermal waters from the Çesme- Seferihisar area, Izmir (W. Turkey). In: Piskin, Ö., Savaşçın, M.Y., Ergün M. and Tarcan, G. (Eds.), Proceedings International Earth Sciences Colloquium on the Aegean Region, 9-14 Oct. 1995, vol. 2, pp. 669-679.

Craig, H. 1961. "Isotopic Variations in Meteoric Waters". Science. 133 (3465): 1702–1703.

Delaloye, M. and Bingol, E. 2000. Granitoids from Western and Northwestern Anatolia: geochemistry and modeling of geodynamic evolution. International Geology Review 42, 241– 268.

Demirtaş, R. 2015. Seferihisar Yükselimi - Cumaovası Çöküntüsü'nün Jeolojik – Tektonik Özellikleri. December 2015 – Ankara (in Turkish)

Dewey, J.F. ve Şengör, A.M.C. 1979. Aegean and surrounding regions: complex multiple and continuum tectonics in a convergent zone. Geological Society of America Bulletin, 90, 84–92.

Drahor, M.G., Sarı, C., Şalk, M. 1999. Self-Potential And Gravity Studies In The Seferihisar Geothermal Field. Volume: 1 Issue: 3 p. 97-112 October 1999 (in Turkish)

Ekingen, A. 1970. İzmir-Urla Seferihisar bölgesinin gravite yöntemiyle incelen- mesi. MTA Raporları No. 4312, Ankara. (İn Turkish)

Eldorado Gold Corporation. 2019. Technical Report Efemçukuru Gold Mine Turkey, 1188 Bentall 5 - 550 Burrard Street Vancouver, BC V6C 2B5

Emre, Ö., Barka, A. 2000. Gediz grabeni-Ege Denizi arasının (İzmir yöresi) aktif fayları. Batı Anadolu'nun Depremselliği Sempozyumu (BADSEM 2000), 24-27 Mayıs 2000, İzmir, 131-132.

Emre, Ö., Özalp, S. 2011. 1:250.000 Ölçekli Türkiye Diri Fay Haritası Serisi, Urla (NJ 35-6) Paftası, Seri No: 5. Maden Tetkik ve Arama Genel Müdürlüğü Yayını, Ankara.

Emre, Ö., Özalp, S., Doğan, A. 2006. 17-21 Ekim 2005 Sığacık Depremleri ve İzmir yöresi diri faylarının deprem potansiyelleri. Aktif Tektonik Araştırma Grubu 10. Toplantısı, 2-4 Kasım 2006, İzmir, 21-22.

Emre, Ö., Özalp, S., Doğan, A., Özaksoy, V., Yıldırım, C., GöktaĢ, F. 2005. İzmir yakın çevresinin diri fayları ve deprem potansiyelleri. Maden Tetkik ve Arama Genel Müdürlüğü Rapor No: 10754, Ankara (unpublished).

Erentöz, C., Ternek, Z. 1968. Türkiye'de Termomineral Kaynaklar ve Jeotermik Enerji Etüdleri, MTA Dergisi, 70.

Erdoğan, B. 1990. İzmir-Ankara Zonu'nun, İzmir ile Seferihisar arasındaki bölgede stratigrafik özellikleri ve tektonik evrimi. TPJD Bülteni, 2, 1-20.

Eşder, T. and Şimşek, S. 1975. Geology of İzmir (Seferihisar) Geothermal Area, Western Anatolia of Turkey: Determination of Reservoirs by Means of Gradient Drilling. Proceedings of the 2nd UN Symposium on the Development and Use of Geothermal Resources, San Francisco, 349-361.

Eşder, T., Şimşek, Ş. 1977. The relationship between the temperature-gradient distribution and geological structure in the İzmir-Seferihisar Geothermal Area, Turkey. In: Proc. of the Symp. on the Geothermal Energy, Ankara, pp. 93-114.

Eşder, T., Akkuş, İ., Demirci, S., Çiçekli, K., Yılmazer, S. 1983. İzmir-Seferihisar Cumali-1 jeotermal araması kuyu bitirme raporu (in Turkish). MTA report No. 8146.

Eşder, T. 1990. The crust structure and convection mechanism of geothermal fluids in Seferihisar geothermal area. In: Savaşcın, M.Y., Eronat, H. (Eds.), Proceedings International Earth Sciences Congress on Aegean Regions, İzmir, Turkey, vol. 1, pp. 135-147.

Eşder, T., Ölmez, E., Aydın, H., Gür, Ş. 1995. Doğanbey Ilıcası (Seferihisar-İzmir) jeotermal enerji kuyusunun bitirme raporu (in Turkish). MTA report No. JT-134.

Eyidoğan, H. and Jackson, J. A. 1985. A seismological study of normal faulting in the Demirci, Alaşehir and Gediz earthquake of 1969,1970 in western Turkey: implications for the nature and geometry of deformation in the continental crust. Geophysical Journal of Royal Astronomical Society, 81, 569-607.

Filiz, Ş. and Tarcan, G. 1993. Seferihisar (İzmir) güneyindeki jeotermal alanın hidrojeolojisi. TPJD Bülteni, 5, 97-112.

Filiz, Ş., Tarcan, G., Gemici, Ü. 1997. Seferihisar (İzmir) jeotermal alan|ndaki s|cak sular|n Hidrojeokimyasal Içncelemesi (in Turkish). In: Su ve Çevre Sempozyumu 97, 2-5 Haziran 1997, İstanbul, pp. 117-128

Filiz, Ş. 1982. Ege Bölgesindeki Önemli Jeotermal alanların 18O, 2H, 3H, 13C izotoplarıyla incelenmesi (in Turkish). Assoc. Prof. Thesis. E.Ü.Y.B.F., İzmir.

Genç, Ş.C., Altunkaynak, Ş., Karacık, Z., Yazman, M., Yılmaz, Y. 2001. The Çubukludağ, south of İzmir: its significance in the Neogene geological evolution of the western Anatolia. Geodinamica Acta 14, 45-55.

Gemici, Ü., Tarcan, G. 2002. Distribution of boron in thermal waters of western Anatolia, Turkey, and examples of their environmental impacts. Environmental Earth Sciences 43(1):87-98

Gessner, K., Gallardo, L A, Markwitz, V, Ring, U, Thomson, S N. 2013. What caused the denudation of the Menderes Massif: Review of crustal evolution, lithosphere structure, and dynamic topography in southwest Turkey, Gondwana Research Volume 24, Issue 1, July 2013, Pages 243-27

Gessner, K., Markwitz, V. and Güngör, T. 2017. Crustal fluid flow in hot continental extension: tectonic framework of geothermal areas and mineral deposits in western Anatolia: Geological Society, London, Special Publications, v. 453, p. 1-23.

Göktaş, F. 2011. Urla (izmir) çöküntüsündeki Neojen tortullaşmasi ve volkanizmasinin jeolojik etüdü. Maden Tetkik ve Arama Genel Müdürlügü Rapor No: 11568, 112 s., Ankara (unpublished).

Göktaş, F. 2019. Stratigraphy of the Neogene Sedimentation and Volcanism in Çubukludağ Basin, Western Anatolia, Geological Bulletin of Turkey, 63-98 (in Turkish)

Göktaş F., Çakmakoğlu A. 2017. 1:100.000 ölçekli Türkiye Jeoloji Haritaları Serisi, Urla-L17 Paftası, Maden Tetkik ve Arama Genel Müdürlüğü, Ankara.

Havazlı, E., Özener, H. 2021. Investigation of strain accumulation along Tuzla fault – western Turkey. Turkish J Earth Sci. 30: 449-459

Hinsbergen, D.J.J. 2010. A key extensional metamorphic complex reviewed and restored: The Menderes Massif of western Turkey. Earth-Science Reviews, 102,60-76.

İlkışık, O.M. 1992. Silica Heat Flow Estimates and Lithospheric Temperature in Anatolia, Proceedings, XI. Congress of World Hydrothermal Organization, Mayıs 13-18, 92-104.

International Atomic Energy Agency. 1981. Stable isotope hydrology, Deuterium and oxygen–18 in the water cycle, Technical Reports Series No. 210, IAEA, Vienna.

İzmir Geothermal Energy Industry Trade Inc. (IGEI). 2008. Izmir Jeotermal Enerji San. ve Tic. A.S., Seferihisar jeotermal alaninin jeokimyasal degerlendirilmesine iliskin rapor (in Turkish)

Jackson, J. and McKenzie, D. 1984. Active tectonics of the Alpine-Himalayan Belt between western Turkey and Pakistan. Geophysical Journal of the Royal Astronomical Society, 77, 185-264.

Jolivet, L., Menant, A., Sternai, P., Rabillard, A., Arbaret, L., Augier, R., Laurent, V., Beaudoin, A., Grasemann, B., Huet, B., Labrousse, L., Le Pourhiet, L. 2015b. The geological signature of a slab tear below the Aegean. Tectonophysics 659 (166–182), 166–182.

Karat, H. I., Aydın, I. 2004. Report on Preparation of the Curie Isotherm Depth Map of Turkey, MTA, Unpublished Report, 10638.

Kaya M.N. 2019. Hydrogeochemical investigation of thermal and mineral waters of Izmır-Ilıkpınar, PhD Thesis, Hacettepe University, p69. (in Turkish)

Koralay, E., Candan, O., Akal, C., Dora, Ö., Chen, F., Satır, M., Oberhanslı, R. 2011. Menderes Masifindeki Pan-Afrikan ve Triyas Yaşlı Metagranitoyidlerin Jeolojisi ve Jeokronolijisi, Batı Anadolu, Türkiye.

Korkmaz, D. 2010. Türkiye Jeotermal Enerji Potansiyelinin Araştirilmasi, Doktora Tezi, İTÜ.

Lachenbruch A.H. 1968. Preliminary geothermal model of the Sierra Nevada. Journal of Geophysical Research 73, 6977-6989.

Leaman, P., and Staude, J.-M. 2002. Metallogenic evolution of the western Tethys of Turkey and Iran, in Metal Mining Agency of Japan, Presentation from a forum on mineral potential of Asia: Mineral Resource Information Center, 42p., CD ROM.

Magri, F., Pekdeger, A., Akar, T., Gemici, Ü. 2018. Numerical simulations of density viscosity-dependent hot fluids in a geothermal field: The Seferihisar- Balçova Area example (Turkey)

Menant, A., Jolivet, L., Tuduri, J., Loiselet, C., Bertrand, G. and Guillou-Frottier, L. 2018. 3D subduction dynamics: A first-order parameter of the transition from copper-to gold-rich deposits in the eastern Mediterranean region: Ore Geology Reviews, v. 94, p. 118-135.

Mıhçakan, M., Öcal, M. 1998. A Survey on Geothermal Gradient Distribution in Turkey, Bildiriler Kitabı, 12. Uluslararası Petrol Kongresi ve Sergisi, 12-15 Ekim, Ankara.

Okay A. 1989. Tectonic units and sutures in the Pontides, northern Turkey. In: Şengör, A.M.C. (ed), Tectonic Evolution of the Tethyan Region. Kluwer Academic Publications, Dordrecht, 109-115.

Okay, A., Altiner, D. 2007. A Condensed Mesozoic Succession North of İzmir: A Fragment of the Anatolide-Tauride Platform in the Bornova Flysch Zone, Turkish Journal of Earth Sciences 16, pp. 257-279

Okay, I. A. ve Tüysüz, O. 1999. Tethyan sutures of northern Turkey. Geological Society, London, Special Publications, 156, 475-515.

Okay, A.I. 2008. Geology of Turkey: A Synopsis: Anschnitt 21, 19-42.

Okay, A. & Siyako, M. 1993. The revised location of the İzmir-Ankara Suture in the region between Balıkesir and İzmir (in Turkish). In: Ozan Sungurlu Symposium Proceedings, Tectonics and Hydrocarbon Potential of Anatolia and Surrounding Regions (ed. S. Turgut), Ankara, 333-355.

Okay, A.I., İşintek, İ., Altıner, D., Özkan-Altıner, S., Okay, N. 2012. An olistostrome- mélange belt formed along a major suture: Bornova Flysch Zone, western Turkey. Tectonophysics, 568-569, 282-295.

Oyman, T., Minareci, F. ve Piskin, O. 2003. Efemcukuru B-rich epithermal gold deposit (Izmir Turkey). Ore Geology Reviews 23, 35– 53.

Oyman, T. 2019. Epithermal Deposits in Turkey, Springer Nature Switzerland AG 2019, F. Pirajno et al. (eds.), Mineral Resources of Turkey, Modern Approaches in Solid Earth Sciences 16

Öngür, T. 2001. İzmir Agamemnon kaplıcaları-Balçova jeotermal alan jeolojisi ve yeni kavramsal jeoloji modeli (unpublished)

Özdemir, A., Arabacı, F., Palabıyık, Y. 2021. Reevaluation of Geothermal Potential of Çubukludağ Graben (Western Anatolia, Turkey). International Journal of Earth Sciences Knowledge and Applications. 3 (2) 70-88.

Özener, H., Doğru, A., Acar, M. 2013. Determination of the displacements along the Tuzla fault (Aegean Region-Turkey): Preliminary results from GPS and precise leveling techniques. Journal of Geodynamics 67 13–20

Özgür N., Pala E.A., Degirmenci S. 2017. Hydrogeological, hydrogeochemical and isotope

geochemical features of the geothermal waters in Seferihisar and environs, Western Anatolia, Turkey IOP Conf. Ser.: Earth Environ. Sci. 95 022039.

Parlaktuna, M., Akın, S., Sayık, T., Karahan, Ç., Bakraç, S. 2010. Interpretation of the Short-Term Production Test of Seferihisar Geothermal Field. Proceedings World Geothermal Congress 2010 Bali, Indonesia, 25-29 April 2010

Pirajno, F. 2009. Hydrothermal processes and mineral systems. Springer, Berlin, p 1250

Rybach, L. 1976. Radioactive Heat Production: A Physical Property Determined by the Chemistry. In: R.G.I. Strens (Editor), The Physical and Chemistry of Minerals and Rocks. Wiley-Interscience Publication, New York, USA, pp. 245-276.

Seyitoğlu, G.and Scott, B. 1991. Late Cenozoic crustal extension and basin formation in west Turkey. Geological Magazine, 128, 15-166.

Sharp, I.R.ve Robertson, A.H.F. 2006. Tectonic-sedimentary evolution of the western margin of the Mesozoic Vardar Ocean: evidence from the Pelagonian and Almopias zones, northern Greece. Tectonic Development of the Eastern Mediterranean Region. Geological Society, London, Special Publications, 260,373-412.

Somerville, M., Wyborn, D., Chopra, P., Rahman, S., Don Estrella, Theo Van der Meulen. 1994. Hot Dry Rock Feasibility Study. Energy Research and Development Corporation, unpublished report. 214 p.

Sözbilir, H. 2000. Bati Anadolu"dan örneklerle aktif faylar ve potansiyel aktif faylar. Bati Anadolu"nun Depremselligi Sempozyumu (BADSEM 2000), 24-27 Mayis 2000, Izmir,133-142.

Sözbilir, H., Sümer, Ö., Uzel, B., Ersoy, Y., Erkül, F., İnci, U., Helvacı, C. 2005. İzmir'deki deprem dizilerinin nedeni, faylardaki çiçek yapısı, Cumhuriyet Bilim Teknik, Deprem Araştırmaları, 3.12.2005, Sayı: 976, 18-19.

Sözbilir, H., Uzel, B., Sümer, Ö., İnci, U., Ersoy, Y. Koçer, T., Demirtaş, R., Özkaymak, Ç. 2008. D-B uzanımlı İzmir Fayı ile KD uzanımlı Seferihisar Fayı'nın birlikte çalıştığına dair veriler: İzmir Körfezi'ni oluşturan aktif faylarda kinematik ve paleosismolojik çalışmalar, Batı Anadolu. Türkiye Jeoloji Bülteni 51, 2, 91-114.

Sözbilir, H., Kaymakçı, N., Langereis, C., Uzel, B., Özkaymak, Ç., Özkaptan, M. & Gülyüz, M. 2009. Transfer zonlarının jeolojik evrimi ve bu zonların Batı Anadolu'daki K-G genişleme tektoniğine katkısı: İzmir-Balıkesir Transfer Zonu (Geological evolution of transfer zones and their contribution to N-S Extensional tectonics in western Anatolia: İzmir-Balıkesir Transfer Zone). 13th Meeting of Active Tectonics Research Group, Abstracts, p. 51.

Sözbilir, H., Sarı, B., Uzel, B., Sümer, Ö. and Akkiraz, S. 2011. Tectonic implications of transtensional supradetachment basin development in an extension-parallel transfer zone: the Kocacay Basin, western Anatolia, Turkey, basin research, 423-448.

Sözbilir H., Softa M., Eski S., Tepe Ç., Akgün M., Pamukçu O., Çırmık A., Utku M., Özdağ Ö., Özden G., Özçelik Ö., Altun Evlek D., Çakır R., Baba A., Uzelli T., Tatar O. 2020. Dokuz Eylül University Earthquake Research and Application Center (DAUM), 30 October 2020 Samos (Samos) Earthquake (MW 6.9) Assessment Report, 109 p. November (in Turkish).

Şalk, M., Göktürkler, G., Özel, M., Karamanderesi, I.H. ve Sarı, C. 1999. Crustal temperature distributions in the Western Turkey. Second Balkan Geophysical Congress and Exhibition, İstanbul, Turkey, July 5-9, Book of Abstracts, 174-175.

Şengör, A.M.C. and Yılmaz, Y. 1981. Tethyan Evolution of Turkey: A Plate Tectonic Approach. Tectonophysics, 75, 181-241

Şengör, A.M.C., Görür, N. ve Şaroğlu, F. 1985. Strike-slip faulting and related basin formation in zones of tectonic escape: Turkey as a case study. In: Biddle, K. ve Christie-Blick, N. (Eds.), Strike-Slip Deformation, Basin Formation and Sedimentation. Society of Economic Paleontologists and Mineralogists, Special Publications 37, 227, 64.

Şengör, A.M.C. 1987. Cross-faults and differential stretching of hanging walls in regions of low-angle normal faulting: examples from western Turkey. In: Coward, M.P., Dewey, J.F., Hancock, P.L. (Eds.), Continental Extensional Tectonics. Geological Society Special Publication, 28, 575-589.

Tan, O., Tapırdamaz, C. & Yörük, A. 2008. The Earthquake Catalogues for Turkey. Turkish Journal of Earth Sciences, 17, 405–418.

Tarcan, G., Filiz, Ş., Gemici, Ü. 1999. Balçova-Seferihisar (İzmir) jeotermal alanlarında karşılaştırılmal| hidrojeokimyasal incelemeler ve jeotermometre uygulamaları (in Turkish). 1. Bat| Anadolu Hammadde Kaynaklar| Sempozyumu Bildiriler Kitabı, 8-14 Mart, İzmir, pp. 346-358.

Tarcan, G. and Gemici, Ü. 2003. Water Geochemistry of the Seferihisar Geothermal Area, İzmir, Turkey. Journal of Volcanology and Geothermal Research, 126, 225-242.

Tezcan, A. K. and Turgay, M. I.: Heat flow and temperature distribution in Turkey, edited by: Cermak, V., Haenal, R., and Zui, V. 1991. Geothermal atlas of Europe, Herman Haack Verlag, Gotha, Germany, 84–85.

Tezel, T., Shibutani, T. and Kaypak, B. 2013. Crustal thickness of Turkey determined by receiver function. Journal of Asian Earth Sciences, 75: 36-45.

Timur, E. and Sındırgı, P. 2006. Cumalı (Seferihisar/İzmir) Jeotermal alanında yapılan manyetik ve SP çalışmaları. Türkiye 17. Uluslararası Jeofizik Kongre ve Sergisi, Ankara (İn Turkish)

Timur, E. 2017. Assessment of Vertical Magnetic Gradient Data of Tuzla Fault Using Boundary Analysis and 3-D Inversion Techniques Journal of Power and Energy Engineering, 33-45.

Uzel B., Sözbilir H. 2008. A first record of strike-slip basin in western Anatolia ve its tectonic implication: The Cumaovası basin as an example, Turkish Journal of Earth Sciences, 17:559–591.

Uzel, B., Sözbilir, H. ve Özkaymak, Ç. 2012. Neotectonic Evolution of an Actively Growing Superimposed Basin in Western Anatolia: The Inner Bay of Izmir, Turkey. Turkish Journal of Earth Sciences, 21, 439-471.

Uzel, B., Sözbilir, H., Özkaymak, Ç., Kaymakcı, N. ve Langereis, C. 2013. Structural evidence for strike-slip deformation in the Izmir–Balıkesir transfer zone and consequences for late Cenozoic evolution of western Anatolia (Turkey). Journal of Geodynamics, 65, 94-116.

Uzel, B. 2013. Geologic Evolution of İzmir-Balikesir Transfer Zone: A Crustal-Scale Structure Reorganizing Extensional Tectonics in Western Anatolia. D.E.U. Graduate School of Natural And Applied Sciences, Ph.D. Thesis, İzmir.

Ünalan, G., Öngür, T. 1979. Geothermal Gradient and Temperature Investigation at 1000 m Depth at Some Basins of Turkey, 1. Ortadoğu Jeoloji Kongresi-GEOCOME, 4-7 Eylül, Ankara.

Voudouris, P. ve Melfos, V. 2014. Intrusion related polymetallic ore system of Lavrion, Southern Attica, Greece: A. Miskovic (Eds.), Field Guide: MDRU Short Course 80, Athens, Greece: MDRU. The University of British Columbia.

World Bank. 2021. Turkey – Assessment of Opportunities and Interest in Direct Uses of Geothermal Energy, Project Final Report Workshop Presentation, World Bank, ESMAP, Stantec and Reykjavik Geothermal, 15 September 2021

Yılmaz, Y. 1990. Comparison of young volcanic associations of western and eastern Anatolia formed under a compressional regime: a review. Journal of Volcanology and Geothermal Research, 44, 69– 87.

Yılmaz, H., Oyman, T., Arehart, G.B., Çolakoğlu, A.R., Billor, Z. 2007. Low-sulphidation type Au-Ag mineralisation at Bergama, İzmir, Turkey. Ore Geol Rev 32:81–124

Yılmaz, H., Sönmez, F.N., Akay, E., Şener, A.K., Tufan, S.T. 2013. Low-sulphidation epithermal Au-Ag mineralisation in the Sındırgı District, Balıkesir Province, Turkey. Turk J Earth Sci 22:485–522

Yılmazer, S. 1984. Ege Bölgesindeki bazı sıcak su kaynaklarının hidrojeoloji ve jeokimyasal incelemeleri (in Turkish). D.E.Ü. Fen Bilimleri Enstitüsü, M.Sc. Thesis, İzmir.

Yılmazer, S. 2001. Kıyı Ege ve İzmir ilindeki Jeotermal kaynakların degelenlendirilmesi. (In Turkish) Yeraltı Suları ve Çevre Sempozyumu, 21-23 Mart 2001, İzmir, Bildiriler, pp.371-379.

Yiğit, O. 2006. Gold in Turkey—a missing link in Tethyan metallogeny. Ore Geology, 28, 147–179.

Yiğit O. 2009. Mineral deposits of Turkey in relation to Tethyan metallogeny: implications for future mineral exploration. Econ Geol 104:19–51

8 CONCLUDING REMARKS ABOUT THE STUDY AREAS

This report is a published product of the 'CRM-geothermal' project - an EU-funded, Horizon Europe project which aims to develop a novel and potentially disruptive technology solution that can help satisfy the European needs for critical raw materials combined with energy production (both heat and power). As a consequence, it will deploy solutions to help Europe fulfil the strategic objectives of the EU Green Deal and the Agenda for Sustainable Development. As part of this process, it is important to make full use of pre-existing information, as well as new data, as a foundation for updated datasets and new models. Hence, in this report we bring together sources of information, in order that more detailed investigations in both this and other projects can more efficiently access the data they need.

This report identifies sources of pre-existing data that underpin datasets and models for the sites being investigated in the 'CRM-geothermal' project. A considerable amount of information exists about these sites, which are:

- High enthalpy volcanic geothermal areas - Reykjanes, Iceland; Tuzla, Turkey
- Low salinity water in fractured crystalline rock – Cornwall, UK
- Saline water in sedimentary basins - Groß Schönebeck, northern Germany
- Alkaline geothermal area – Olkaria, Kenya
- Metamorphosed flysch – Seferihisar, Turkey

Information on each of the above sites is reported in a separate chapter. This report provides a brief introduction to the study areas and identifies the broad types of data and datasets already generated. It does not discriminate between open-file and restricted information, just identifying what information exists. There has been no attempt to interpret those data in the report – this will be part of other Work Packages within the project.